Acknowledgments

I would like to express my sincere thanks and deep gratitude to ***Dr. Ahmad K. Ahmad*** *for suggesting the present research, and for helpful comments and simulating discussions throughout the research.*

I would like to thank ***Dr. Fatin Abdul Jalil Al-Mudarris*** *For her valuable assistance during the work.*

I am grateful to the Dean of College of science and the staff of the Department of physics at Al-Nahrain University for their valuable support and cooperation. My special thanks are also due to ***Mr. Ahmad Al-Tabbakh****.*

The assistance given from my best friend ***Mr. Hussain Ali Al Hussaini*** *is highly appreciable and I would thank all my colleagues specially (****Ms. Fatma Nafaa, Mrs. Noor mohammed, and Ms. Zeena mowafaq****) ,and my friend* ***Mr. Ali Ihsaan.***

Last but not least, I would like to record my deep affection and thanks to ***my parent*** *for their moral support and patience throughout this work.*

Mohammed

Certification

I certify that this thesis entitled **"Design of an Ion Mirror as an Aberrations Corrector Using Boundary Values Method"** is prepared be **Mr. Mohammed Salam Mzahem Al-Obaidy** under my supervision at the College of Science of Al-Nahrain University in partial fulfillment of the requirements for the degree of **Master of Science in Physics**.

Supervisor: Dr. Ahmad K. Ahmad
Title: Assistant Professor
Date: / /2007

In view of the recommendations, we present this thesis for debate by the examination committee.

Dr. Ahmad K. Ahmad
Title: Assistant Professor
(Head of Physics Department)
Date: / /2007

4. CONCLUSIONS AND FUTURE WORK

4.1 Conclusions

It appear that the concepts put forward in the present investigation with regard to the mathematical expressions for the potential and the ion beam to produce the trajectories for ion mirrors are successful and gave rise to excellent result from the ion-optical point of view. Two and three-electrodes of electrostatic ion mirror have been achieved which can be useful for application in studying a specimen surface.

The ion mirrors achieved in the present investigation are useful for studying surfaces of specimens when infinite magnification ray path and by using Bimurzaev technique are considered as mirror trajectories. Comparison between the electrostatic mirrors achieved in this investigation and those reported in the literature have shown that the performance of the present work mirrors are excellent and highly desirable in ion optics. Thus it is worthwhile paying the suggested mirrors considerable attention for future application in experimental ion-optical columns.

4.2 Recommendations for Future Work

The following topics are put forward for future investigations within the framework of the present research.

(a) The electrostatic ion mirrors can, in principle, be used to correct aberration of many ion-optically instruments such as TOFMS (Time-of-flight mass spectrometer) can be performed when the advantage of the approach put forward in the present work are taken into account.

(b) An investigation on the effect of the geometrical parameters on the performance of various types of electrostatic mirrors.

(c) The following potential equations gave rise to achieve the electron or ion mirror action where the path of charge particles deviates towards the optical axis in a nearly linear manner,

$$U(z) = \frac{a}{1 + \left(\frac{z}{b}\right)^2} \qquad (4\text{-}1)$$

$$U(z) = \pm a * sec\,h\left(\frac{z}{c}\right) \pm b * cosh\left(\frac{z}{c}\right) \qquad (4\text{-}2)$$

$$U(z) = \pm a \pm tanh\left(\frac{z}{b}\right) \qquad (4\text{-}3)$$

Contents

الاسم :محمد سلام مزاحم

عنوان السكن : م- 308 ز- 58 د- 9

رقم الهاتف : 07901802945

الايميل : alobaidy1983@yahoo.com

تاريخ المناقشه :17-5-2007

عنوان الرساله : تصميم مرآة أيونيه تعمل كمصحح للزيوغ باستخدام طريقه القيم الحدوديه

Examination Committee Certification

We certify that we have read the thesis entitled **"Design of an Ion Mirror as an Aberrations Corrector Using Boundary Values Method"** and as an examination committee, examined the student **Mr. Mohammed Salam Mzahem Al-Obaidy** on its contents, and that in our opinion it is adequate for the partial fulfillment of the requirements of the degree of **Master of Science in Physics**.

Signature:
Name: **Dr. Inaam S. Al-Nakeshli**
Title: **Professor**
(Chairman)
Date: **/ /2007**

Signature:
Name: **Dr. Ayad A. Al-Ani**
Title: **Assistant Professor**
(Member)
Date: **/ /2007**

Signature:
Name: **Dr. Samir K. Al-Ani**
Title: **Assistant Professor**
(Member)
Date: **/ /2007**

Signature:
Name: **Dr. Ahmad K. Ahmad**
Title: **Assistant Professor**
(Supervisor)
Date: **/ /2007**

Approved by the University Committee of Postgraduate studies

Signature:
Name: **Dr. Laith Abdul Aziz Al- Ani**
Title: **Assistant Professor**
(Dean of the College of Science)
Date: **/ /2007**

1. INTRODUCTION

1.1 Electrostatic Electron Mirror

The idea of using an electron mirror to correct the chromatic and spherical aberration of around lens dates back more than half of century. Extensive studies of electrons mirrors have been performed by the **Kelman, Rempfer, Shao,** and **Rose** and co-workers **[Barnett and Nixon 1966]**. In **Rempfer's** work and the work of **Preikszas** and **Rose**, it was found that an electron mirror could correct the spherical and chromatic aberrations of the accelerating field of an immersion objective lens **[Schmid et al 2005].**

An electron mirror is create when an electrode with sufficiently high negative potential is placed in the path of an electron beam. The negative electrode forms a potential hill that decelerates the incident electrons. The electrons lose their kinetic energy before reaching the electrode and are re-accelerated in the reverse direction away from the electrode **[Kuehler 1960]**.

An electron mirrors are capable of introducing chromatic and spherical aberrations of arbitrary sign. Hence, we can utilize mirrors to compensate for the corresponding aberrations of round lenses **[Preikszas and Rose 1997]**. Unlike a light optical mirror, where the reflection occurs at the physical surface, the electron mirror represents a "soft" mirror, which allows the electrons to penetrate into the inhomogeneous reflecting medium formed by the electrostatic potential **[Rose and Wan 2005]**.

By introducing a reflection in the electron path using an electron mirror, the electron beam direction reverses and the electron velocity changes sign, thus the **Scherzer** theorem no longer applies **[Feng et al 2005].** The depth of penetration depends on the energy and the direction of the electron in front of the mirror. Mirrors which are suited for compensating the chromatic and spherical aberrations of round lenses, must be concave in the paraxial region and the convex in the outer zone as depicted in figure 1.1 **[Rose and Wan 2005]**.

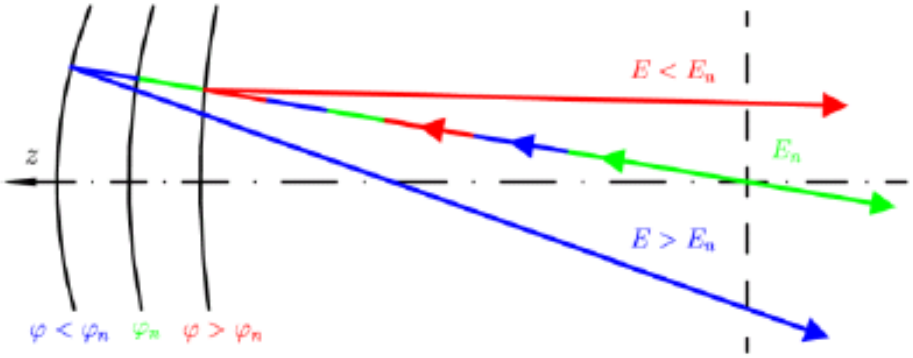

(*a*) *Correction of chromatic aberration*

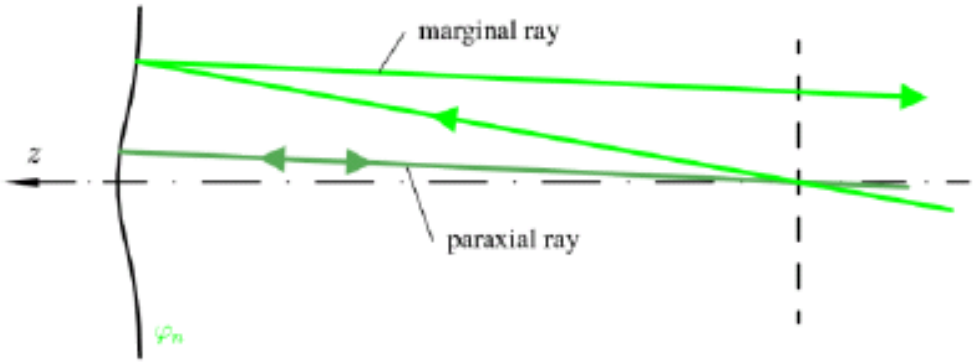

(b) Correction of spherical aberration

Figure (1.1) Path of rays illustrating chromatic and spherical aberration correction by the mirror [Rose and Wan 2005].

The mirror field is usually confined between two electrodes a negative (mirror) electrode and a positive electrode (anode) which may be a ground potential. The electrodes can be shaped to provide the desired focusing effects along with reversing effect **[Rempfer et al 1997]**. An electrostatic mirror is formed when the negative potential buildup on the specimen is strong enough to repel the primary electron beam, giving image of the SEM (Scanning Electron Microscope) specimen chamber instead of the specimen **[Wong et al 1997].**

The resolution and sensitivity of the electrostatic electron microscope with the mirror objective lens free of spherical and axial chromatic aberrations are higher than those of a similar microscope with an electron lens **[Bimurzaev et al 2003]**. Any electrostatic mirror is in actuality a space-filling electrostatic field shaped by the surrounding electrodes **[Henkelman and Ottensmeyer 1973]**.

An example of electron mirror is shown in figure 1.2. the electron-optical scheme of the transmission electron microscope with a mirror objective. In this scheme the mirror optical axis coincides with the electron microscope optical axis and the objective plane is located near the mirror focal plane. The electron microscope operates as follows. The electron beam (2) formed by the illumination system (1) falls on a studied object placed on the stand (3), at a certain angle with respect to the microscope optical axis. This angle can be selected in a way such that only the electrons that are deviated from their original path due to the interaction with the object can go through the aperture diaphragm (6). The other electrons that have not undergone interactions with the object are stopped by the diaphragm. The electrons (4)

that deviate from their original path, on reflecting from the electrostatic electron mirror (the objective (5)), create a magnified image of the object on the intermediate screen (7) and this image is free of aberration. Then, the devices of observation and registration of the image (8) create a magnified image of that intermediate image in the plane of the screen (9) **[Bimurzaev et al 2004]**.

There are several difficulties associated with the use of the mirror, including that of providing a physical separation between the entering and emerging electron beams **[Crew et al 2000]**. Electron mirrors are made in various geometries according to their function in an electron optical instrument. They can be made in the form of two or three concentric cylindrical electrodes at different potentials for reducing aberration **[Berger and Baril 1982]**.

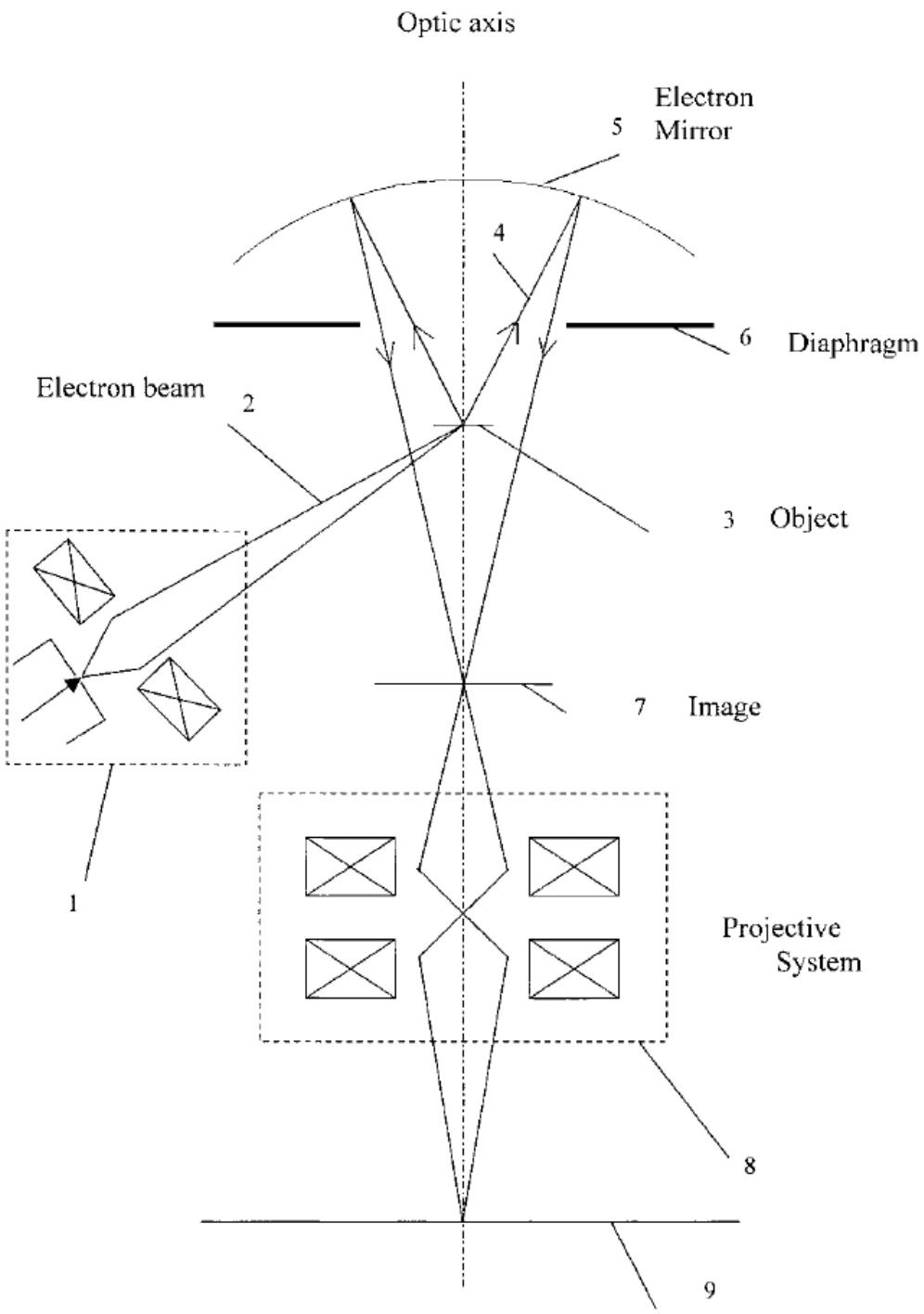

Figure (1.2) Scheme of electron microscope with mirror lens [Bimurzaev et al 2004].

1.2 Electrostatic Ion Mirror

Electrostatic mirrors have previously been utilized for the deflection or energy analysis of beams of ions or electrons. The electrostatic ion mirror was first studied by **Yarnold and Bolton in 1949**.

Ion mirrors are expensive to construct and difficult to optimize and maintain. In addition, the conventional staged designs have two or more regions with significantly different electric field intensities. Electrode shapes could also be used to fabricate effective ion mirrors. These shapes include cylindrical and rectangular shapes **[Zhang et al 2000]**. Ion mirrors work on the principle that faster ions penetrate deeper into the mirror and consequently spend more time in the mirror **[Short and Todd 1994]**.

The field inside a parabolic mirror (reflectron) is curved along the axis and according to the Laplace equation it also has a curvature in a radial (or transverse) direction **[Doroshenko and Cotter 1999]**. In electrostatic ion mirror the electrostatic field continuously changes in the interface region between the retarding and repelling fields, and the electric field extends out from the retarding field region into the field-free drift path **[Scherer et al 2006]**.

There are many types of ion mirrors with different shapes and electric field distributions but perfect compensation for ion kinetic energy differences requires a complex electric field shape in the ion mirror. Practical ion mirrors can be divided into two groups:

a) Gridless ion mirrors: its have the advantage of improved ion transmission but the homogeneity of the electric fields in the radial direction is compromised. This inhomogeneity may cause ion dispersion and temporal defocusing.

b) Grided ion mirrors: it's easier to design and build but the electric field can be distorted in the vicinity of the grids. **[Zhang et al 2000]**.

There is a potential hill in the ion mirror in which a time shift occurs as ion enters the mirror, are decelerated, turn around, and finally accelerate in the opposite direction **[Zhang and Enke 2000]**. In the ion mirror there is no hard reflecting point, this surface does not necessarily coincide with either the physical location of the turnaround point of the ion mirror or a physical electrode surface **[Rockwood 1999]**.

If there is a large distance involved between the ion source and the entrance of the ion mirror it is important to position a set of weakly focusing ion optical lenses in the field free region that controlled the divergence of the beam **[Giannakopulos et al 2002]**.

1.3 Application of Electron and Ion Mirror

Many applications in both physical and biological sciences require higher resolution to resolve even smaller structures. It is unfortunate that the current approach of designing better lenses has reached saturating point **[Shao and Wu 1990]**. Electron microscopy with aberration correctors based on electron mirrors has been proposed by many authors **[Franzen and Taaffe 1980]**.

We can divide the applications and advantages of electrostatic electron mirror in many instruments:

a) PEEM3 (third generation of Photo emission electron microscopy) :

Photo emission microscopy has become a powerful tool in recent years for the investigation of the surface chemical and magnetic properties of materials at high spatial resolution **[Takakusagi et al 2000, Wan et al 2005].** In this instrument the emitted electrons come in a wide range of energies, however, resulting in strong chromatic aberration. One solution has been to restrict the energies of electrons at just a single energy by using the electron mirror. The mirror could also increase the ultimate resolution of these instruments from 70 angstroms to 10 or fewer **[Stokstad 1997]**. An electrostatic mirror, in principle, can be used for the simultaneous correction of chromatic and spherical aberration. The design goal of an aberration corrected PEEM3 (see figure 1.3) is to obtain the highest throughput, at a resolution commensurate with the resolution determined by low energy electron scattering within a sample **[Feng et al 2002]**.

Up to now, an electron mirror is the only device known (through both simulation and experiment) to be able to correct chromatic and spherical aberrations of a PEEM **[Wan et al 2004]**.

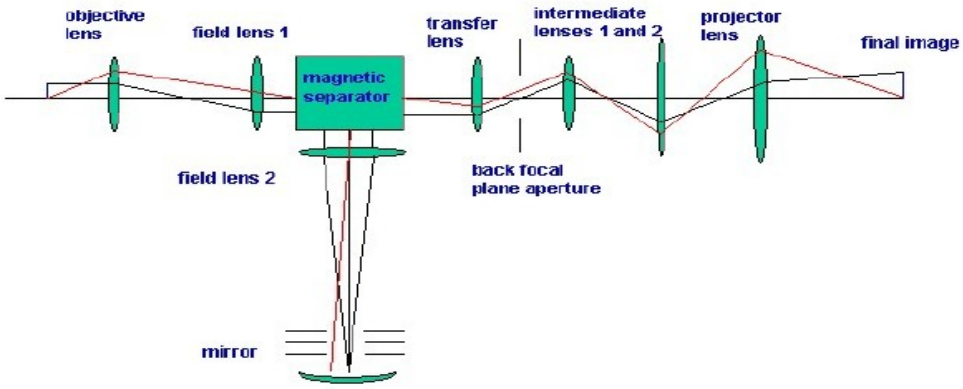

Figure (1.3) The PEEM3 [Wan et al 2004]

b) CMA (Cylindrical Mirror Analyzer) : An electrostatic cylindrical mirror analyzer is an instrument that can be able to analyze a complete energy spectrum simultaneously and can be accept to analyzing the spectrum of energies are emitted over a wide range of angles in the transverse direction . The advantage of CMA is the ability to analyze a narrow energy region with higher resolution **[Read 2002]**. It propose to use such a mirror not for energy analysis of electrons but only as a collecting stage that prepares the beam suitable for the energy analysis **[Belov and Yavor 2000]**.

c) LEEM (Low Energy Electron Microscopy): it is one of the premier technique for studies of surface dynamical processes, such as epitaxial growth, phase transitions, chemisorption and strain relaxation

phenomena. The advantage of electrostatic electron mirror is to improved resolution, improved diffraction capabilities by correction of chromatic and spherical aberration **[Tromp et al 1998, Weißäcker and Rose 2002]**. The LEEM can be also used to image thin film magnetic structures. The image contrast in LEEM is due to variations in electron reflectivity arising from the local chemical, structural, and magnetic properties of the surface **[Grzelakowski 1999, Hannon and Tromp 2003]**.

d) EMIM (Electron Mirror Interference Microscopy) : The principle of EMIM that the specimen serves as a mirror electrode held at a potential negative with respect to cathode from which the electrons are emitted. The advantage of EMIM is the possibility of judging the quality of polished surfaces **[Lichte and Möllenstedt 1979]**.

e) MEM (Mirror Electron Microscopy): Theoretical and experimental work on MEM began with the early developments of electron microscopy in the 1930's. From the very beginning of electron microscopy, mirror microscopy was used as technique of direct surface imaging where the specimen is neither struck by electrons nor emits electrons. The transfer of the specimen information onto the imaging electron beam is obtained indirectly by disturbances in the potential field at the surface of the specimen **[Hawkes and Kasper 1989]**.

The MEM is very sensitive to micro fields and to the step height of objects under study. The lowest step height detectable in the MEM is of the order of 1 nm. Important for the application of the MEM is the contrast due to contact potentials between adjacent area with different value of the work function **[Babout et al 1980, Kleinschmidt and Bostanjoglo 2001]**. The MEM is also a very useful tool for the study of magnetic domains and detecting the influence of magnetic fields. MEM is preferentially applied to the detection of weak field inhomogeneities **[Barnett and Nixon 1966]**.

Electrostatic ion mirrors have also found application in cyclotrons where they may be used to deflect the ion beam, when it is introduce from an external ion source, through 90º into the system for acceleration. The application of ion mirrors has been largely restricted to three areas **[Beanland and Freeman 1976]**:

a) Energy analysis-mainly for electrons.

b) Ion and electron microscopy-for the reflection of very low intensity beams through 180º.

c) Axial beam injectors-to couple low energy, external ion sources into high energy accelerators.

One of the application of electrostatic ion mirror in TOFMS (Time-of-flight mass spectrometer), that the most convenient way to analyze the mass distribution of ions produced from ion source **[Vialle et al 1997]**.

The (TOF) instrument is one of the simplest mass analyzers. Some (TOF) mass analyzers include an ion mirror at the end of flight tube, which reflects ions back through the flight tube to a detector. In this way, the ion mirror serves to increase the length of the flight tube. The ion

mirror also corrects for small energy differences among ions. Both of these factors contribute to an increase in mass resolution **[Graves and Haystead 2002]**. The ion mirror in the (TOF) can compensate the residual energy spread when the geometry and the potentials of the mirror electrodes are chosen properly **[Ishida et al 2005].**

The electrostatic ion mirror is a powerful way in (TOF) to compensating for the spread in the initial energy distribution of the ions is to reflect the beam in an electrostatic field, consider a package of ions having the same mass and approaching the mirror after been accelerated to certain energy. Due to the initial energy distribution some ions will have lower energy and some higher energy than the correct one. Ion with too high energy will penetrate deeper into the mirror before the are reflect back, compared to the ones with correct energy. Thereby they will lose time. Ions with to low energy will not penetrate so deep into the mirror before they are reflected back, compared to the ones with correct energy. Thereby they will gain time. The net effect is a time focusing of the ion package at the detector plane **[Håkansson 1999]**.

The ion mirror is also used in QqTOF (quadrupole-time-of-flight mass spectrometry) to correct both spatial and the resulting energy spread of the ions are originated from the source and this correcting help to improving the resolution of image and getting to high resolution **[Chernushevich et al 2001]**.

The electrostatic mirror becomes a critical part of the spectrometer if high spatial resolution and good image quality required from the system **[Henkelman and Ottensmeyer 1973, Zashkvara et al 1966]**.The simulations with an ion mirror gave us an idea about the necessary potential distribution to solve our problem, so we had to find another geometry providing the same field distribution **[Hohl et al 1999, Rempfer 1990]**.

1.4 Aim of the Research

Due to the practical importance of electrostatic mirror it is aimed in the present investigation at achieving a good design for such device for several reasons. It is found that the aberrations of the experimental electrostatic mirrors reported in the literature are characterized by their values which are ion-optically undesirable. Therefore, in the present work a new approach and new technique by **Bimurzaev** has been followed. Considerable attention has been given to mathematical expressions representing the potential that would give rise to an electrostatic mirror which unfortunately have received only limited attention by the designers.

List of Symbol

a, b	**Constants affecting the voltage ratio (Volt, V)**
c	**Constant affecting the voltage ratio (millimeter, mm)**
C_c	**Chromatic aberration coefficient (mm)**
C_s	**Spherical aberration coefficient (mm)**
e	**Electron charge (Column, C)**
f_o	**Focal length in the object side (mm)**
f_R	**Focal length of the reflect ion beam trajectory (mm)**
G	**Radial displacement of the reflected beam from the mirror (mm)**
G′	**Derivative of the radial displacement of the reflected beam from the mirror with respect to z i.e. dG/dz**
L	**Length of mirror field**
m	**Electron mass (kilogram, kg)**
P	**Radial displacement of the incident beam on the mirror**
P′	**Derivative of the radial displacement of the incident beam on the mirror with respect to z i.e. dP/dz**
R	**Radial displacement of the beam from the optical axis (mm)**
R′	**Derivative of the radial displacement with respect to z i.e. dR/dz**
U=U(z)	**The axial potential distribution (V)**
U', U''	**First and second derivatives with respect to z i.e.** dU/dz **and** d^2U/dz^2
v	**Electron velocity (meter/second, m/s)**
z	**Optical axis (mm)**

References

Ahmad, A. K. (1993)
Computerized investigation on the optimum design and properties of the electrostatic lenses
Ph.D. Thesis, Al-Nahrain University, Baghdad, Iraq

Al-Mudarris, F. A. J. (2001)
Computer-aided design of an ion-optical transport and focusing system
Ph.D. Thesis, Al-Nahrain University, Baghdad, Iraq

Al-Tabbakh, A. A. (2000)
Design of a focusing ion beam (FIB) using the inverse problem procedure
M.Sc. Thesis, Al-Nahrain University, Baghdad, Iraq

Babout, M., Guivarch, M., Pantel, R., Bujor, M., and Guittard, C. (1980)
Mirror electron microscopy applied to the continuous local measurement of work-function variations
J. Phys. D: Appl. Phys., **13**, 1161-1167

Barnett, M. E., and Nixon, W. C. (1966)
A mirror electron microscope using magnetic lenses
Sci. Instrum., **44**, 893-898

Beanland, D. G., and Freeman, J. H. (1976)
The modeling of electrostatic mirrors for the manipulation and focusing of heavy ions
Nucl. Instrum. Meth., **136**, 409-419

Belov, V. D., and Yavor, M. I. (2000)
High-resolution energy analyzer with a large angular acceptance for photoelectron spectromicroscopy applications
Rev. Sci. Instrum., **71**, 1651-1655

Berger, C., and Baril, M. (1982)
Studies of three-cylinder electrostatic mirrors and lenses
J. Appl. Phys., **53**, 3950-3956

Bimurzaev, S. B., Serikbaeva, G. S., and Yakushev, E. M. (2003)
Electrostatic mirror objective with eliminated spherical and axial chromatic aberrations
J. Electron Microsc., **52**, 365-368

Bimurzaev, S. B., Serikbaeva, G. S., and Yakushev, E. M. (2004)
Calculation of focusing quality of the electrostatic mirror objective free of the third-order spherical aberration
Nucl. Instrum. Meth. Phys. Res., **A519**, 70-75

Chernushevich, I. V., Loboda, A. V., and Thomson, B. A. (2001)
An introduction to quadrupole-time-of-flight mass spectrometry
J. Mass Spectrom., **36**, 849-865

Crewe, A. V., Ruan, S., Korda, P., and Tsai, F. C. (2000)
Studies of a magnetically focused electrostatic mirror
I. Experimental test of the first order properties
J. Microscopy., **197**, 110-117

Doroshenko, V. M., and Cotter, R. J. (1999)
Ideal velocity focusing in a reflection time-of-flight mass spectrometer
J. Am. Soc. Mass Spectrom., **10**, 992-999

El-kareh, K. B., and El-Kareh, J. C. J. (1972)
Electron beam, lenses and optics, Vol.1 and 2
(Academic press: New York and London)

Feng, J., Forest, E., Macdowell, A. A., Marcus, M., Padmore, H., Raoux, S., Robin, D., Scholl, A., Schlueter, R., Schmid, P., Stöhr, J., Wan, W., Wei, D. H., and Wu, Y. (2005)
An x-ray photoemission electron microscope using an electron mirror aberration corrector for the study of complex materials
J. Phys: Condens. Matter., **17**, 1339-1350

Feng, J., Padmore, H., Wei, D. H., Anders, S., Wu, Y., Scholl, A., and Robin, D. (2002)
Modeling the acceleration field and objective lens for an aberration corrected photoemission electron microscope
Rev. Sci. Instrum., **73**, 1514-1517

Franzen, W., and Taaffe, J. (1980)
Theory of modified cylindrical mirror electron spectrometer free of third-order aberration
J. Phys. E: Sci. Instrum., **13**, 719-723

Giannakopulos, A. E., Thomas, B., Colburn, A. W., Reynolds, D. J., Raptakis, E. N., Makarov, A. A., and Derrick, P. J. (2002)
Tandem time-of-flight mass spectrometer (TOF-TOF) with a quadratic-field ion mirror
Rev. Sci. Instrum., **73**, 2115-2123

Graves, P. R., and Haystead, T. A. J. (2002)
Molecular biologist's guide to proteomics
Microbiol. Mol. Biol. Rev., **66**, 39-63

Grivet, P. (1972)
Electron optics
(Pergamon : Oxfords and New York)

Grzelakowski, K. (1999)
The novel surface science instrument: Double reflection electron emission microscope
Rev. Sci. Instrum., **70**, 3346-3350

Håkansson, P. (1999)
An introduction to the time-of-flight technique
Brazilian. J. Phys., **29**, 422-427

Hannon, J. B., and Tromp, R. M. (2003)
Low-energy electron microscopy of surface phase transitions
Annu. Rev. Mater. Res., **33**, 263-288

Hawkes, P. W., and Kasper, E. (1989)
Principles of electron optics
Vol. **1**, p. 261, (Academic New York)

Henkelman, R. M., and Ottensmeyer, F. P. (1973)
An electrostatic mirror
J. Phys. E: Sci. Instrum., **7**, 176-178

Hohl, M., Wurz, P., Scherer, S., Altwegg, K., Balsiger, H. (1999)
Mass selective blanking in a compact multiple reflection time-of-flight mass spectrometer
International J. Mass spectrometry, **188**, 189-197

Ishida, Y., Wada, M., and Wollnik, H. (2005)
A multi-reflection time-of-flight mass spectrometer for mass measurements of short-lived nuclei.
Nucl. Instr. and meth. in Phys. Res. B, **241**, 983-985

Kleinschmidt, H., and Bostanjoglo, O. (2001)
Pulsed mirror electron microscope: A fast near-surface imaging probe
Rev. Sci. Instrum., **72**, 3898-3901

Kuehler, J. D. (1960)
A new electron mirror design
J. IBM of research and development . **4**. 202-204

Lichte, H., and Möllenstedt, G. (1979)
Measurement of the roughness of supersmooth surfaces using an electron mirror interference microscope
J. Phys. E: Sci. Instrum., **12**, 941-944

Munro, E. (1975)
A set of computer programs for calculating the properties of electron lenses
Department of Engineering Report CUED/B. Elect. TR45, University of Cambridge, UK

Paszkowski, B. (1968)
Electron optics
(Itiffe Book: London)

Preikszas, D., and Rose, H. (1997)
Correction properties of electron mirrors
J. Electron Microsc., **46**, 1-9

Read, F. H. (2002)
The parallel cylindrical mirror electron energy analyzer
Rev. Sci. Instrum., **73**, 1129-1139

Rempfer, G. F. (1990)
A theoretical study of the hyperbolic electron mirror as a correcting element for spherical and chromatic aberration in electron optics
J. Appl. Phys., **67**, 6027-6040

Rempfer, G. F., Desloge, D. M., Skoczylas, W. P., and Griffith, O. H. (1997)
Simultaneous correction of spherical and chromatic aberration with an electron mirror: an electron optical achromat
Microsc. Microanal., **3**, 14-27

Risley, J. S. (1972)
Design parameters for the cylindrical mirror energy analyzer
Rev. Sci. Instrum., **43**, 95-103

Rockwood, A. L. (1999)
Stability conditions for multiply reflection electrostatic ion trap
J. Am. Soc. Mass Spectrom., **10**, 241-245

Rose, H., and Wan, W. (2005)
Aberration correction in electron microscopy
Proc. IEEE, Particle Accelerator Conference, Knoxville, Tennessee,. 44-48

Scherer, S., Altwegg, K., Balsiger, H., Fischer, J., Jäckel, A., Korth, A., Mildner, M., Piazza, D., Reme, H., and Wurz, P. (2006)
A novel principle for an ion mirror design in time-of-flight mass spectrometry
International J. Mass spectrometry, **251**, 73-81

Schmid, P., Feng, J., Padmore, H., Robin, D., Rose, H., Schlueter, R., Wan, W., Forest, É., and Wan, Y. (2005)
Correction and alignment strategies for the beam separator of the photoemission electron microscope 3 (PEEM 3)
Rev. Sci. Instrum., **76**, (023302-1)-(023302-14)

Shao, Z., and Wu, X. D. (1990)
Properties of a four-electrode adjustable electron mirror as an aberration corrector
Rev. Sci. Instrum., **61**, 1230-1235

Short, R. T., and Todd, P. J. (1994)
Improved energy compensation for time-of-flight mass spectrometry
J. Am. Soc. Mass Spectrom., **5**, 779-787

Skoczylas, W. P., Rempfer, G. F., and Griffith, O. H. (1994)
Electron optical benches for in-line and branched systems. A new bench designed for mirror-based aberration correction and low energy electron microscopy
Rev. Sci. Instrum., **65**, 3183-3193

Stokstad, E., (1997)
Electron mirror gives a clearer view
Science, New series, **275**, 1069-1070

Szilagyi, M. (1984)
Reconstruction of electrodes and pole pieces from optimized axial field distributions of electron and ion optical system
Appl. Phys. Lett., **45**, 499-501

Szilagyi, M. (1988)
Electron and ion optics
(Plenum Press: New York)

Szilagyi, M., and Szép, J. (1987)
A systematic analysis of symmetric three-electrode electrostatic lenses
IEEE Trans., ED**34**, 2634-2642

Takakusagi, S., Kato, M., Sakai, Y., Fukui, K., Asakura, K., and Iwasawa, Y. (2000)
Development of an X-ray photoemission electron microscopy system with multi-probes, and its application to surface imaging at static and dynamic states
J. Microscopy, **200**, 240-250

Tromp, R. M., Mankos, M., Reuter, M. C., Ellis, A. W., and Copel, M. (1998)
A new low energy electron microscope
Surface Rev. lett., **5**, 1189-1197

Vialle, J. L., Baguenard, B., Bourgey, A., Cottancin, E., Lermé, J., Palpant, B., Pellarin, M., Valadier, F., and Broyer, M. (1997)
A cylindrical reflectron time-of-flight mass spectrometer
Rev. Sci. Instrum., **68**, 2312-2318

Wan, W., Feng, J., and Padmore, H. A. (2005)
Design study of a new beam separator for PEEM3
Proc. IEEE. Particle Accelerator Conference, Knoxvill, Tennessee,. 3985-3987

Wan, W., Feng, J., Padmore, H. A., and Robin, D. S. (2004)
Simulation of a mirror corrector for PEEM3
Nucl. Instrum. Meth. Phys. Res., **A519**, 222-229

Weißbäcker, C., and Rose, H. (2002)
Electrostatic correction of the chromatic and of the spherical aberration of charged-particle lenses (part II)
J. electron Microsc., **51**, 45-51

Wong, W. K., Phang, J. C. H., and Thong, J. T. L. (1997)
Estimation of the second crossover in insulators using the electrostatic mirror in the scanning electron microscope
Appl. Phys. Lett., **71**, 1270-1272

Zashkvara, V. V., Korsunskii, M. I., and Kosmachev, O. S. (1966)
Focusing properties of an electrostatic mirror with a cylindrical field
Sov. Phys. Tech. Phys., **11**, 96-99

Zhang, J., and Enke, C. G. (2000)
Simple cylindrical ion mirror with three element
J. Am. Soc. Mass Spectrom., **11**, 759-746

Zhang, J., Gardner, B. D., and Enke, C. G. (2000)
Simple geometry gridless ion mirror
J. Am. Soc. Mass Spectrom., **11**, 765-769

3. RESULTS AND DISCUSSIONS

3.1 An Electrostatic Mirror for Infinite Magnification Ion Mirror

3.1.1 Suggested potential for the electrostatic ion mirror

A potential distribution function has been suggested to represents an electrostatic mirror operating in the accelerating mode under infinite magnification condition. It has the following form:

$$U(z) = a * \sec h\left(\frac{z}{c}\right) + b * \tanh\left(\frac{z}{c}\right) \qquad \textbf{(3-1)}$$

where *U* (z) is the axial potential along the optical axis z. Solving the paraxial ray equation (2-1) using the axial potential distribution equation (3-1) and its first and second derivatives by the fourth order Runge-Kutta method one can have the electron or ion trajectory and its first derivative and thus one can determine the first and third order optical properties of the mirror. The potential distribution *U* (z) is constant at the boundaries, and then its first and second derivatives are zero at these boundaries. The second derivatives of the potential has two inflection points, hence the mirror has three electrodes [**Szilagyi 1988]**.

The constants a**, b** and **c** in equation (3-1) is affects the properties of this suggested potential and have been given the following values: **a** = 500, 1000, 1500; **b** = 0.01, 0.02, 0.03, 0.04, 0.05 and **c** = 0.95, 1.0, 1.05, 1.1, and 1.15. The effect of these constants on *U* (z) has been investigated independently. The choice of the function given in equation (3-1) is justified by the results that will be discussed later. The units of the constants **a**, **b**, and **c** are such that the net result of the right- hand of the equation (3-1) has the unit of volt in order that *U*(z) is maintained in

volts. The present investigation have shown that as far as the relative spherical and chromatic aberration coefficients C_s / f_o and C_c / f_o are concerned respectively, where it is highly favorable values of the constants **a**, **b** and **c** at 500, 0.01, 1.05 respectively. In order to achieve the electron or ion-optically acceptable aberrations where C_s / f_o = -0.26 and C_c / f_o = -0.26, a value will below unity. Figure (3.1) shown the favorable axial potential *U*(z) and its corresponding first and second derivatives respectively based on the proposed expression given in equation (3-1) at the above value of the constant **a**, **b**, **c**. The length **L** of the mirror in this case is 17.8 mm. The potential *U (z)* has a maximum value of 500 V at z = 0 and diminishes at about z = 8 mm and z = -8 mm.

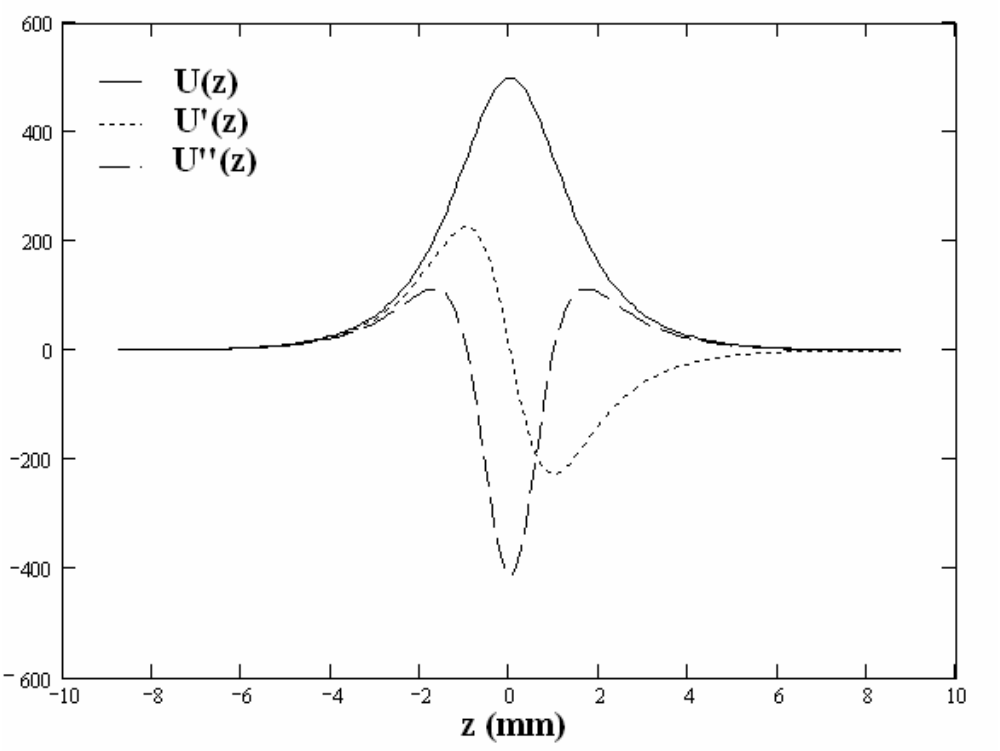

Figure(3.1) The axial potential distribution U(z) and its first and second derivatives U'(z) and U''(z) respectively of the electrostatic mirror when a = 500 volt, b = 0.01 Volt, c = 1.05 mm, and mirror length L = 17.8 mm.

When the proposed expression given in equation (3-1) is investigated at other values of **a**, **b**, and **c** besides the various values of the mirror length **L**. The main difference will lies in the value of the maximum potential which always appears at a fixed axial position where z = 0. By taking various values of the mirror length **L** into account such as 12, 14, 16, 18, 20 mm the calculation have shown that their effect appears in the region of reducing potential only where **z = L** provided **a**, **b**, and **c** remain constant.

When the mirror length is increases, the value of the potential at **z = L** increases. For each value of **L** given above, the effect of each of the constants **a**, **b**, and **c** have been investigated independently. The computation have shown that the maximum value of the potential increases in the manner of increasing value of **a** as shown in figure (3.2). The maximum value of the potential is not effect by the various values of **b** and **c** where by varying the values of **b** or **c** with keeping **a** constant causes a changing in the potential at the terminals peak where the increasing of **b** causes decreasing of potential at the negative part of **z** and increasing of potential at the positive part of **z** with keeping **a** and **c** constant as shown in figure (3.3). By keeping **a** and **b** constant the increasing of the value of **c** causes increasing the potential at the terminals peak in both positive and negative part of **z** but with different ratio as shown in figure (3.4). One would expect such a result since at **z** = 0, *U* (z) = **a**; hence *U (z)* increases with increasing **a** where **b** and **c** have no effect on the maximum potential.

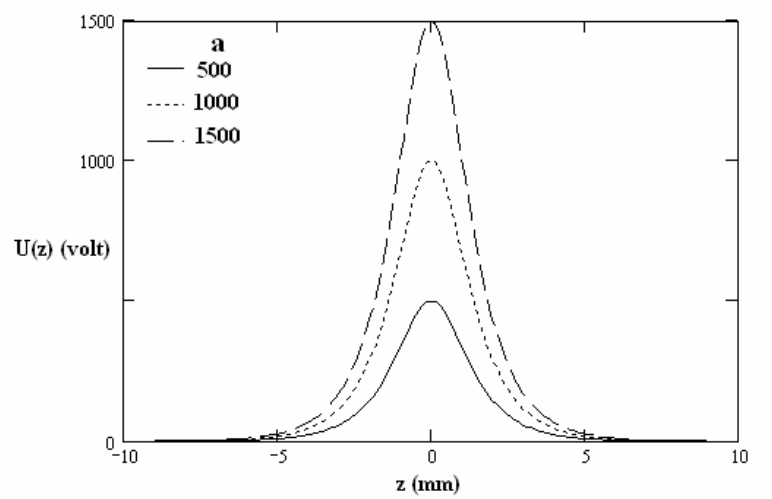

Figure(3.2) Show the axial potential distribution U(z)at various values of a (Volt) , and mirror length L = 17.8 mm.

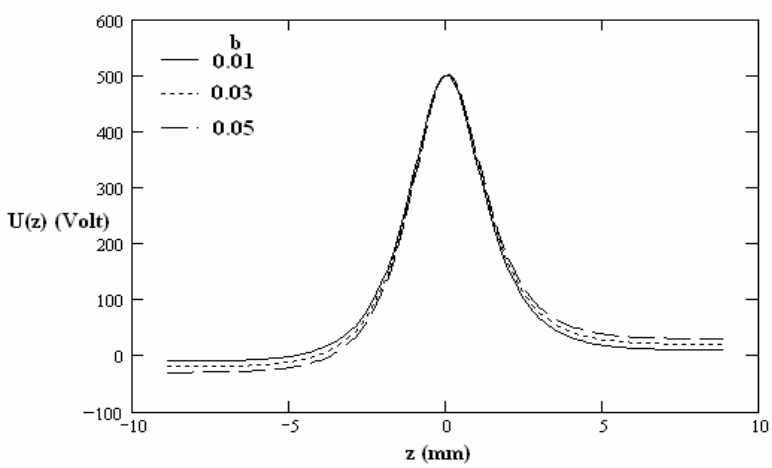

Figure(3.3) Show the axial potential distribution U(z)at various values of b (Volt) , and mirror length L = 17.8 mm.

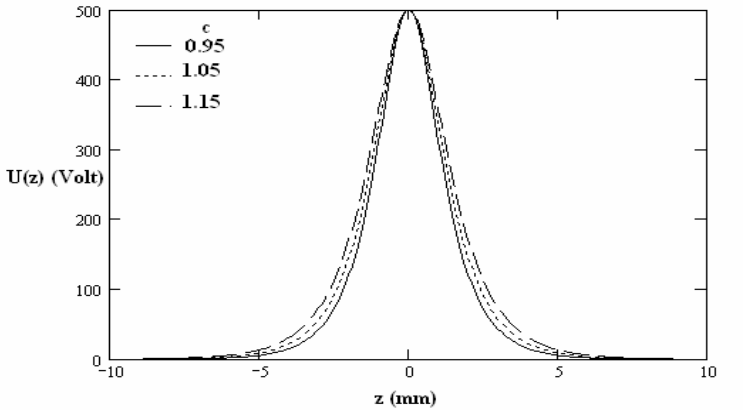

Figure(3.4) Show the axial potential distribution U(z)at various values of c (mm) , and mirror length L = 17.8 mm.

3.1.2 Ion beam trajectory under infinite magnification condition.

The ion beam path along the electrostatic mirror field under infinite magnification condition and accelerating mode of operation has been considered. Taking various values of the constant **a**: 500, 1000, and 1500 under consideration, it has been found that as far as the relative aberration coefficients are concerned the effect of **a** is very little irrespective of the values of **b** and **c**. Thus the value **a** = 500 has been maintained as a constant one in computing the field and the trajectory at various values of **b** and **c**. For example, from the figure (3.5) It is can be shown that the values of the objective focal length f_o increases with **b** where the increasing of **b** deducing increasing in the objective focal length f_o at the same mirror length where **L** = 12 mm, **a** = 500, and **c** = 1.05. Figures (3.6), (3.7), and (3.8) shows the trajectories of an ion beam traversing the electrostatic mirror field at various values of mirror lengths **L** = 14, 16, 18 mm. These trajectories have been computed with taking into account various values for the constant **c** =0.95, 1.0, 1.05, 1.1, 1.15, and **b** = 0.01, 0.02, 0.03, 0.04, 0.05, with keeping **a** constant at 500. These trajectories are similar in their general form. It is seen that as the mirror length **L** increases, the radial displacement **R** of the beam decreases. Each trajectory represents a mirror of a specific length **L**.

At the values of the mirror length **L** = 14, 16, 18 mm and keeping **a** and **b** constants at 500 and 0.01 respectively, figure (3.6) shows the effect of various values of the constants **c** on the radial displacement with keeping **a** = 500 and **b** = 0.01**.** Theses trajectories at the three values of **L** = 14, 16, 18 suggested that the most favorable mirror trajectories

appear when **c** = 1.05 and 1.1 because at these values of **c** we get at the best values of an aberration coefficients and other optical properties compared with other values of **c**. At the above values of **L** the effect of the constant **c** on the trajectory has been reconsidered when **a** and **b** are maintained constant at the value of 500 and (0.01, 0.03, 0.05) respectively, these trajectories are shown in figures (3.6), (3.7), and (3.8), it also suggested that the most favorable mirror trajectories are found when **c** = 1.05 and 1.1. And for **a** = 500 and **b** = 0.05, the effect of the constant **c** on the trajectories has been investigated at different values of **L** are shown in figure (3.8). Again these trajectories indicate that the most favorable mirror trajectories are found when **c** = 1.05 and 1.1. From the investigation it is noted that the mirror focal length has a negative sign that is meaning the type of mirror is divergence mirror.

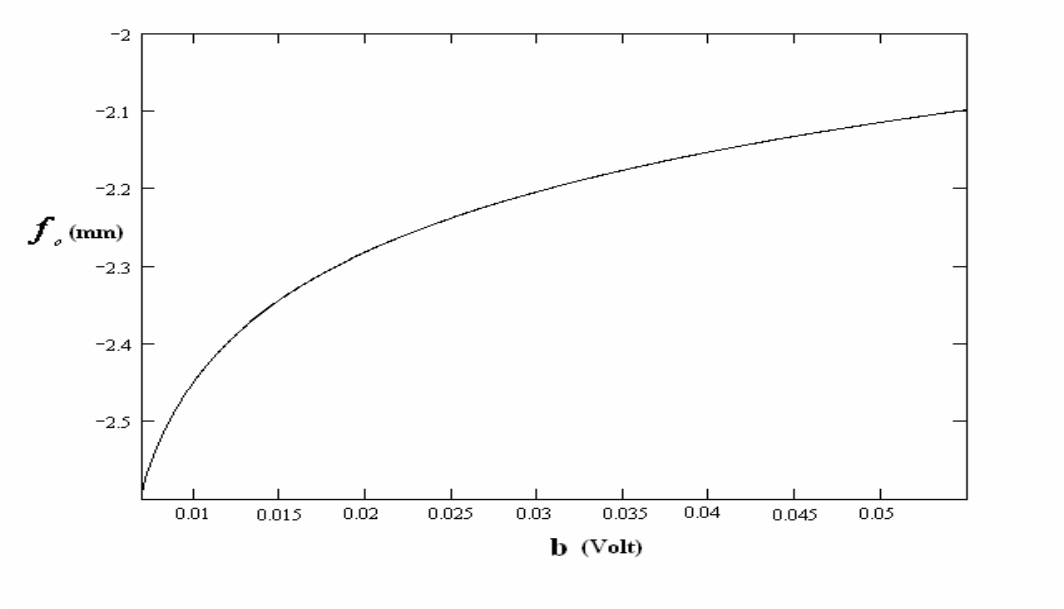

Figure(3.5) show the variation between values of b and the values of the object focal length f_o (mm) when L=12 mm, c=1.05 mm, and a=500 Volt.

(a)

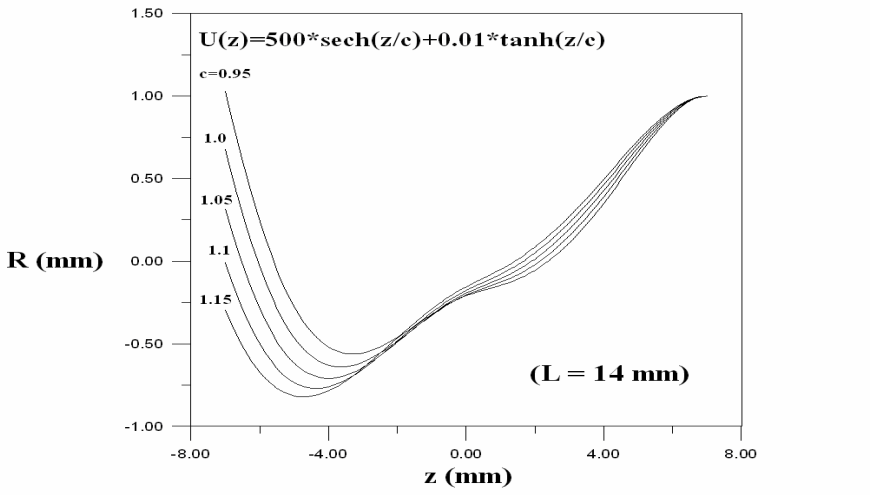

(b)

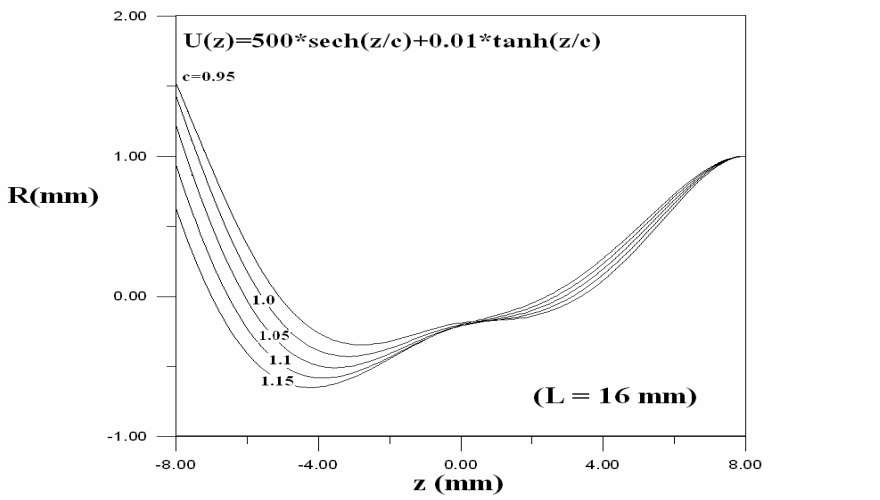

(c)

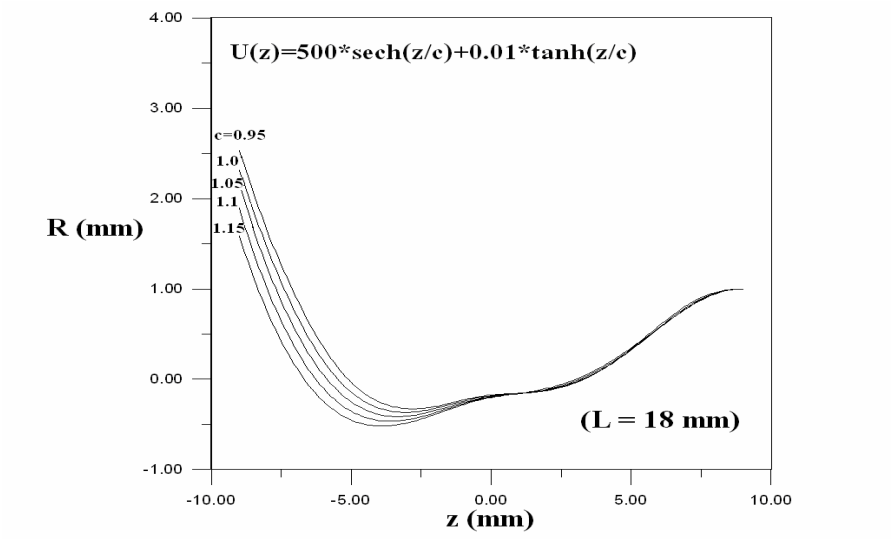

Figure (3.6) The ion beam trajectory in an electrostatic mirror under infinite magnification condition at various value of c (mm) when a=500 volt, b=0.01 volt, and mirror length L=14, 16, 18 mm at figures (a), (b), and (c) respectively.

(a)

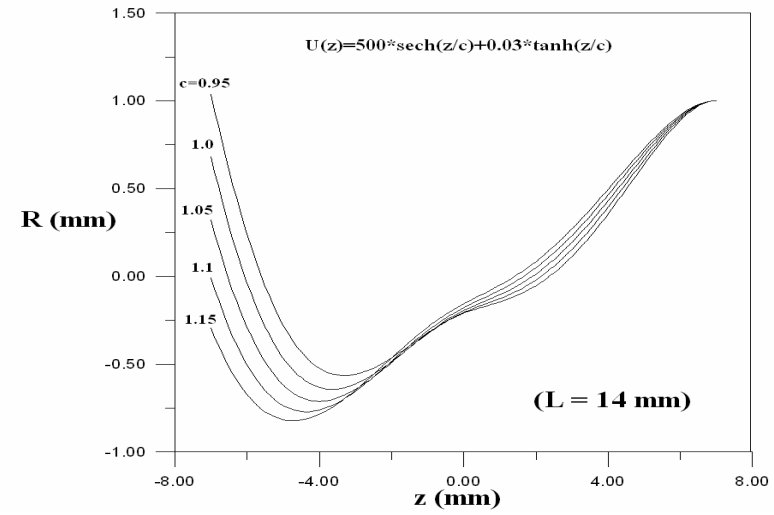

(b)

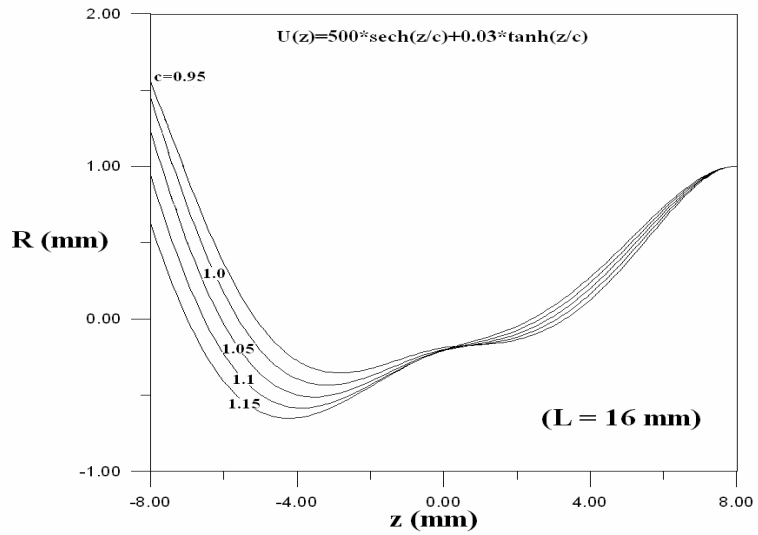

(c)

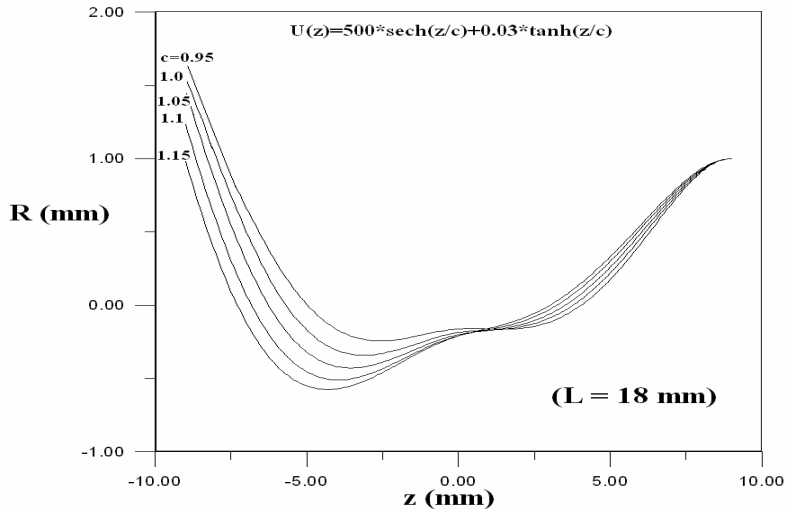

Figure (3.7) The ion beam trajectory in an electrostatic mirror under infinite magnification condition at various value of c (mm) when a=500 volt, b=0.03 volt, and mirror length L=14, 16, 18 mm at figures (a), (b), and (c) respectively.

(a)

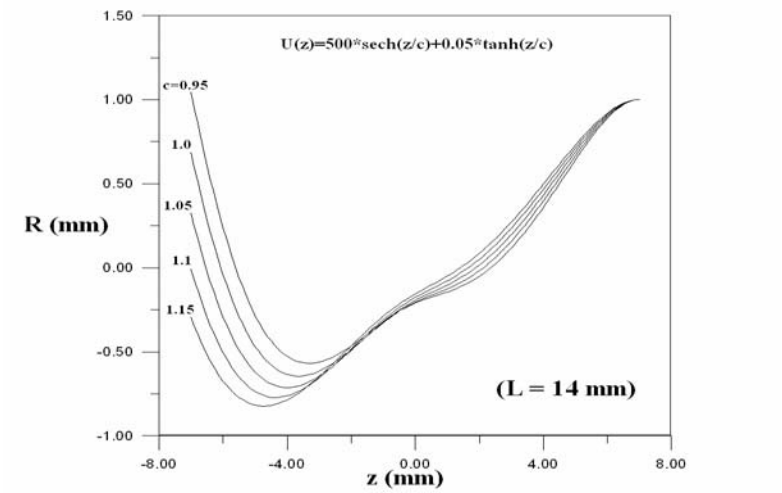

(b)

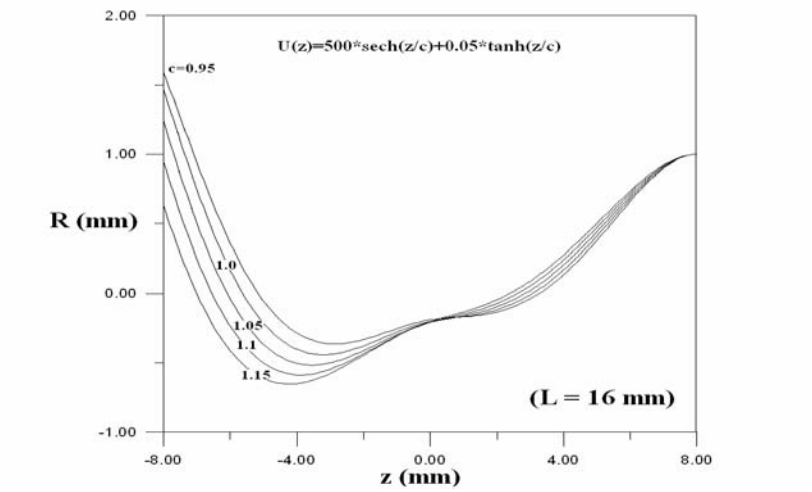

(c)

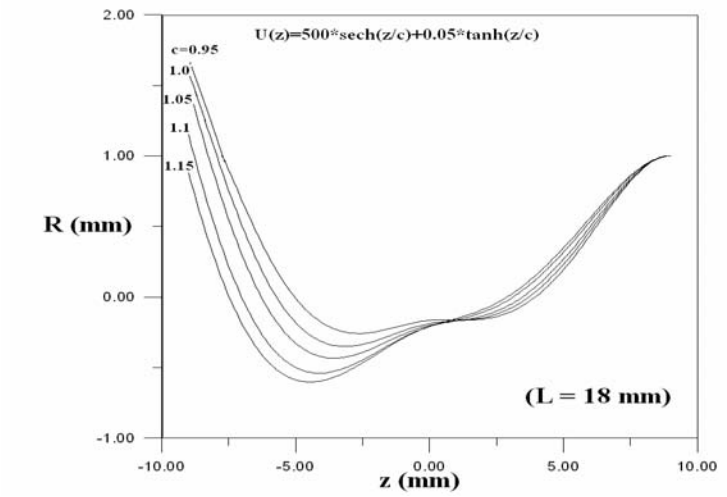

Figure (3.8) The ion beam trajectory in an electrostatic mirror under infinite magnification condition at various value of c (mm) when a=500 volt, b=0.05 volt, and mirror length L=14, 16, 18 mm at figures (a), (b), and (c) respectively.

From the figure (3.9) It is seen that the objective focal length f_o increases with increasing mirror length **L** at a constant **a** = 500, **b** = 0.01, and **c** = 1.05.

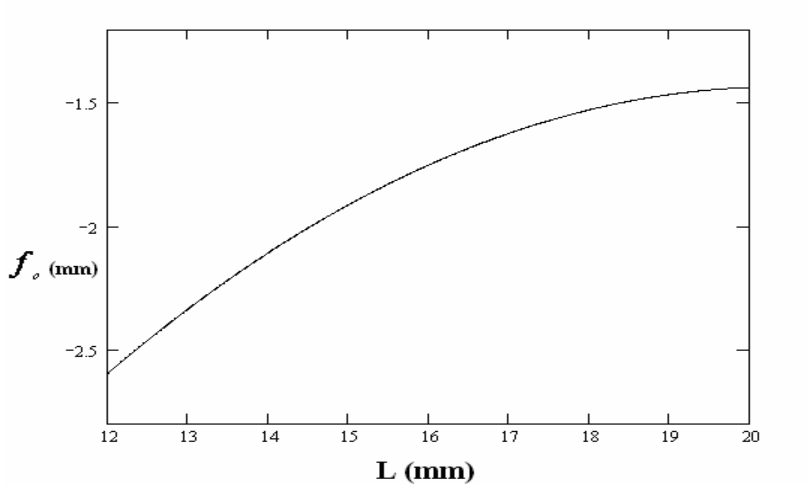

Figure(3.9) show the variation between values of mirror lengths L and the values of the object focal length f_o (mm) when a=500 volt , b=0.01 volt and c=1.05 mm.

By taking the values of **a** = 500 and **b** = 0.01 the increasing values of **c** causes to decreasing in the object focal length at the same mirror length **L** = 12 mm as shown in figure (3.10).

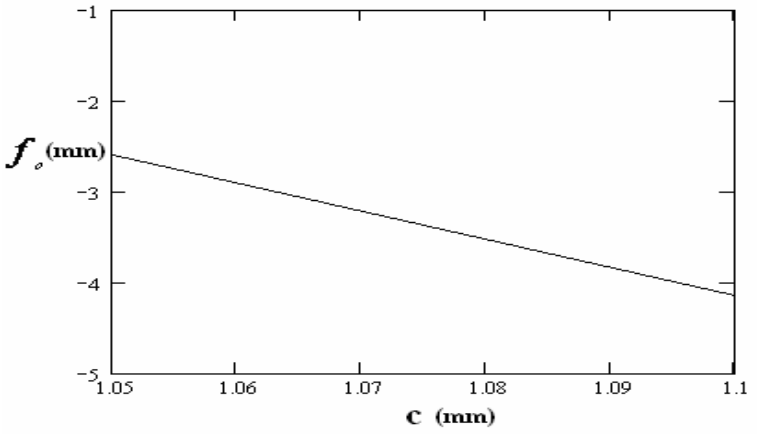

Figure(3.10) show the variation between the values of the object focal length f_o (mm) and values of c (mm) when a=500 volt , b=0.01 volt and L=12 mm.

The effect of the constant **b** at various values of the mirror length **L** = 12, 14, 16, 18, 20 mm on the beam trajectory has been investigated are shown in figure (3.11), and (3.12). When **a** = 500 and taking into account the most favorable values of **c** (i.e. 1.05 or 1.1) that have been deduced. Five values for the constant **b** have been taken into consideration **b** = 0.01, 0.02, 0.03, 0.04, 0.05 and **c** = 1.05, the trajectories shown in figure (3.11) have been studied thoroughly with regard to the aberrations where the most favorable value of the constant **b** will be determined. Figure (3.12) shows the ion beam trajectories at the values of **c** = 1.1.

(a)

b=0.01

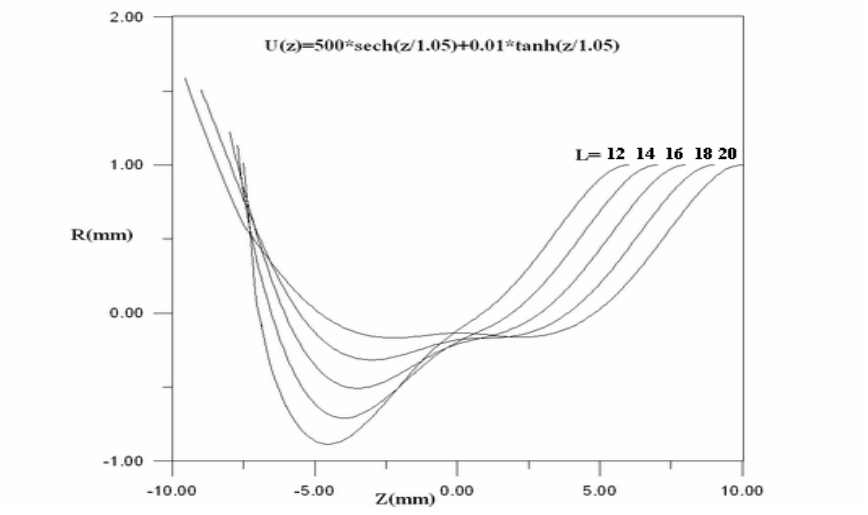

(b)

b=0.02

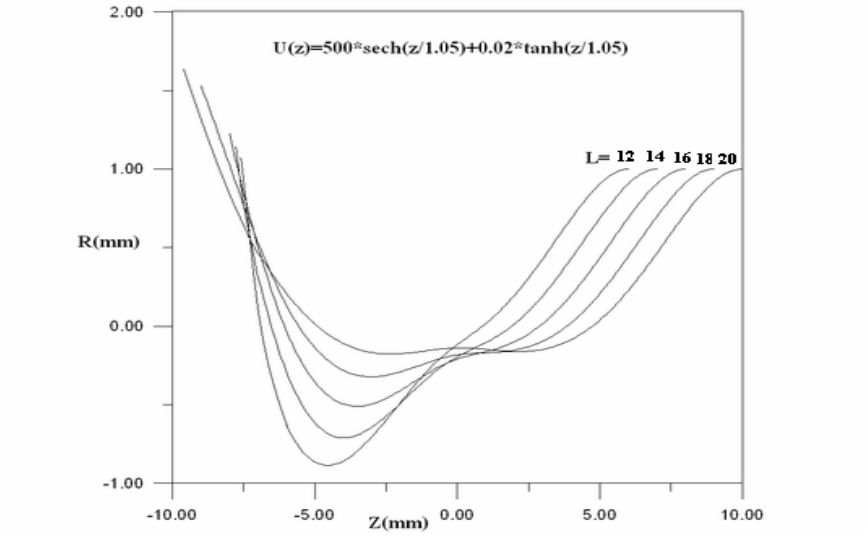

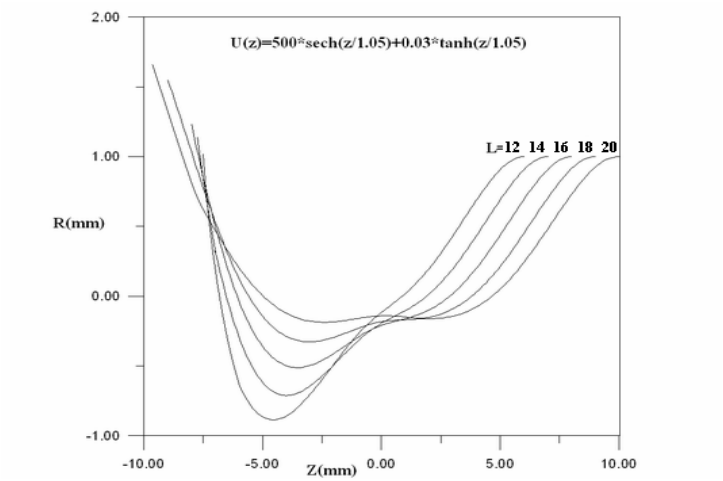

(c)
b=0.03

(d)
b=0.04

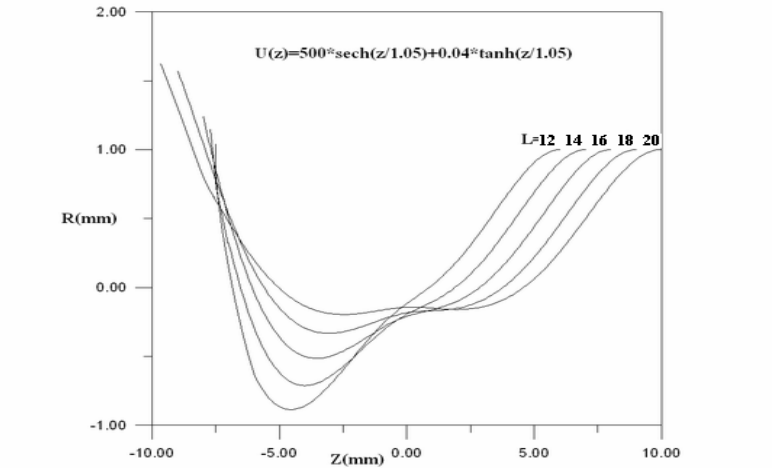

(e)
b=0.05

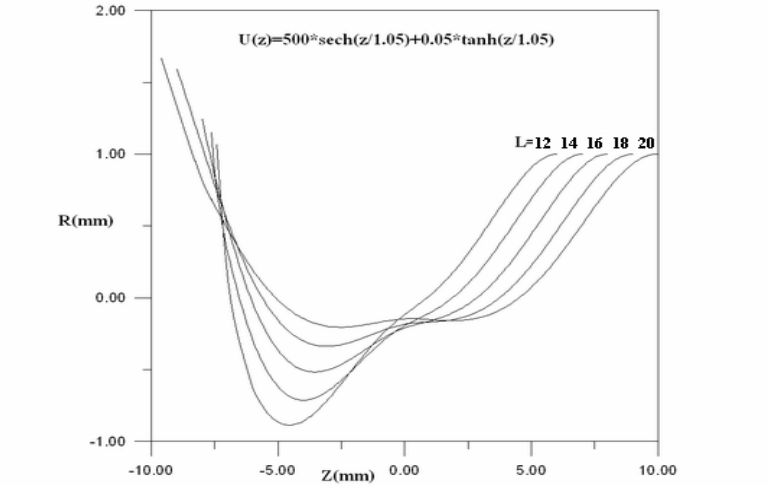

Figure (3.11) The ion beam trajectories in an electrostatic mirror under infinite magnification condition at various value of b (volt) when a=500 volt, c=1.05 mm, and mirror length L=12, 14, 16, 18, 20 mm.

(a)
b=0.01

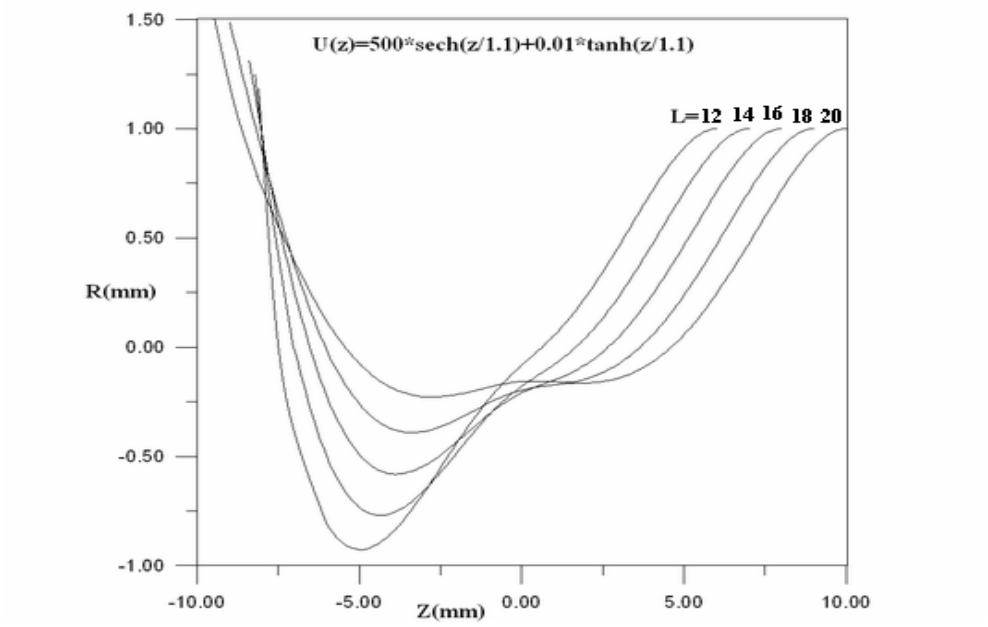

(b)
b=0.02

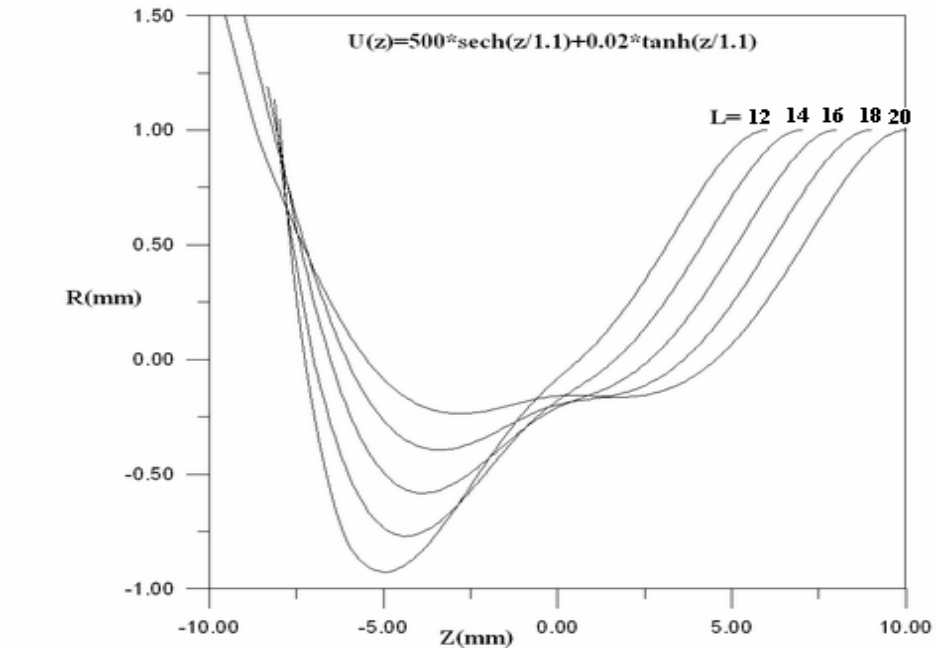

(c)
b=0.03

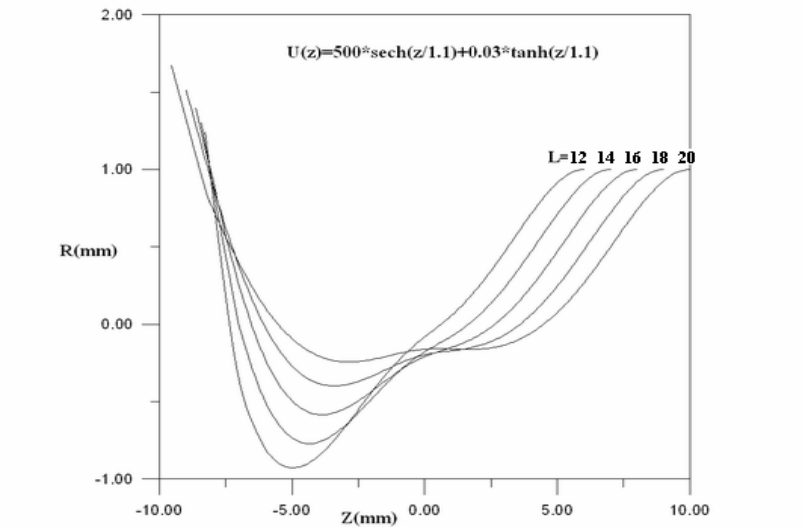

(d)
b=0.04

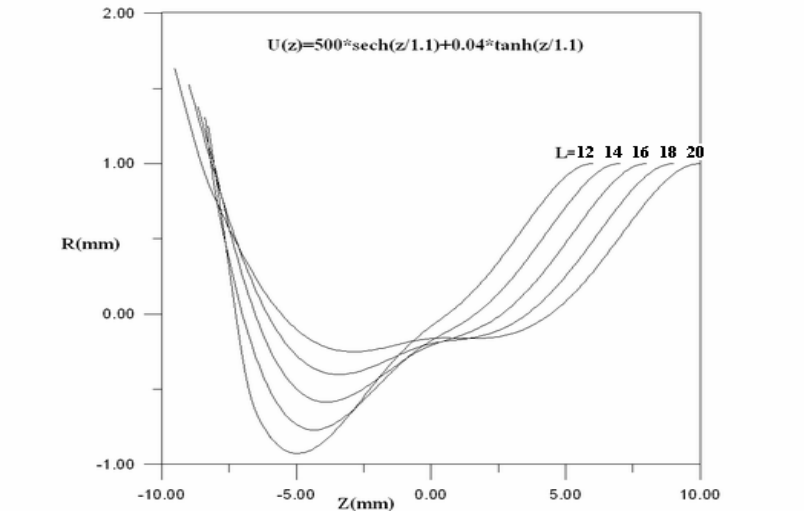

(e)
b=0.05

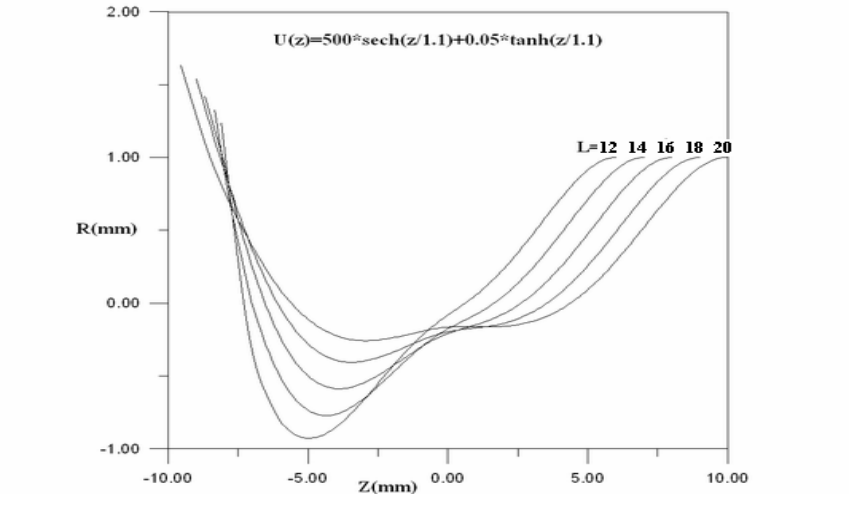

Figure (3.12) The ion beam trajectories in an electrostatic mirror under infinite magnification condition at various value of b (volt) when a=500 volt, c=1.1 mm, and mirror length L=12, 14, 16, 18, 20 mm.

3.1.3 Relative aberration coefficients of the infinite magnification electrostatic mirror

The spherical and chromatic aberration coefficients have been given a considerable attention in the present work since they are the two most important aberrations in the optical systems. The investigation has been focused at their effect on the object side, and has been normalized in terms of the object side focal length, i.e. the relative values of C_s / f_o and C_c / f_o are investigated as figures of merit which are dimensionless.

a. Relative spherical aberration coefficient

Figure (3.13) shows the relative spherical aberration coefficient C_s / f_o of the immersion electrostatic mirror as a function of the relative mirror length L / f_o and the figure (3.14) shows the relative spherical aberration coefficient C_s / f_o of electrostatic mirror as a function of the mirror lengths **L** = 12, 14, 16, 18, and 20 mm at a various values of constant **b** (keeping **a**=500 and **c**=1.05) under infinite magnification condition where the mirror action is achieved. The trajectories shown in figures (3.11) have been used for computing the aberration coefficients and objective focal length f_o at the values of **b** = 0.01, 0.02, 0.03, 0.04, and 0.05. It is seen that as L / f_o decreases, C_s / f_o increases irrespective of the values of **b**. It is seen that the values of C_s / f_o increases with increases the values of **b** with keeping **a** and **c**

constants at the same value of the mirror length, for example at **a** = 500, **c**=1.05, and mirror length **L** = 18 mm can be shown in table (3.1).

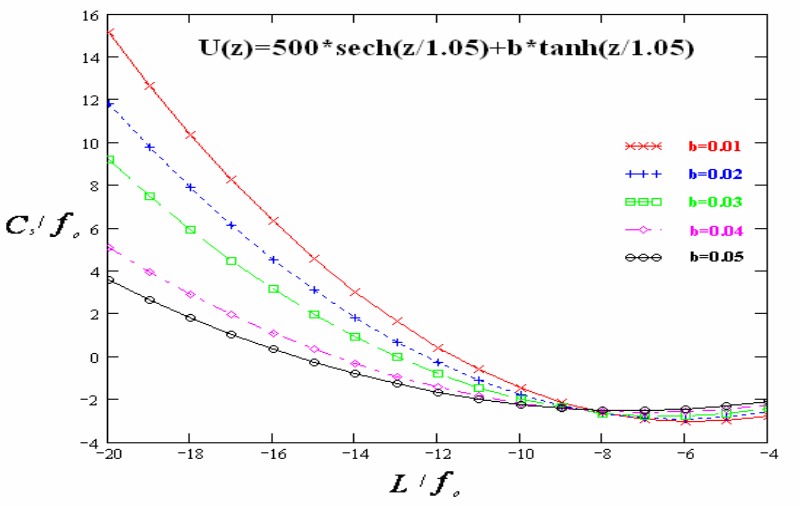

Figure (3.13) The relative spherical aberration coefficient C_s / f_o ***as a function of the relative mirror length*** L / f_o ***at various values of b (volt) keeping a=500 volt and c=1.05 mm.***

By taking different values of the mirror length **L** into account such as 12, 14, 16, 18, 20 mm the computations have shown that the relative spherical aberration C_s / f_o increases with increasing values of the mirror lengths with keeping **a** and **c** constants where in this case **a** = 500 and **c** = 1.05 in figure (3.11) .

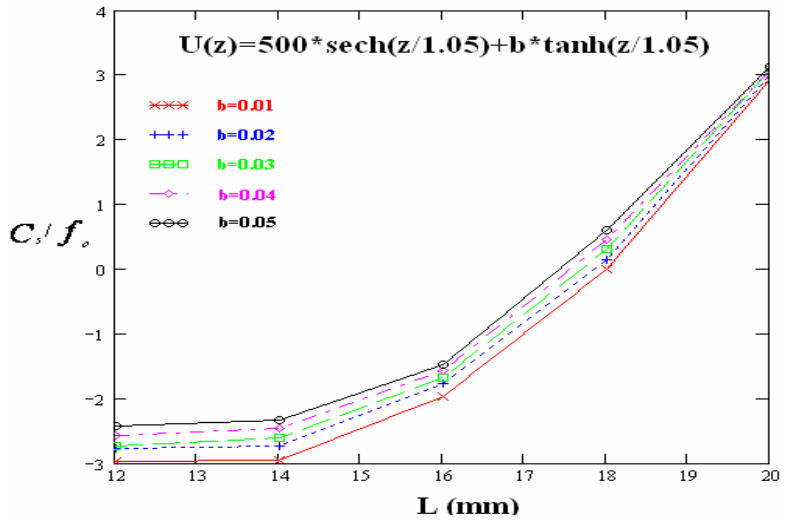

Figure (3.14) The relative spherical aberration coefficient C_s / f_o ***as a function of the mirror length L (mm) at various values of b (volt) with keeping a=500 volt and c=1.05 mm.***

Table (3.1) Shows the changeability values between the values of relative spherical aberration C_s / f_o and the values of b with keeping a=500 volt and c=1.05 mm and the mirror length L = 18 mm.

At a = 500 and c = 1.05	
b	C_s / f_o
0.01	-0.003
0.02	0.152
0.03	0.305
0.04	0.454
0.05	0.604

A similar investigation of C_s / f_o as a function of L / f_o and **L** have been carried out by giving **c** the other favorable value of 1.1, where The trajectories shown in figure (3.12) have been used for computing the aberration coefficients and the objective focal length f_o at the values of **b** = 0.01, 0.02, 0.03, 0.04, and 0.05. The results of $C_s / f_o, L / f_o$ and **L** are plotted in figures (3.15) and (3.16) respectively with keeping a constant value of **a** = 500.

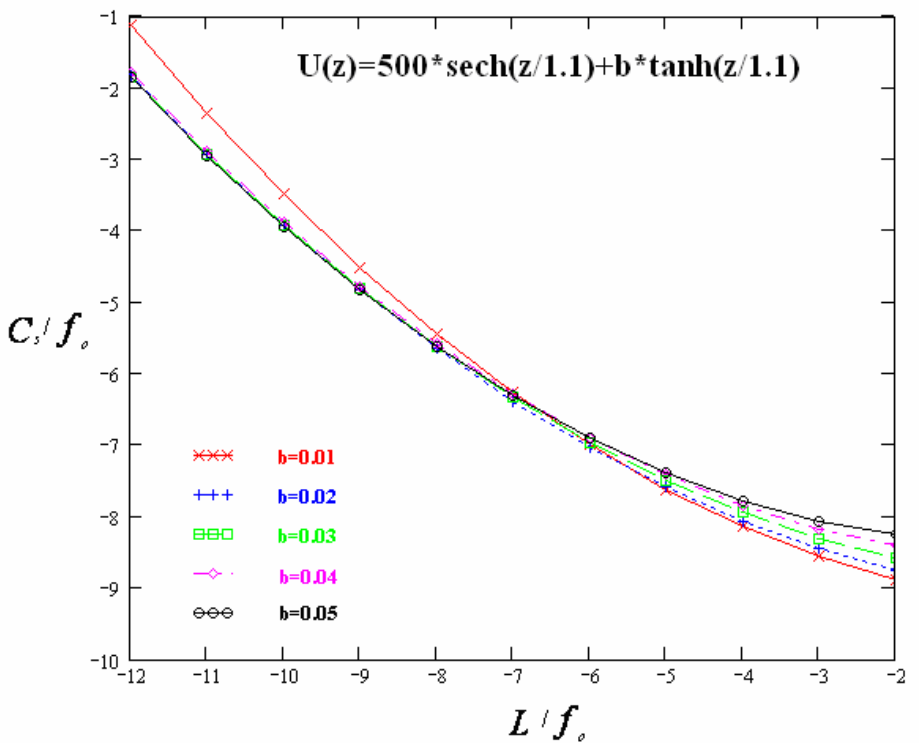

Figure (3.15) The relative spherical aberration coefficient C_s / f_o as a function of the relative mirror length L / f_o at various value of b (volt) with keeping a=500 volt and c=1.1 mm.

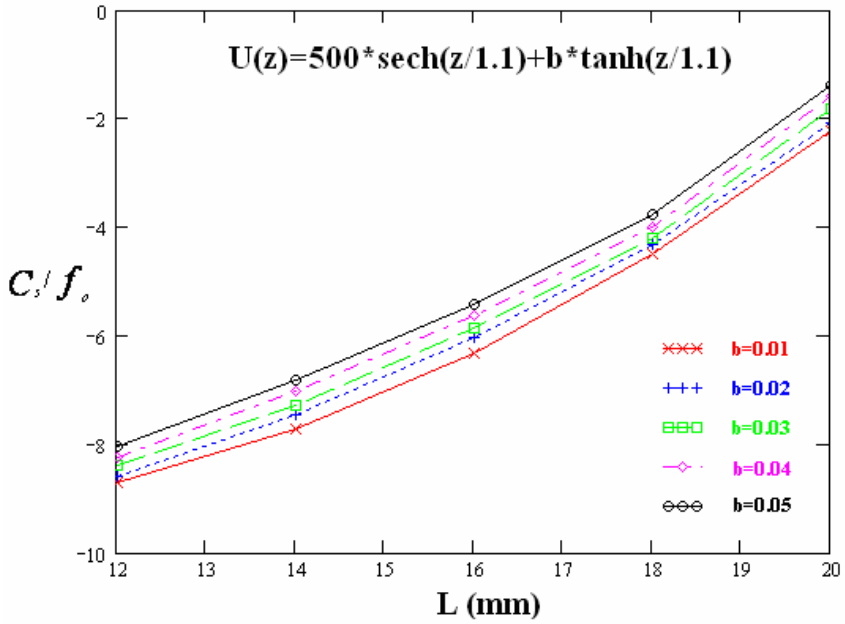

Figure (3.16) The relative spherical aberration coefficient C_s / f_o as a function of the mirror length L (mm) at various values of b (volt) with keeping a=500 volt and c=1.1 mm.

It is seen that the values of the relative spherical aberration C_s / f_o proportional inversely with **c** where as increasing the value of **c** causes the decreasing of C_s / f_o with remains **a** and **b** constant, for example at **a** = 500, **b**=0.01 and the mirror length **L** = 18 mm can be shown in table (3.2).

Table (3.2) Shows the changeability values between the values of relative spherical aberration C_s / f_o and the values of c with keeping a=500 and b=0.01 and the mirror length L = 18 mm.

At a=500 and b=0.01		
L (mm)	c	C_s / f_o
18	1.05	-0.003
	1.1	-4.5

One may deduce from figures (3.13), (3.14) that as far as the relative spherical aberration coefficient is concerned, the values of the constant should be as follows: **a** = 500, **b** = 0.01 and **c** = 1.05. Under theses conditions the highly favorable values of C_s / f_o that has been achieved in this work is -0.003 when L / f_o = -11.749. The value of f_o in this case is -1.532 mm; hence L is equal to 18 mm, an acceptable value from the practical point of view. Figures (3.17) show the behavior of spherical aberration in the present investigation it is relatively similar to the behavior of spherical aberration in the paper that published by **Shao and Wu (1990)**.

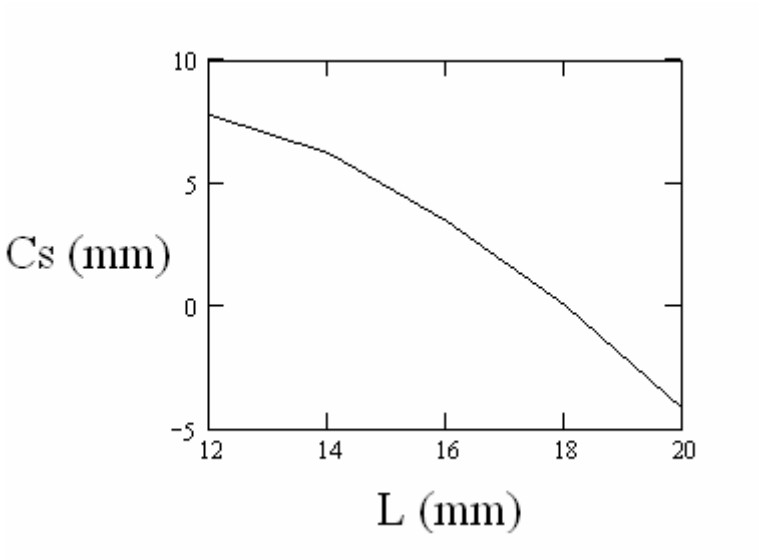

(*a) Spherical aberration coefficient as shown in present work*

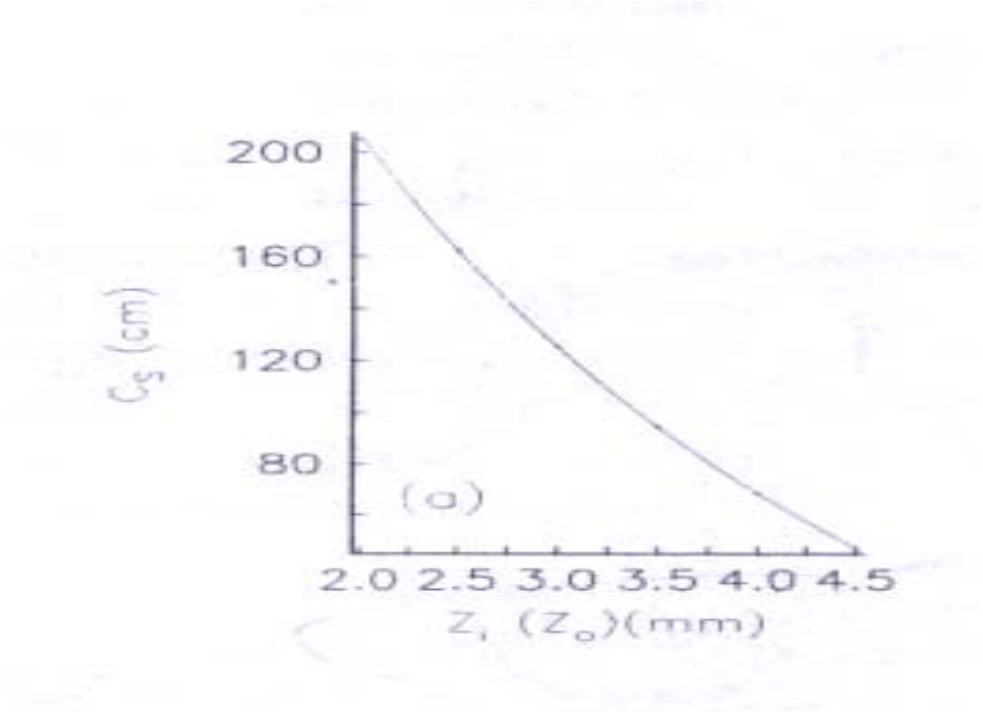

(b) Spherical aberration coefficient as shown in Shao and Wu (1990)

Figure(3.17) Show the behavior of the spherical aberration in (a) the present work and (b) the paper that published by Shao and Wu (1990) respectively.

b. Relative chromatic aberration coefficient

Figure (3.18) shows the variation of the relative chromatic aberration coefficients C_c / f_o as a function of the relative mirror length L / f_o and the figure (3.19) shows the variation of the relative chromatic aberration C_c / f_o with the mirror lengths **L** = 12, 14, 16, 18, and 20 mm at various values of **b** = 0.01, 0.02, 0.03, 0.04, and 0.05, keeping **a** and **c** constants at 500 and 1.05 respectively.

These parameters have been computed with the aid of trajectories plotted in figure (3.11). It is seen that as L / f_o decreases, C_c / f_o decreases irrespective of the values of **b**.

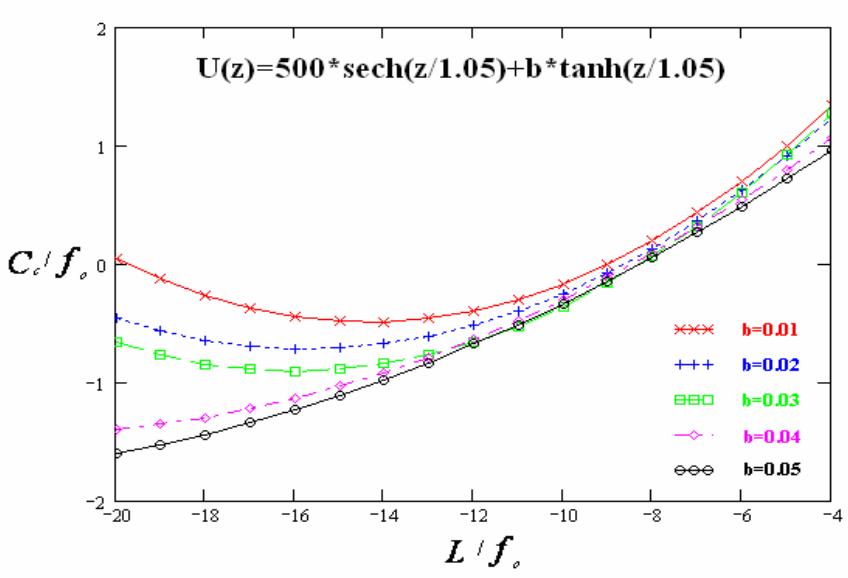

Figure (3.18) The relative chromatic aberration coefficient C_c / f_o as a function of the relative mirror length L / f_o at various values of b (volt) with keeping a=500 volt and c=1.05 mm.

By taking various values of the mirror length **L** into account such as 12, 14, 16, 18, 20 mm the computations have shown that the values of the relative chromatic aberration C_c / f_o decreases with increasing values of the mirror lengths keeping **a** and **c** constants where in this case **a** = 500 and **c** = 1.05 in figure (3.19).

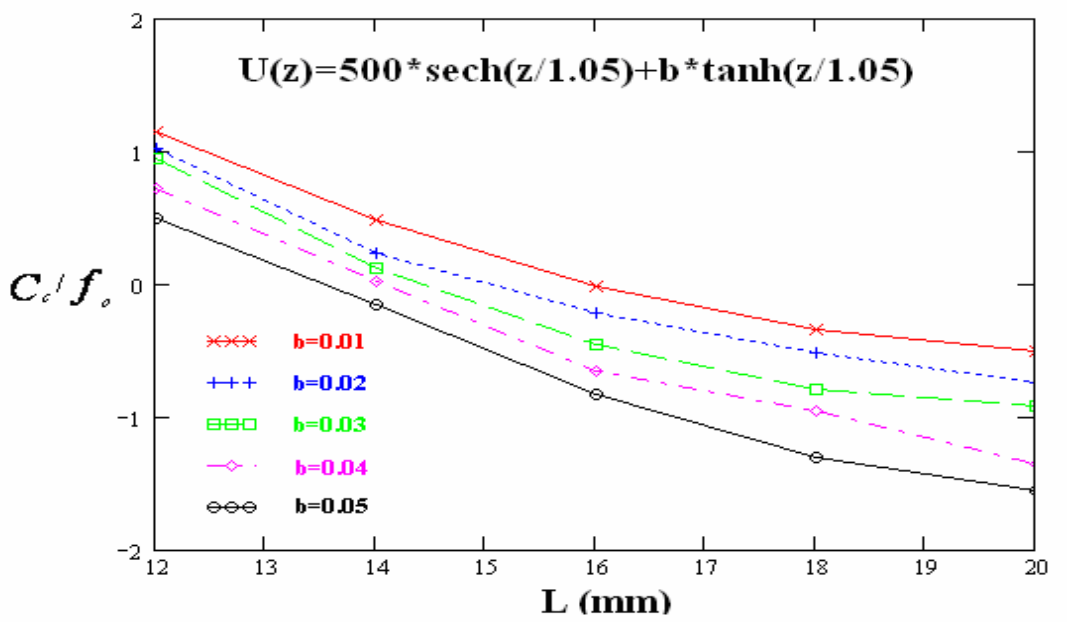

Figure (3.19) The relative chromatic aberration coefficient C_c / f_o as a function of the mirror length L (mm) at various values of b (volt) with keeping a=500 volt and c=1.05 mm.

It is seen that the values of C_c / f_o decreases with increases the values of **b** with keeping **a** and **c** constants at the same length of the mirror, for example at **a** = 500, **c** = 1.05, and mirror length **L** = 16 mm can be shown in table (3.3).

Table (3.3) Shows the changeability values between the values of relative chromatic aberration C_c / f_o and the values of b with keeping a=500 volt, c=1.05 mm, and the mirror length L = 16 mm.

At a = 500 and c = 1.05	
b	C_c / f_o
0.01	0.01
0.02	-0.15
0.03	-0.35
0.04	-0.78
0.05	-0.88

By taking **c** = 1.1, the computation of C_c / f_o as a function of L / f_o and **L** have been repeated and shown in figure (3.20), and (3.21) respectively at **a** = 500 and **b** = 0.01, 0.02, 0.03, 0.04, and 0.05, and **c** = 1.1 where the trajectories shown in figure (3.12) have been used for computing the aberration coefficients and the objective focal length f_o.

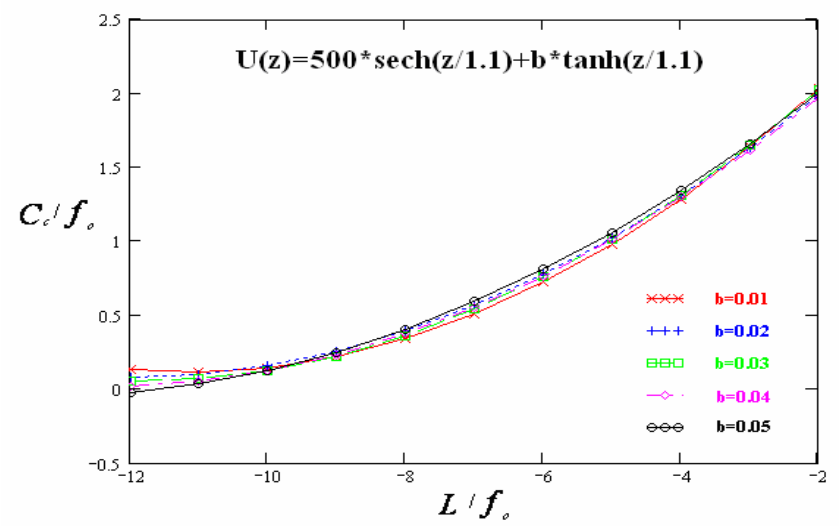

Figure (3.20) The relative chromatic aberration coefficient C_c / f_o as a function of the relative mirror length L / f_o at various values of b (volt) with keeping a=500 volt and c=1.1 mm.

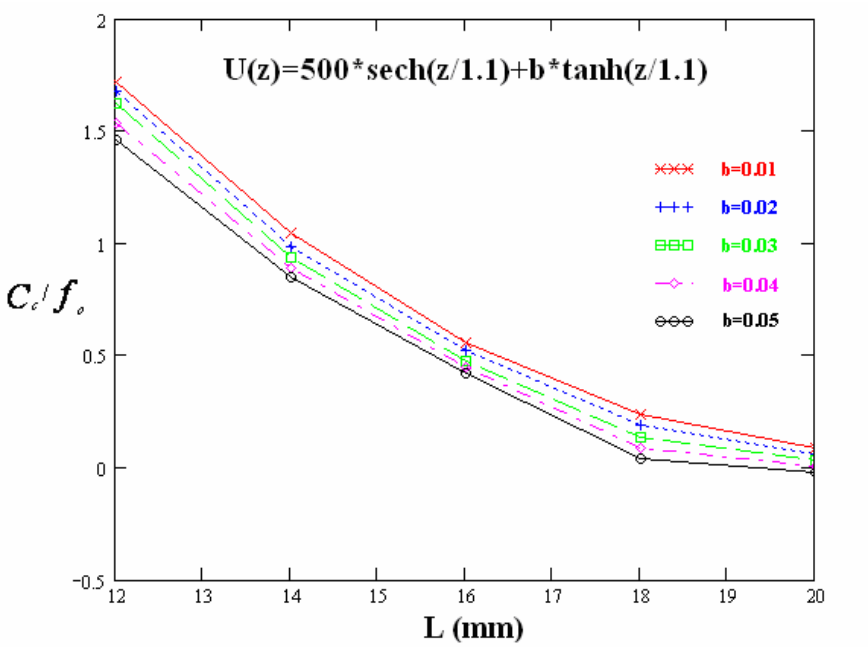

Figure (3.21) The relative chromatic aberration coefficient C_c / f_o as a function of the mirror length L (mm) at various values of b (volt) with keeping a=500 volt and c=1.1 mm.

It is seen that the relative values of the chromatic aberration coefficients C_c / f_o directly proportional with **c** where the increasing of **c** causes to increasing the values of C_c / f_o with remains **a** and **b** constant , for example at **a** = 500, **b** = 0.01 and the mirror length **L** = 16 mm can be shown in table (3.4).

Table (3.4) Shows the changeability values between the values of relative chromatic aberration C_c / f_o and the values of c (mm) with keeping a=500 volt and b=0.01 volt and the mirror length L = 16 mm.

At a=500 and b=0.01		
L (mm)	c	C_c / f_o
16	1.05	-0.02
	1.1	0.554

One may deduce from figures (3.18), and (3.19) that as far as the relative chromatic aberration coefficient is concerned, the values of the constant should be as follows: **a** = 500, **b** = 0.05 and **c** = 1.05. Under theses conditions the highly favorable values of C_c / f_o is -0.0017 when L / f_o = -10.256. The value of f_o in this case is -1.56 mm; hence L is equal to 16 mm, an acceptable value from the practical point of view. Figure (3.22) shown the behavior of chromatic aberration in the present investigation it is relatively similar to the behavior of chromatic aberration in the paper published by **Shao and Wu (1990)**.

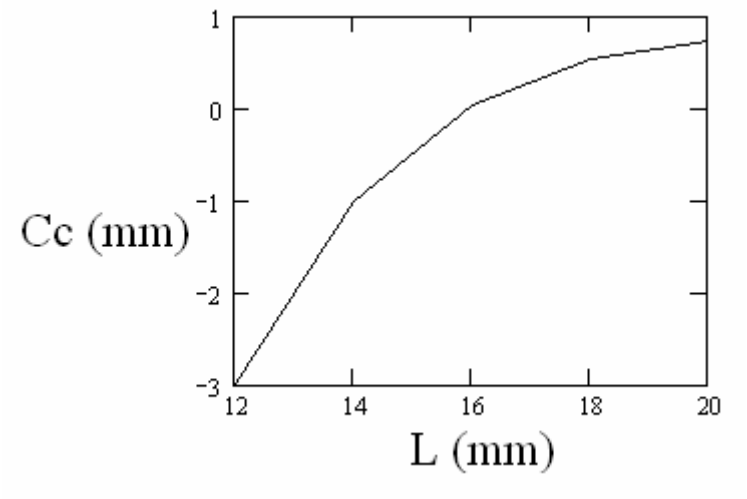

(a) Chromatic aberration coefficient as shown in present work

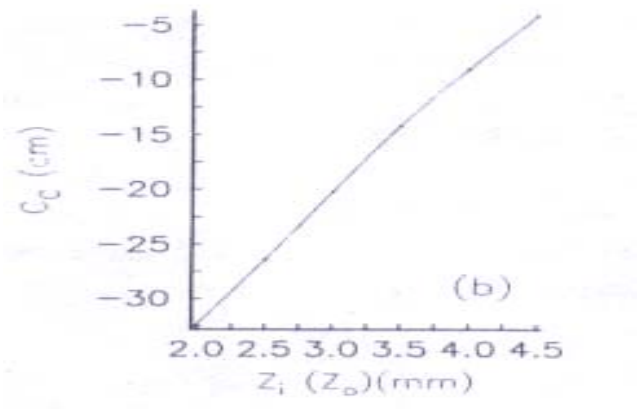

(b) Chromatic aberration coefficient as shown in Shao and Wu (1990)

Figure(3.22) Show the behavior of the chromatic aberration in (a) the present work and (b) the paper that published by Shao and Wu (1990) respectively.

c. Comparison between the relative spherical and chromatic aberration coefficients

It is important to make a systematic comparison between the two relative aberration coefficients under infinite magnification conditions. The above computations achieved the most favorable values of the constants **a**, **b**, and **c** with regard to the relative aberration coefficients. By taking the constants **a** and **c** the values 500 and 1.05 respectively, the relative spherical and chromatic aberration coefficients C_s / f_o and C_c / f_o have been plotted in figure (3.23) as a function of mirror length L at five different values of **b**. It is seen that C_s / f_o increases as C_c / f_o decreases with increasing **L**.

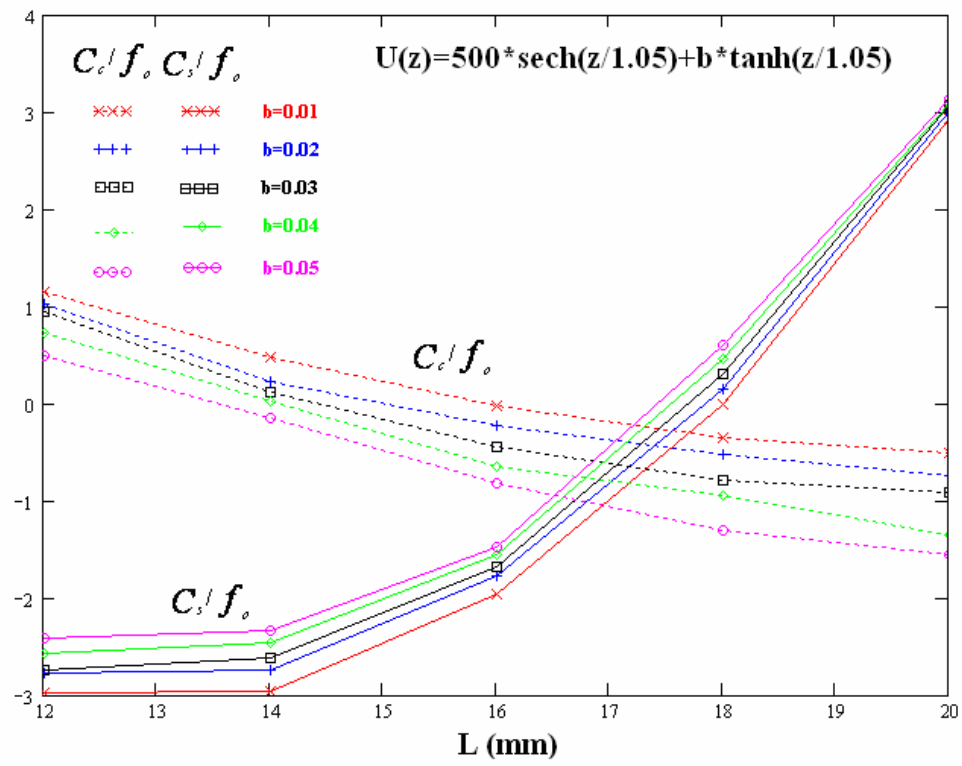

Figure (3.23) The object-side relative spherical and chromatic aberration coefficients C_s/f_o and C_c/f_o respectively as a function of the mirror length L (mm) for an electrostatic mirror under infinite magnification conditions at various values of b (volt) with keeping a=500 volt, c=1.05 mm.

The plots in figure (3.23) suggested that when 18 > **L** > 16 mm, C_s/f_o and C_c/f_o having the same values approximately between -0.26 and -1.0 when the constant **b** = 0.01, and 0.05 respectively. An investigation similar to the above has been carried out when **c** = 1.1. Plots of C_s/f_o and C_c/f_o as a function of mirror length **L** are shown in figure (3.24) at a various values of **b**.

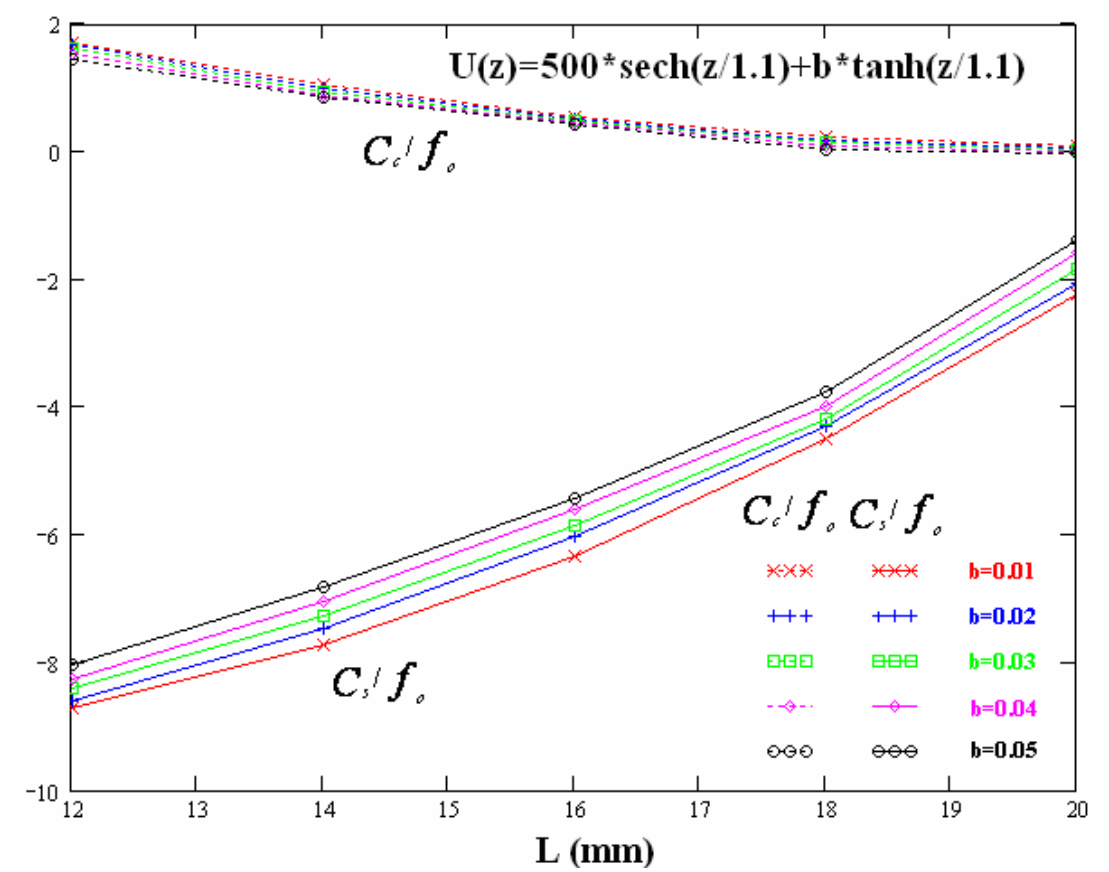

Figure (3.24) The object-side relative spherical and chromatic aberration coefficients C_s/f_o and C_c/f_o respectively as a function of the mirror length L (mm) for an electrostatic mirror under infinite magnification conditions at various values of b (volt) with keeping a=500 volt, c=1.1 mm.

It is seen that the increases values of **c** cause to decreases values of the C_s / f_o and increases values of C_c / f_o much more than when the value of **c** = 1.05 but the intersection region between C_s / f_o and C_c / f_o not found when **c** = 1.1 because its may be need to more mirror lengths greater than the mirror lengths that can be used in this project. One can get the optical properties when the mirror length 18 > **L** > 16 where its only at **c** = 1.05 we can get at the best and the same values of C_s / f_o and C_c / f_o ;therefore, the choice of the mirror depends on the operational requirements, where best value of C_s / f_o = -0.26 is achieved if **a** = 500, **b** = 0.01, **c** = 1.05 and **L** ≈ 17.8 mm, and best value of C_c / f_o = -0.26 is found when **a** = 500, **b** = 0.01, **c** = 1.05 and **L** ≈ 17.8 mm. A general comparison is made concerning the variation of C_s / f_o and C_c / f_o with L / f_o at various values of **b** with keeping **a** = 500 and **c** = 1.05 can be shown in figure (3.25).

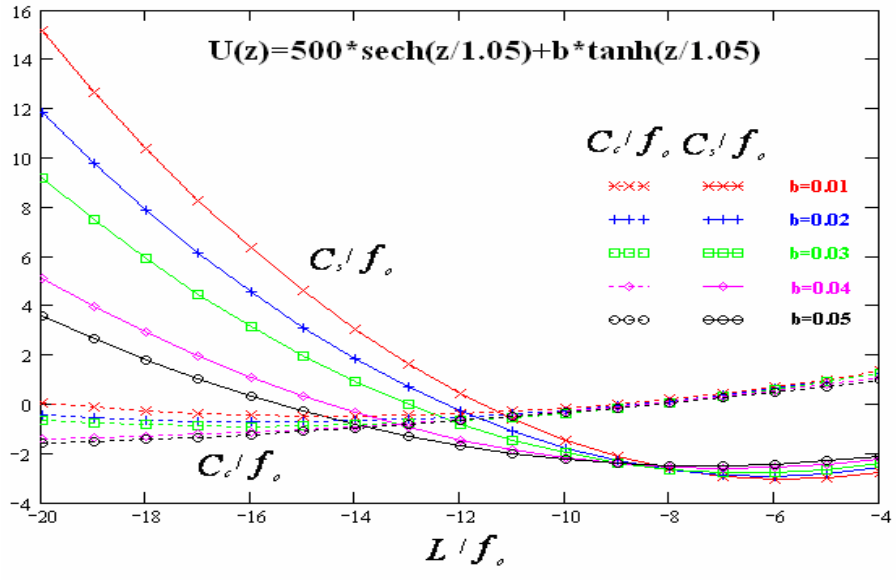

Figure (3.25) The object-side relative spherical and chromatic aberration coefficients C_s / f_o ***and*** C_c / f_o ***respectively as a function of the relative mirror length*** L / f_o ***for an electrostatic mirror under infinite magnification conditions at various values of b (volt) keeping a=500 volt, c=1.05 mm.***

It is seen from this figure that the relative spherical aberration C_s / f_o increases with decreases values of the relative focal length L / f_o and the relative chromatic aberration C_c / f_o decreasing with decreases values of the object focal length L / f_o. The best value of C_s / f_o and C_c / f_o is locate in the region when the relative object focal length -10.5 > L / f_o >-14 where the values of $C_s / f_o = C_c / f_o$ = -0.003 at **a** = 500, **b** = 0.01 and **c** = 1.05 and when **b** = 0.05 with keeping **a** = 500 and **c** = 1.05 at the intersection points of C_s / f_o and C_c / f_o is decreases where $C_s / f_o = C_c / f_o$ = -1.05. By taking **c** = 1.1 with keeping **a** = 500 at various value of **b** = 0.01, 0.02, 0.03, 0.04, and 0.05 the comparison between the variation between C_s / f_o and C_c / f_o with L / f_o can be shown in figure (3.26).

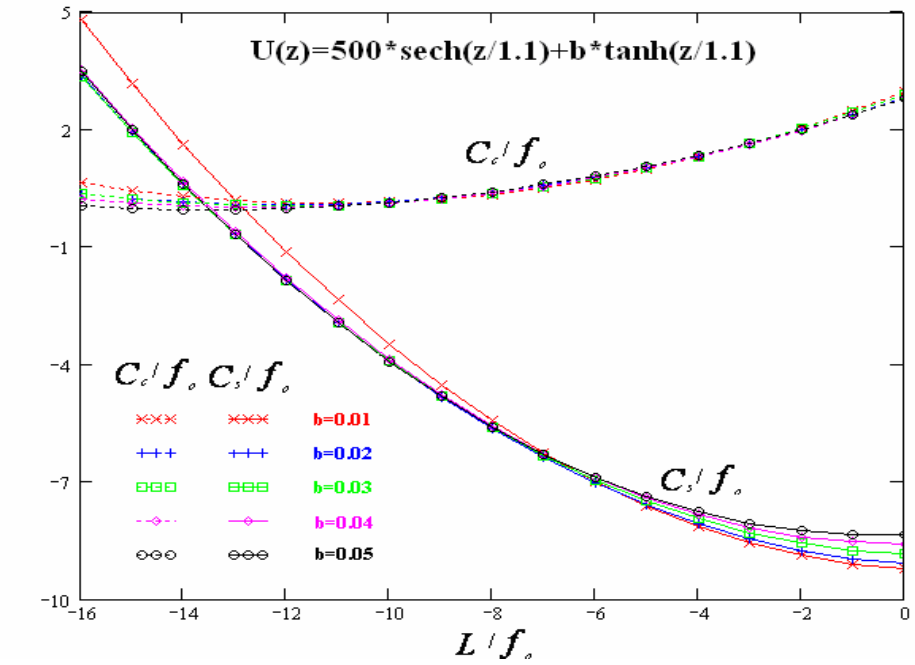

Figure (3.26) The object-side relative spherical and chromatic aberration coefficients C_s / f_o ***and*** C_c / f_o ***respectively as a function of the relative mirror length*** L / f_o ***for an electrostatic mirror under infinite magnification conditions at various values of b (volt) keeping a=500 volt, c=1.1 mm.***

The increasing value of **c** causes to get at a narrow intersecting region between C_s / f_o and C_c / f_o as a function of L / f_o comparing with the intersecting region when c = 1.05 where the intersecting region at c = 1.1 is -12.5 > L / f_o >-13, furthermore, the increasing value of **c** causes to decreases of C_s / f_o much more than when **c** = 1.05 and increase C_c / f_o more than when **c** = 1.05. Thus under these condition the most favorable mirror is deduced having the following parameters: **a** = 500, **b** = 0.01, **c** = 1.05, f_o =-1.618 mm, **L** = 17.8 mm , C_s = 0.42 mm and C_c = 0.42 mm. this mirror is the most favorable one as far as the spherical and chromatic aberrations are concerned, in the present work must be note that the results of spherical and chromatic aberration are nearly similar to the values that published by **[Shao and Wu 1990]**.

3.1.4 Mirror electrodes shape

The shape of the electrodes of the mirror that this properties are found before have been determined with aid of equation (2-8). The computer program that has been used for determining the electrodes shape is described in detail by Ahmad (1993). The parameters of the mirror are as follows:

a = 500, **b** = 0.01, and **c** = 1.05 where *U*(z) = 500 volt at **z** = 0 (figure 3.1), C_s = 0.42 mm, C_c = 0.42 mm, and f_o =-1.618 mm. the mirror's operational condition is done for infinite magnification condition. Figure (3.27) show the profile of the mirror electrodes. This mirror has three electrodes since the second derivatives of its potential *U*(z) have two inflection points **[Szilagyi 1988]**. The three electrodes have rotational symmetry about the optical axis. Each electrode has a central hole to allow passage for the ion beam. The two outer electrodes are geometrically identical having a shape of a hat, where the electrode at the left hand side have relative inner radius **R/L** = 0.18 at **z/L** = -0.073; the relative outer radius of this electrode is **R/L** = 0.023 at **z/L** = -0.483. The electrode at the right hand side have relative inner radius **R/L** = 0.18 at **z/L** = 0.073; the relative outer radius of this electrode is **R/L** = 0.026 at **z/L** = 0.5. The middle electrode have inner radius **R/L** = 0.001 at **z/L** = 0; the relative outer radius at both side of this electrode **R/L** = 0.396 at **z/L** = -0.051 and **z/L** = 0.051. The three electrodes are separated by two air gap of relative length **z/L** = 0.022.

Since the favorable value of **L** for this mirror is found to be 17.8 mm, hence the parameters of the three electrodes will be as follows:

1) the electrode at the right hand side of the figure (3.27) has entrance for the ion beam of radius **R** = 0.409 mm at **z** = -8.9 mm. the beam emerges from this electrode at the region where **z** = -1.299 mm and the electrode's radius = 3.204 mm.

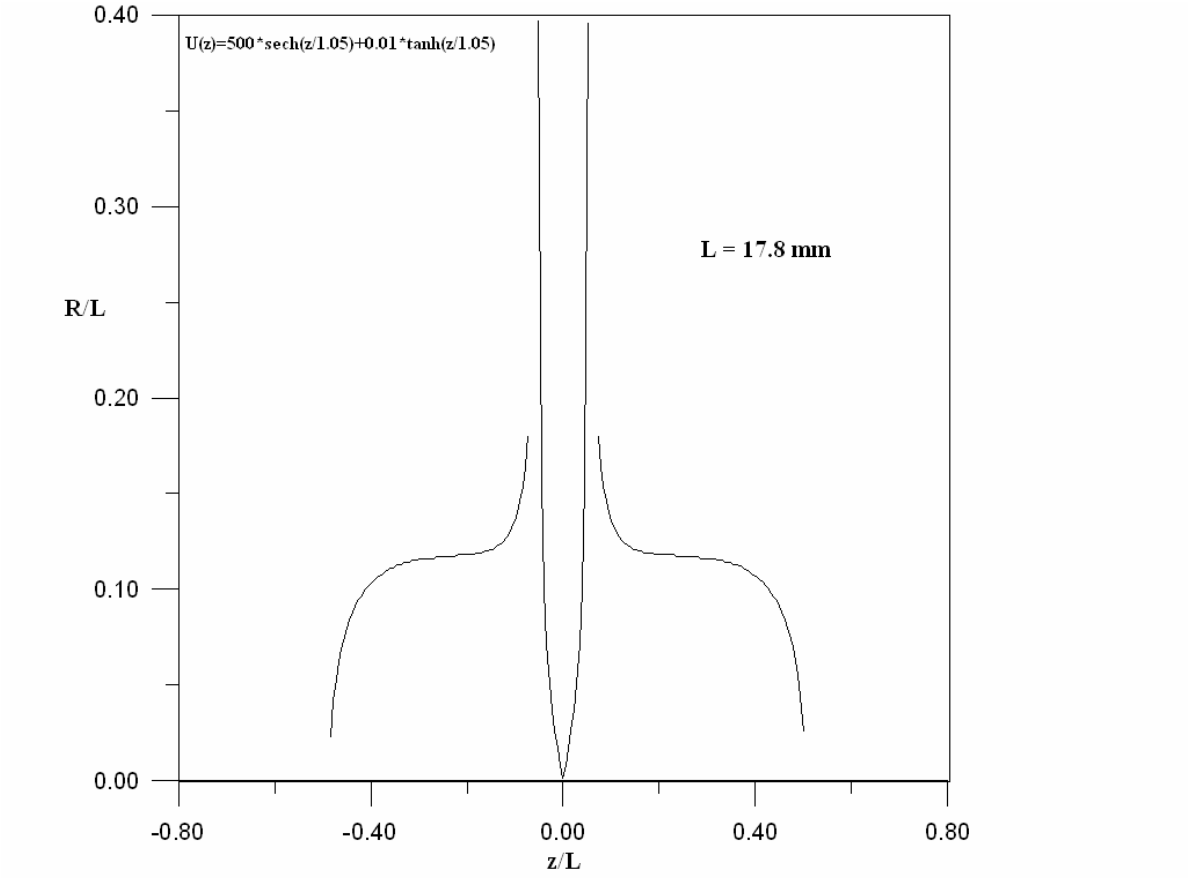

Figure (3.27) the electrodes profile of the three electrode electrostatic mirror under infinite magnification condition when the constant a = 500 volt, b = 0.01 volt, and c = 1.05 mm.

2) The middle electrode of figure (3.27) has an entrance radius **R** = 0.0178 mm at **z** = 0 mm and have both outer radius have the same value where **R** = 7.04 mm at both **z** values where **z** = -0.907 and 0.907 mm.

3) The electrode at the left hand side similar the electrode at the right hand side where its found that the entrance value of the outer radius of the left hand side electrode have **R** = 3.204 mm at **z** = 1.299 mm and the ion beam emerges from this electrode at the region where **z** = 8.9 mm and the electrode radius **R** = 0.462 mm. The two air gap separating the three electrodes is 0.3916 mm.

The trajectory of this mirror type when the specimen is positioned at the vicinity of the turning point of the beam thus the specimen material should be of the kind that would not distort the mirror's field.

3.2 Design an Electrostatic Mirror by using "Bimurzaev technique"

3.2.1 Suggested potential model

The principle of the Bimurzaeav technique is depend on using two boundary conditions the first one representing the incident beam on the mirror before reflecting and the second condition representing the reflecting beam from the mirror, and the second condition is very important because the optical properties computed from this part. The suggested potential model given in the present work is given by equation (3-2) representing an electrostatic mirror has been modified to achieve a mirror with accelerating mode.

$$U(z) = a * \tanh\left(\frac{z}{c}\right) + b * \cosh\left(\frac{z}{c}\right) \qquad \textbf{(3-2)}$$

Where U (z) is the axial potential along the optical axis **z**. The constants **a**, **b**, and **c** are affecting the properties of this suggested potential and have been given the following values: **a** = 150, 160, 170, 180, 190; **b** = 13, 14, 15 but the mirrors lengths controlled by using a specific values of the constant **c**. The values of **c** for each mirror length can be shown in the following table:

Table (3.5) Shows the values of c (mm) for each values of mirror lengths.

c	Mirror length (mm)
1.1	6
1.5	8
1.9	10
2.3	12
2.7	14

The effect of these constants on *U*(z) has been investigated independently. The units of the constants **a**, **b**, and **c** are such that the net result of the right-hand side of equation (3-2) has the unit of volt. The choice of the function given in equation (3-2) is justified by the results that will be discussed later. Figure (3.28) show the favorable axial potential distribution *U*(z) and its corresponding first and second derivatives. The values of the constants **a**, **b**, and **c** have the values of 150, 15, 2.7 respectively where the **c** value is linked with the length of mirror as shown in the upper table (3.5) where when **c** is 2.7 the length of mirror is 14 mm. from the figure (3.28) also one can notes that there is only one inflection point in the second derivative of the potential distribution, i.e. we have a two electrode mirror.

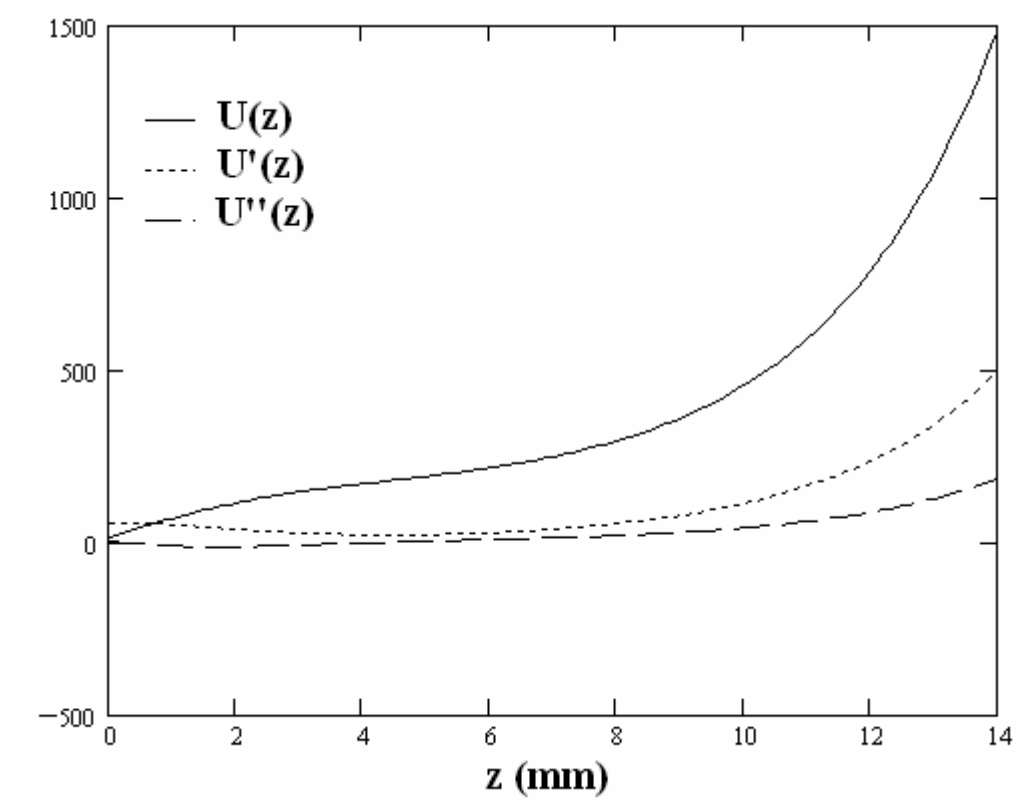

Figure(3.28) The axial potential distribution U(z) and its first and second derivatives U'(z) and U''(z) respectively of the electrostatic mirror when a = 150 volt, b = 15 volt, c= 2.7 mm, and mirror length L= 14 mm.

When the length of the mirror is 14 mm the potential *U*(z) has a maximum value of 1.49×10^3 volt at **z** = 14 mm. The constants in equation (3-2) have no effect on the number of inflection points in second derivative of the potential distribution *U''*(z); By taking various values of the mirror length **L** into account such as 6, 8, 10, 12, 14 mm; the effect of each of the constants **a**, **b** have been investigated independently. For example, the effect of various values of **b** on the potential distribution at specific length of mirror **L** = 14 mm, where **c** = 2.7 and **a** = 150, is shown in figure (3.29):

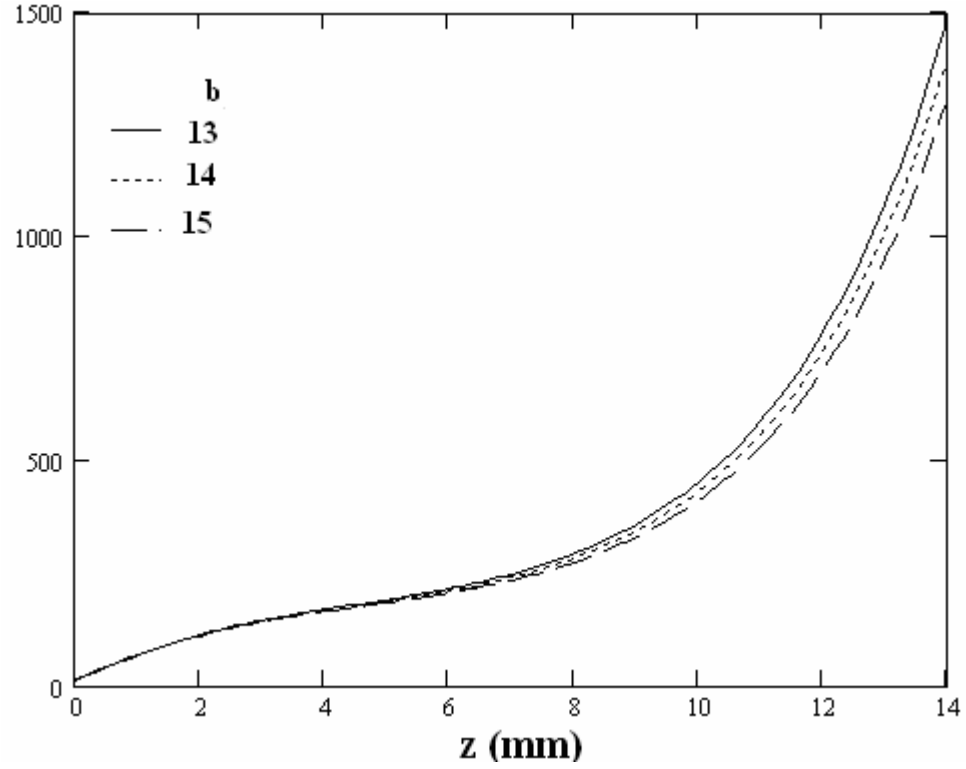

Figure(3.29) The relation between various values of b (volt) and potential distribution at
a = 150 volt, c= 2.7 mm, and mirror length L= 14 mm.

From this figure it is noted that the increasing value of **b** lead to a higher value of the potential distribution *U*(z). One would expect such result since at **z** = 0, *U*(z) = **b**; hence *U*(z) increases with increasing **b**. The effect of varying the constant a on the potential *U*(z) when keeping **b** and **c** constant is found to be insignificant, hence the effect of the constant **b** will be investigated under constant value of **a**.

3.2.2 Ion beam trajectory under Bimurzaev technique

The ion beam path along the electrostatic mirror field using Bimurzaev technique under the accelerating mode of operation has been considered. Examples for trajectories of the electrostatic mirror along various lengths **L** = 6, 8, 10, 12 and 14 of the mirror are given in figures (3.30), (3.31), (3.32), (3.33), and (3.34).

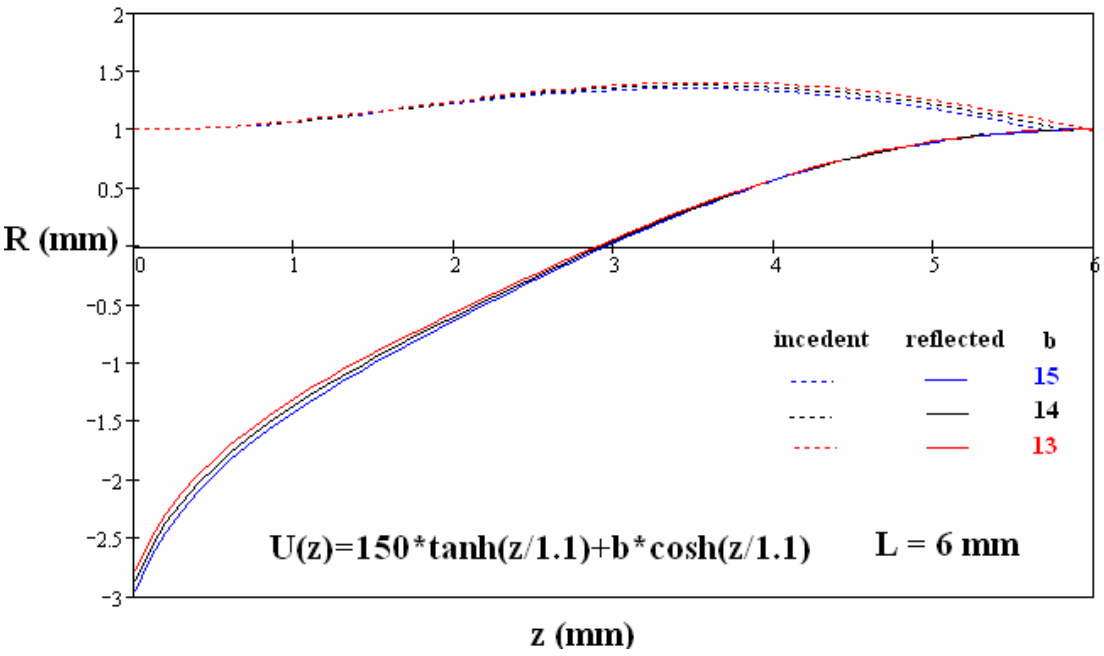

Figure (3.30) The ion beam trajectory for the electrostatic mirror under various value of b (volt) when a=150 volt, c=1.1 mm, and mirror length L=6 mm.

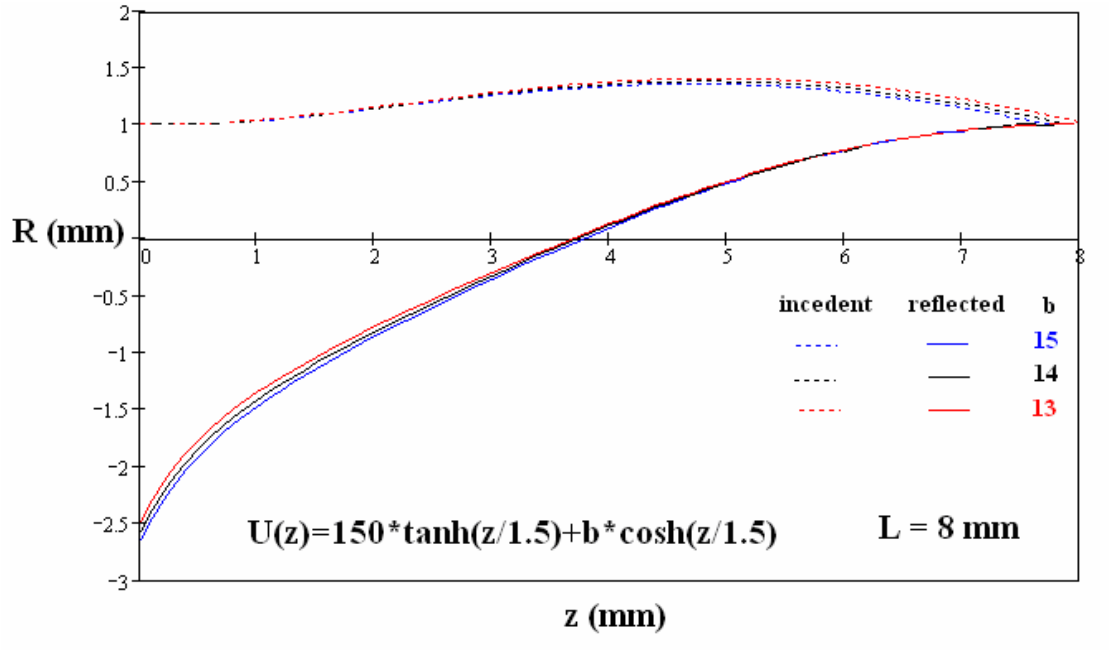

Figure (3.31) The ion beam trajectory for the electrostatic mirror under various value of b (volt) when a=150 volt, c=1.5 mm, and mirror length L=8 mm.

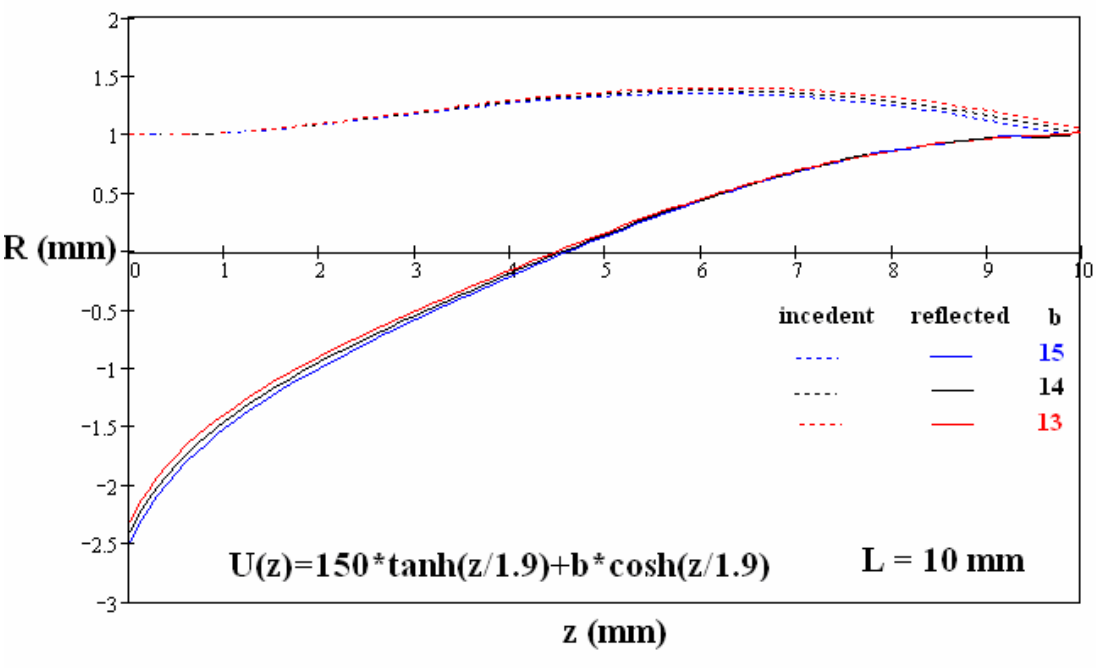

Figure (3.32) The ion beam trajectory for the electrostatic mirror under various value of b (volt) when a=150 volt, c=1.9 mm, and mirror length L=10 mm.

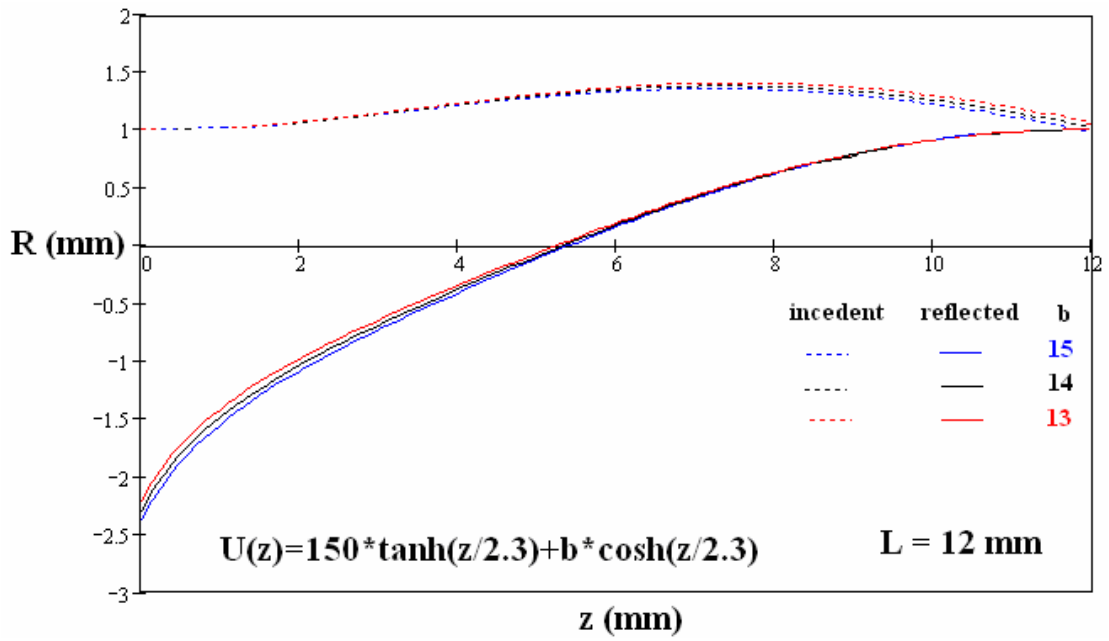

Figure (3.33) The ion beam trajectory for the electrostatic mirror under various value of b (volt) when a=150 volt, c=2.3 mm, and mirror length L=12 mm.

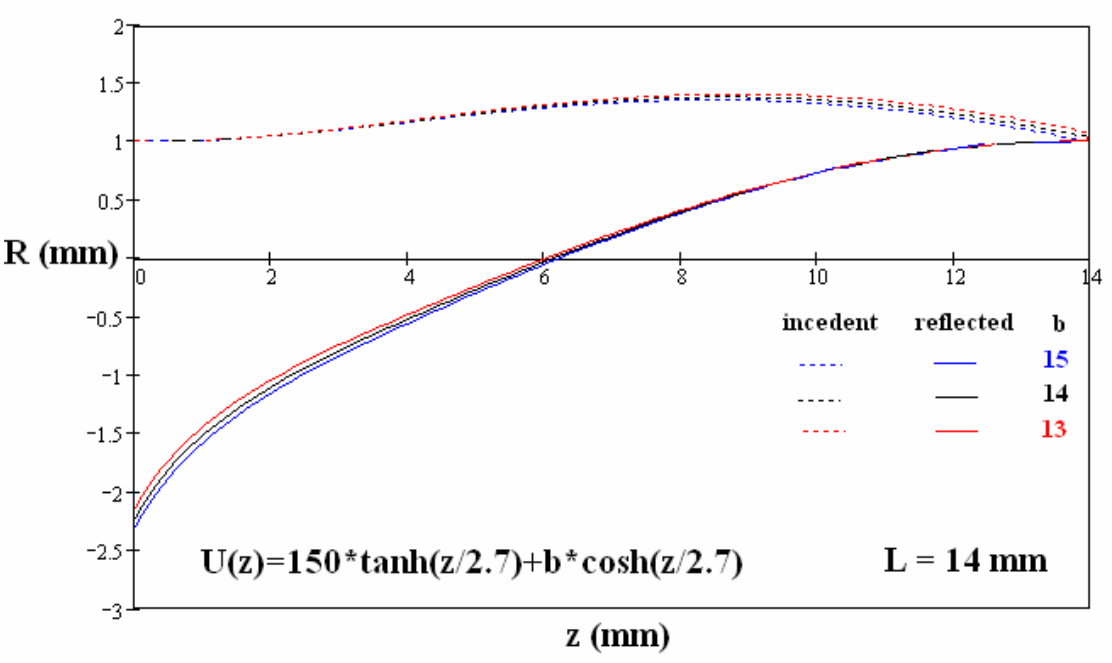

Figure (3.34) The ion beam trajectory for the electrostatic mirror under various value of b (volt) when a=150 volt, c=2.7 mm, and mirror length L=14 mm.

From the above figures (3.30), (3.31), (3.32), (3.33), and (3.34) it is noted that the electrostatic mirror focal length f_R is directly proportional with **b** for all mirror length with **a** = 150, also increases the radial displacement of the reflecting trajectory. The mirror focal length can be determine from the reflect ion beam trajectory where the focal length of the reflect ion beam trajectory represent the mirror focal length f_R, from the result it is noted that the mirror focal length has a positive sign that is mean the mirror type is convergence. For example, from the figure (3.35) It is can be shown that the values of the mirror focal length f_R proportional directly with **b** where increasing the values of **b** deducing increasing in the mirror focal length f_R with keeping **a** = 150 at the mirror length **L** = 14 and **c** = 2.7. For example, It is noted from the figure (3.36) that the values of the mirror focal length f_R proportional inversely with **a** where increasing the values of **a** causes to decrease the values of the mirror focal length f_R with keeping **b** = 15 at the mirror length **L** = 14 and **c** = 2.7.

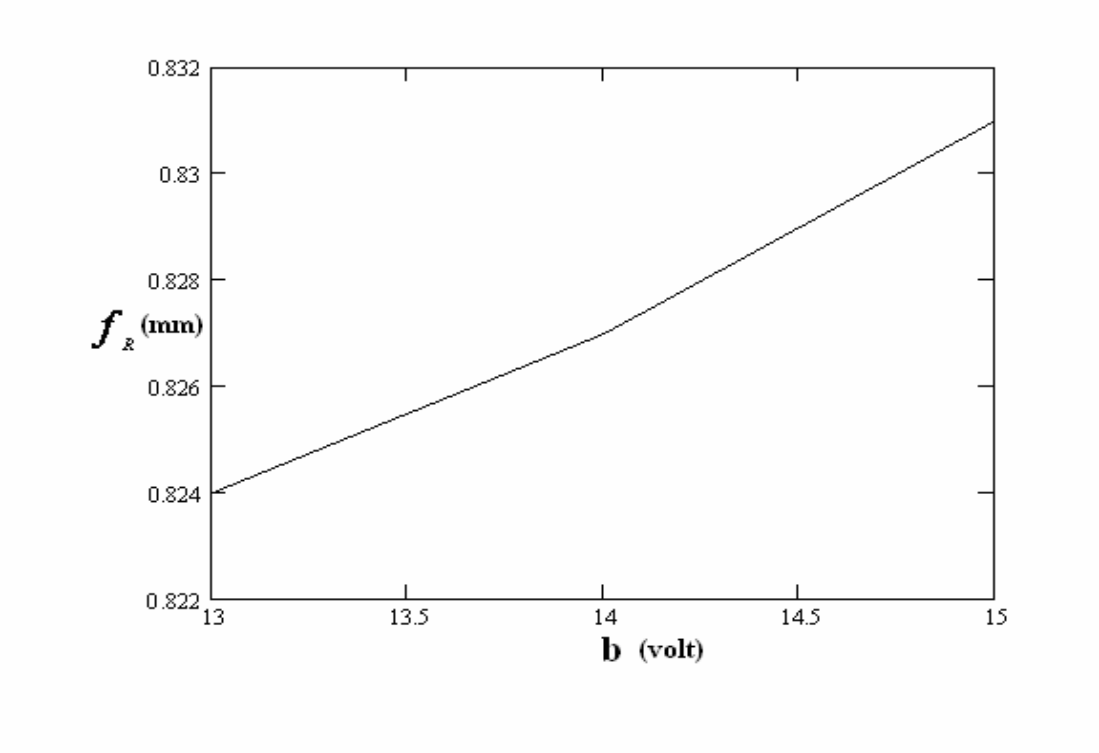

Figure(3.35) show the changeability between values of b (volt) and the values of the mirror focal length f_R (mm) when L=14 mm, c=2.7 mm, and a=150 volt.

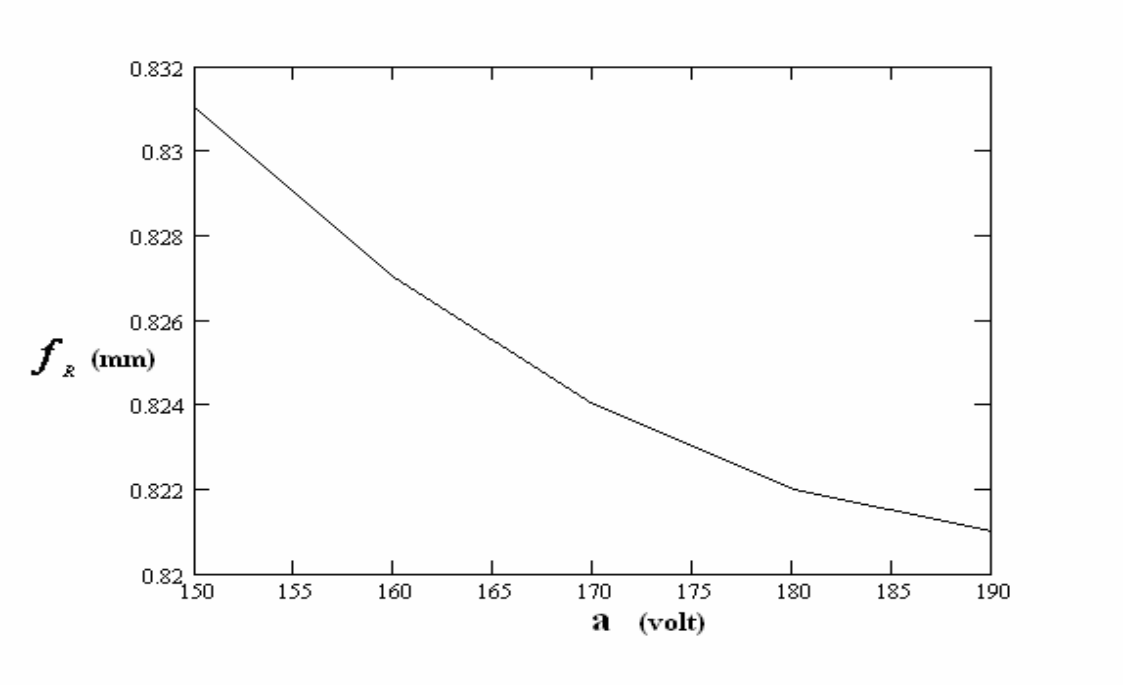

Figure(3.36) show the changeability between values of a (volt) and the values of the mirror focal length f_R (mm) when L=14 mm, c=2.7 mm, and b=15 volt.

The effect of changing the values of constant **a** on the ion beam trajectory for constant **L**, **c** and **b** = 15 are shown in the following figures (3.37), (3.38), (3.39), (3.40), and (3.41).

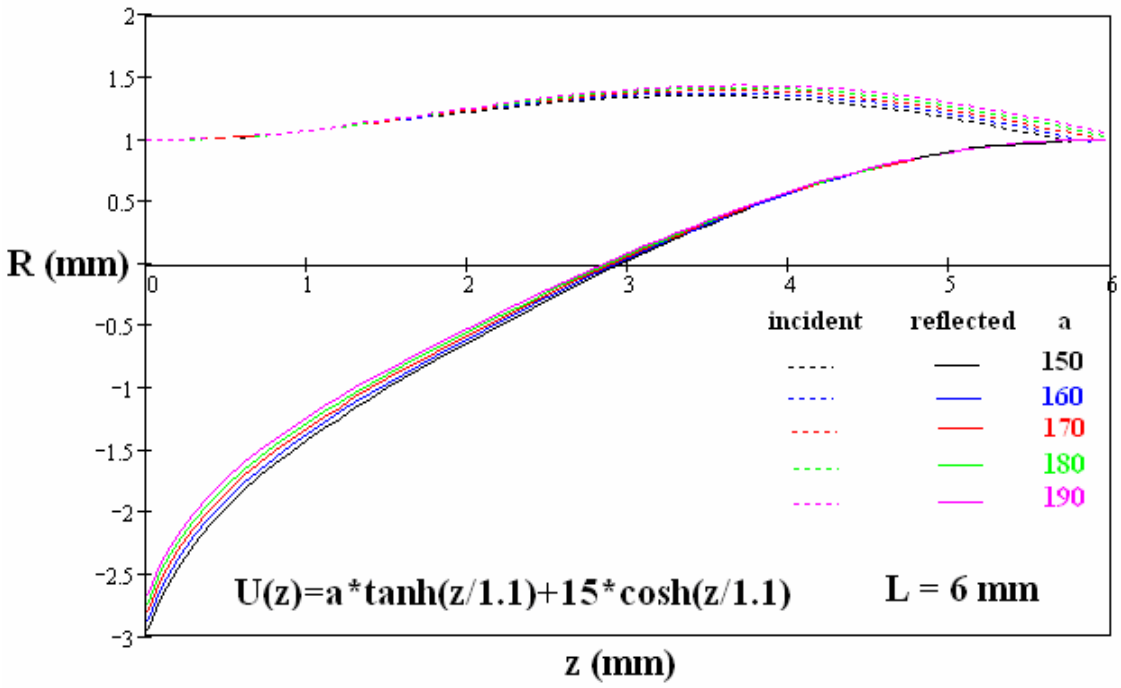

Figure (3.37) The ion beam trajectory for the electrostatic mirror under various value of a (volt) when b=15 volt, c=1.1 mm, and mirror length L=6 mm.

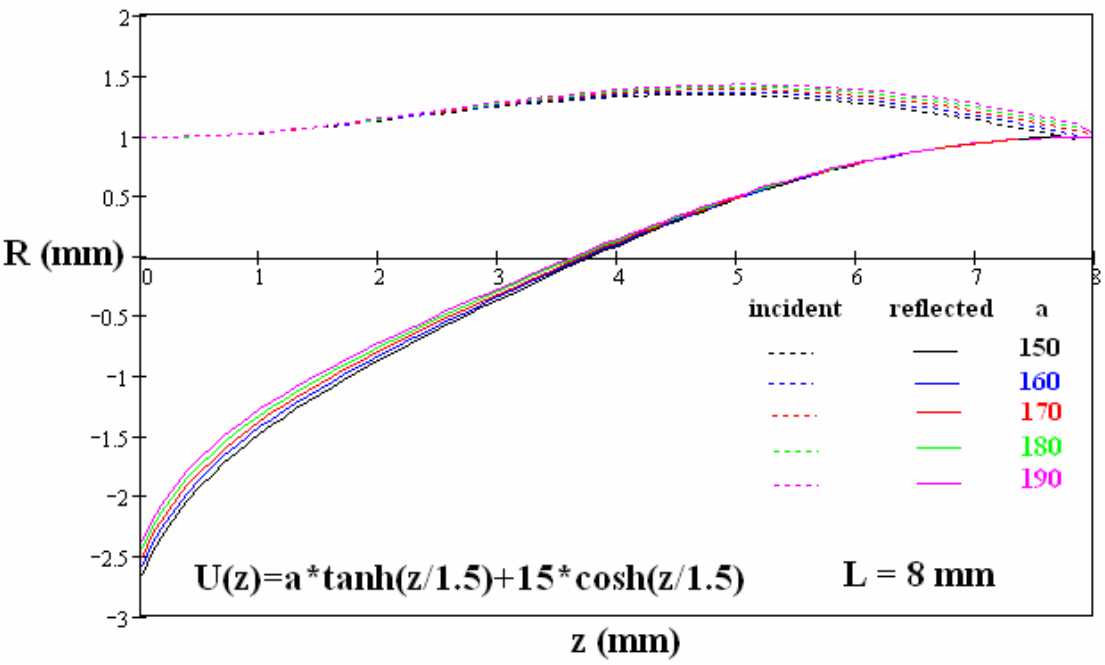

Figure (3.38) The ion beam trajectory for the electrostatic mirror under various value of a (volt) when b=15 volt, c=1.5 mm, and mirror length L=8 mm.

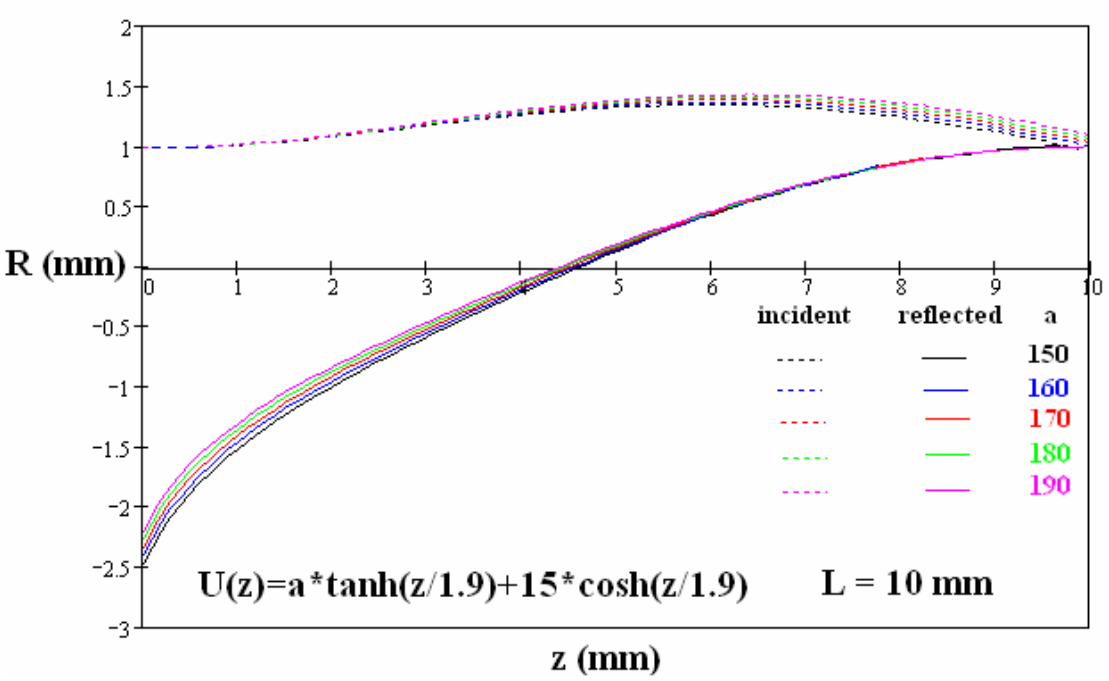

Figure (3.39) The ion beam trajectory for the electrostatic mirror under various value of a (volt) when b=15 volt, c=1.9 mm, and mirror length L=10 mm.

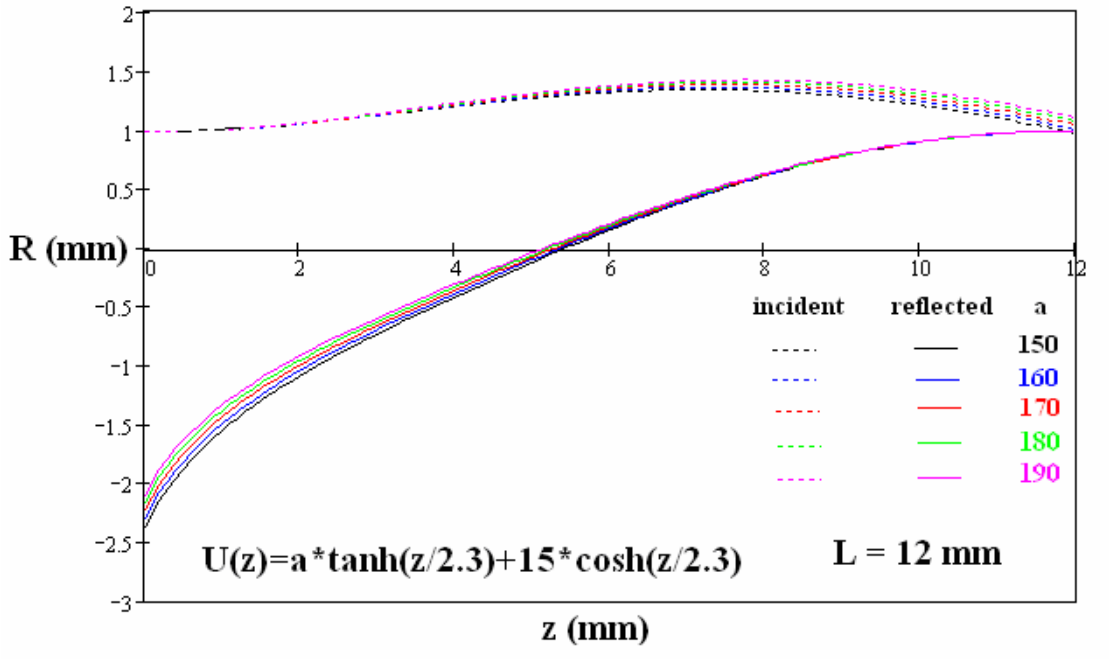

Figure (3.40) The ion beam trajectory for the electrostatic mirror under various value of a (volt) when b=15 volt, c=2.3 mm, and mirror length L=12 mm.

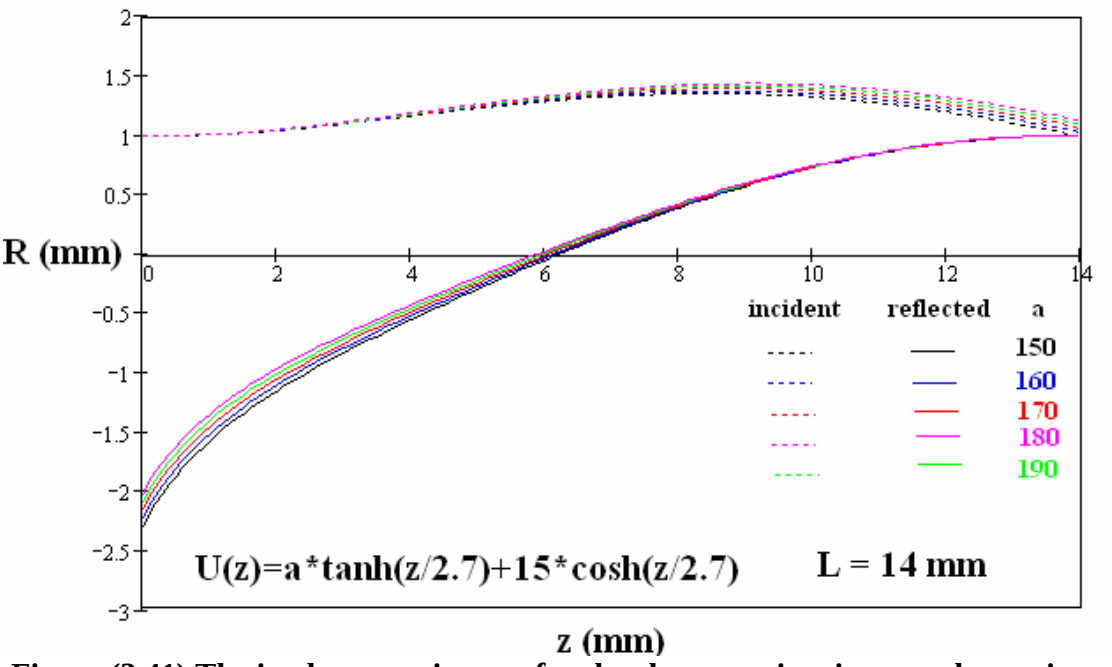

Figure (3.41) The ion beam trajectory for the electrostatic mirror under various value of a (volt) when b=15 volt, c=2.7 mm, and mirror length L=14 mm.

From these figures (3.37), (3.38), (3.39), (3.40), and (3.41) it is noted that by increasing the values of **a** causes to decreasing the values of the electrostatic mirror focal length for all mirror length with **b** = 15 and decreases the radial displacement of the reflecting trajectory. By taking five values of mirrors length **L** = 6, 8, 10, 12, 14 mm with five values of constants **c** = 1.1, 1.5, 1.9, 2.3, 2.7, it is noted that as to keep the equation (3-2) to work in the mirror mode must be increases the constant **c** about 0.4 when the mirrors length increases abut 2 mm and this values are shown in the table (3.5) and the figure (3.42) showing the relation between the mirrors length and the constants **c**.

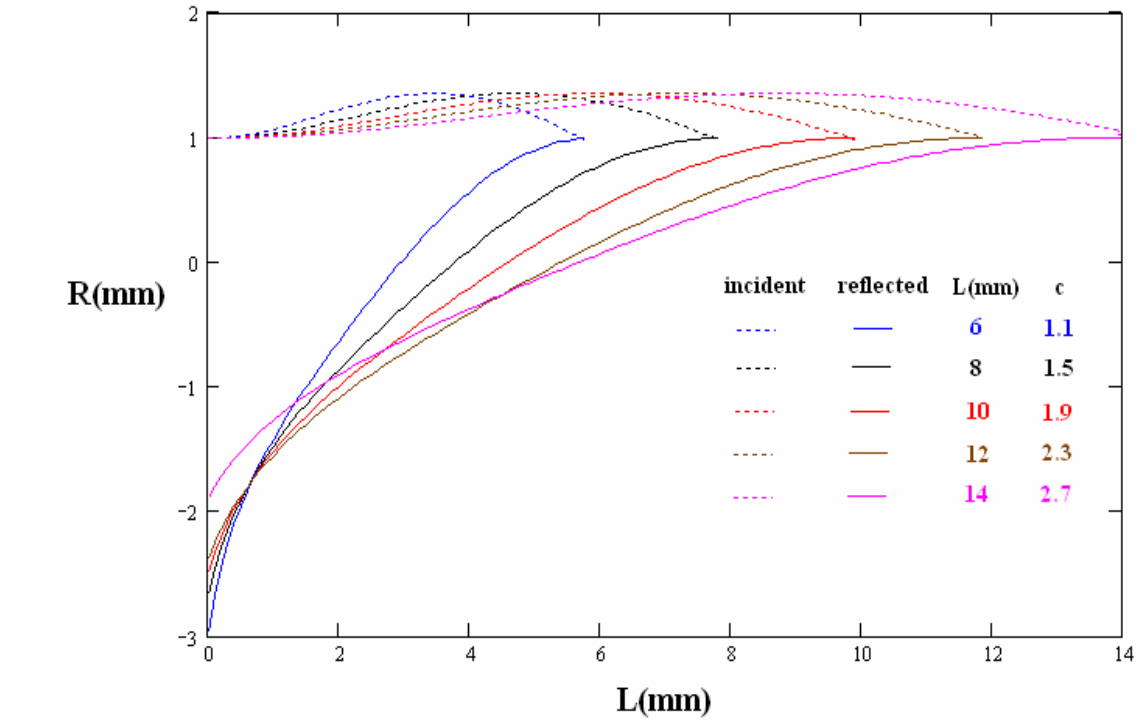

Figure (3.42) show the relation between the mirror length L (mm) and constant c (mm) at a=150 volt and b=15 volt.

3.2.3. Relative aberration coefficients of electrostatic mirror

For each mirror length as an examples **L** = 6, 8, 10, 12, 14 mm, the relative spherical C_s / f_R and chromatic C_c / f_R aberration coefficients have been computed as a function of the relative mirror length L / f_R are shown in the figure (3.43), (3.44), (3.45), (3.46), and (3.47) the effect of both constants **a** and **b** on the relative spherical C_s / f_R and chromatic C_c / f_R aberration coefficients are clear too

Figures (3.43), (3.44), (3.45), (3.46), and (3.47), shows the variations between C_s / f_R and C_c / f_R as a function of L / f_R at various values of **b** where **b** = 13, 14, 15 with keep **a** constant where the most favorable **a** = 150 at mirror length **L** = 6, 8, 10, 12, 14 mm respectively.

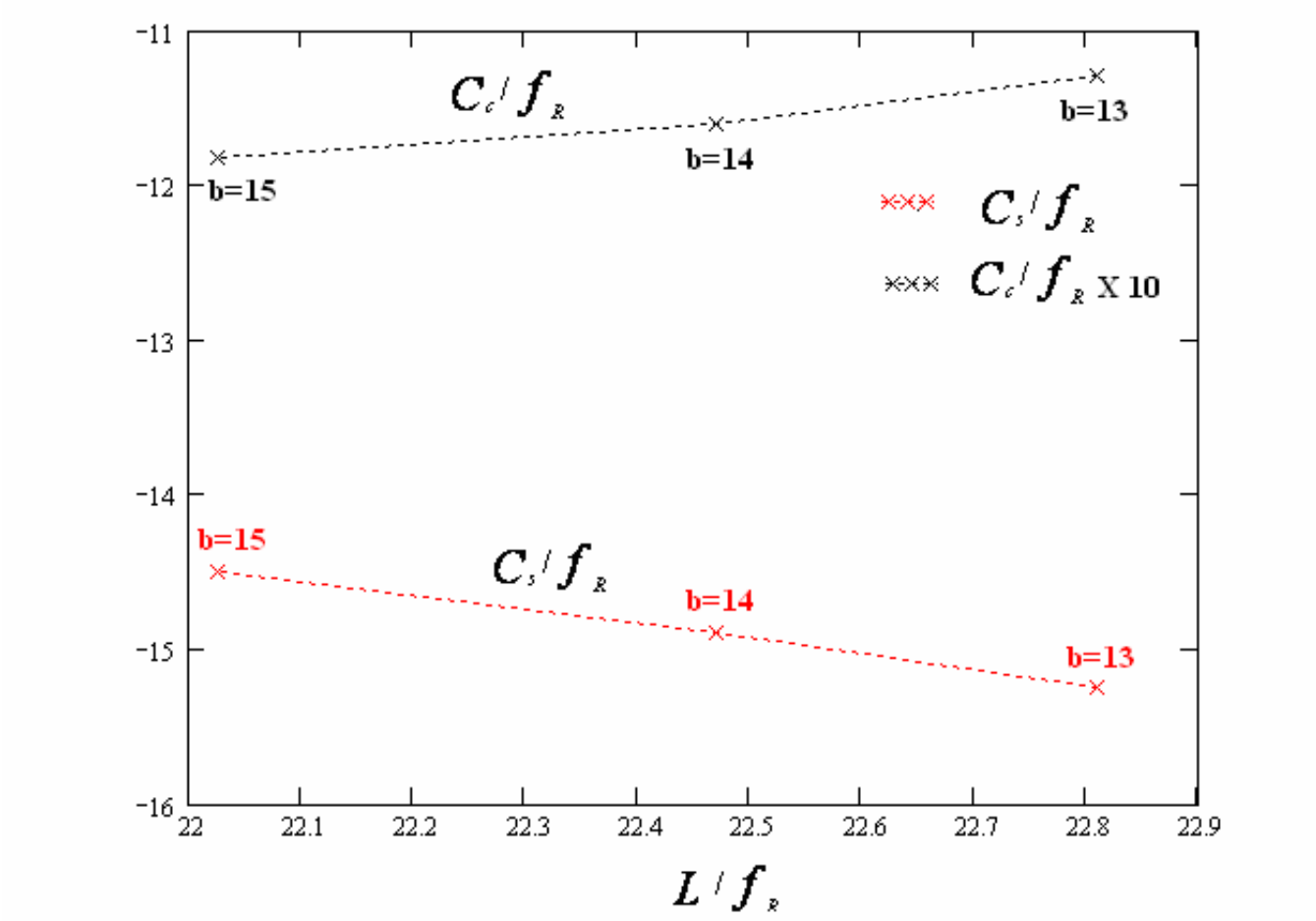

Figure(3.43) show the variation between C_s / f_R and C_c / f_R as a function of relative electrostatic mirror length L / f_R for different values of b (volt) at a = 150 volt, L = 6 mm, and c = 1.1 mm.

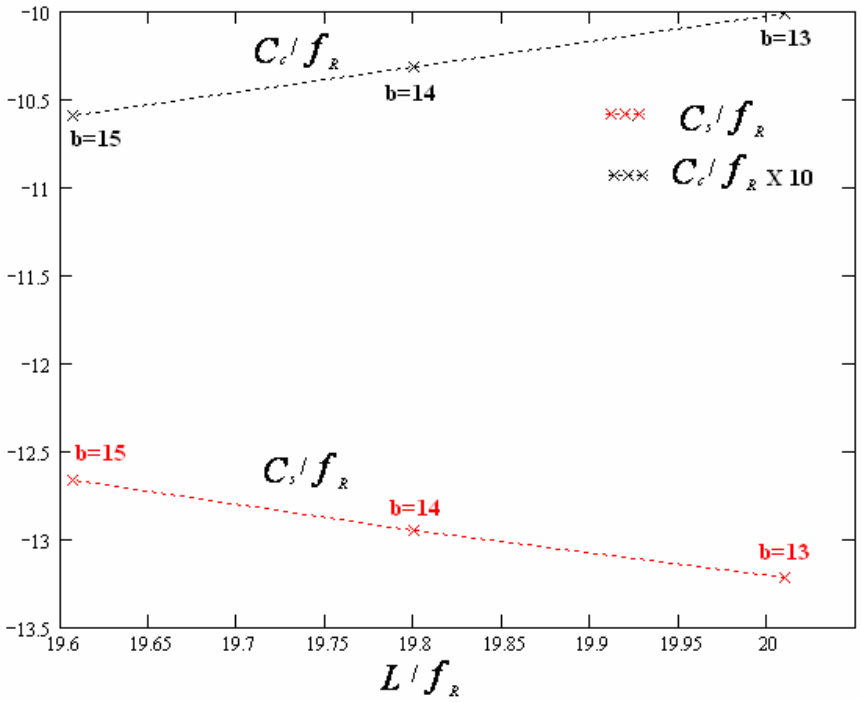

Figure(3.44) show the variation between C_s / f_R ***and*** C_c / f_R ***as a function of relative electrostatic mirror length*** L / f_R ***for different values of b (volt) at a = 150 volt, L = 8 mm, and c = 1.5 mm.***

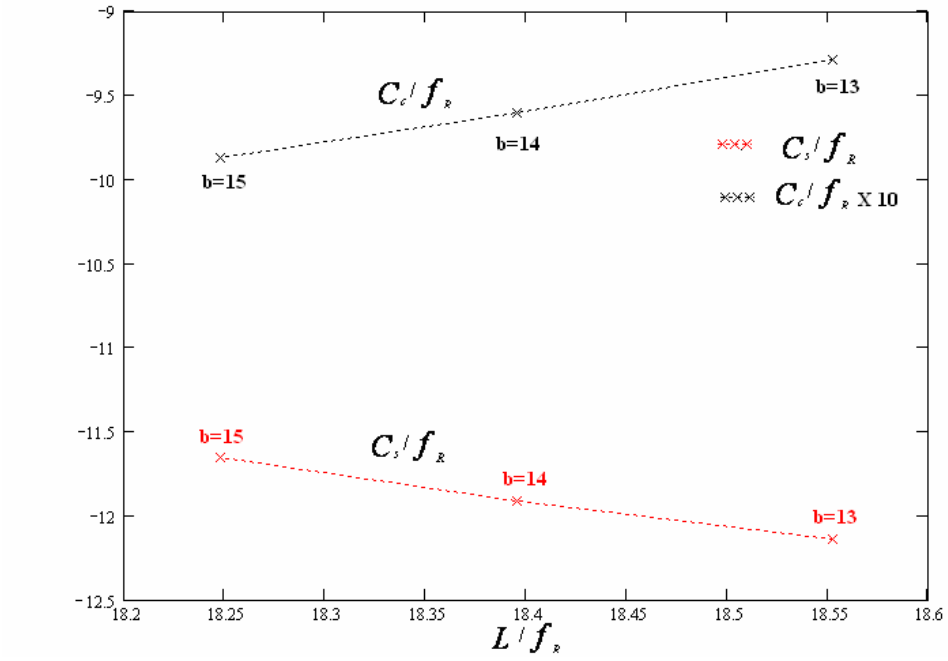

Figure(3.45) show the changeability between C_s / f_R ***and*** C_c / f_R ***as a function of relative electrostatic mirror length*** L / f_R ***for different values of b(volt) at a = 150 volt, L = 10 mm, and c = 1.9 mm.***

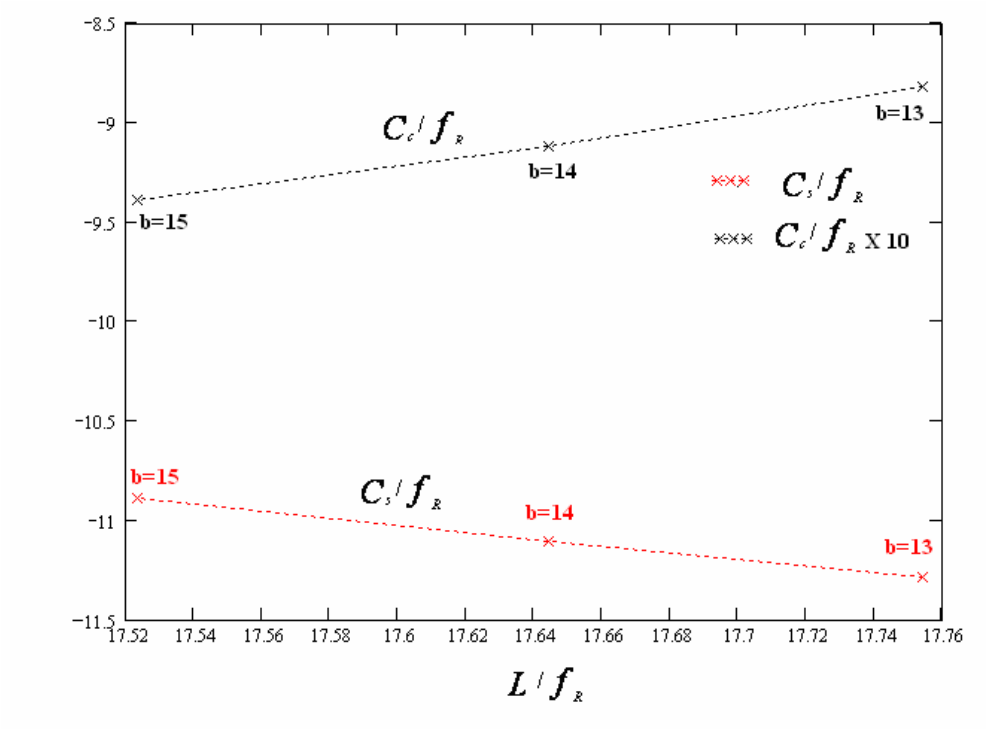

Figure(3.46) show the changeability between C_s / f_R ***and*** C_c / f_R ***as a function of relative electrostatic mirror length*** L / f_R ***for different values of b (volt) at a = 150 volt, L = 12 mm, and c = 2.3 mm.***

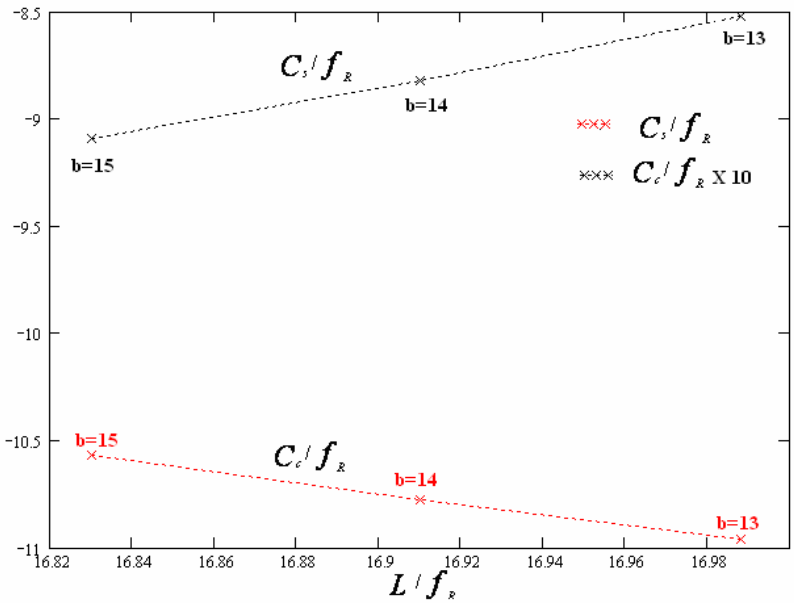

Figure(3.47) show the changeability between C_s / f_R ***and*** C_c / f_R ***as a function of relative electrostatic mirror length*** L / f_R ***for different values of b (volt) at a = 150 volt, L = 14 mm, and c = 2.7 mm.***

Figures (3.48) is an example to show the variation between C_s / f_R and C_c / f_R as a function of the mirror focal length f_R at various values of **b** where **b** = 13, 14, 15 with keep constant **a** = 150, **L** = 14 mm, and **c** = 2.7, where it is noted from this figure that the increasing values of **b** causes to increase the values of both the f_R and C_s / f_R where the values of C_c / f_R decreases .

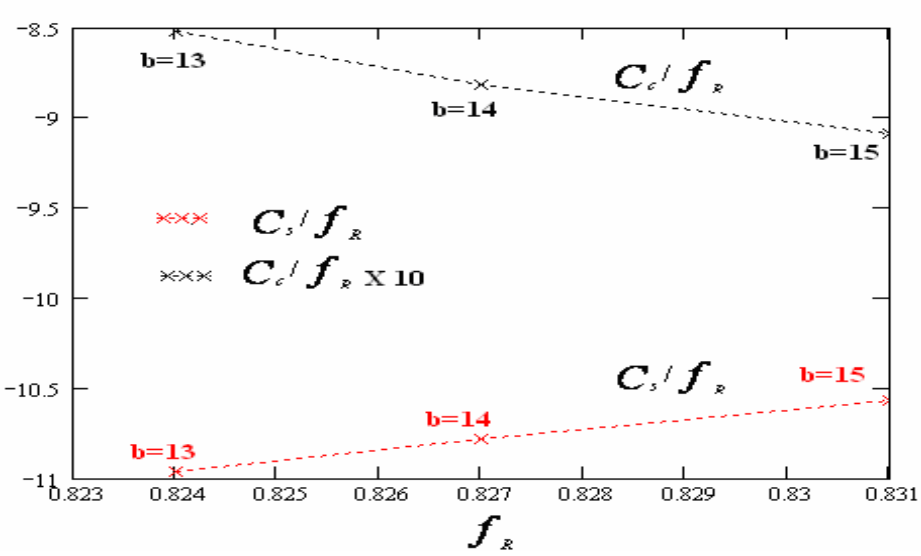

Figure(3.48) show the changeability between C_s / f_R and C_c / f_R as a function of mirror focal length f_R (mm) for different values of b (volt) at a = 150 volt, L = 6 mm, and c = 1.1 mm.

It is noted from figures (3.43), (3.44), (3.45), (3.46), and (3.47) that increasing the values of **b** causes to increases the values of the C_s / f_R, where the values of both C_c / f_R and L / f_R are decreases, with keeping **a** = 150 for all mirror lengths as shown in table (3.5). Figures (3.49), (3.50), (3.51), (3.52), and (3.53), show that increasing the values of **a** causes to increases both of the $C_c / f_R, L / f_R$ and decreasing of the C_s / f_R with keeping **b** = 15 for all mirror lengths with specific constant **c** for each length as shown in table (3.5).

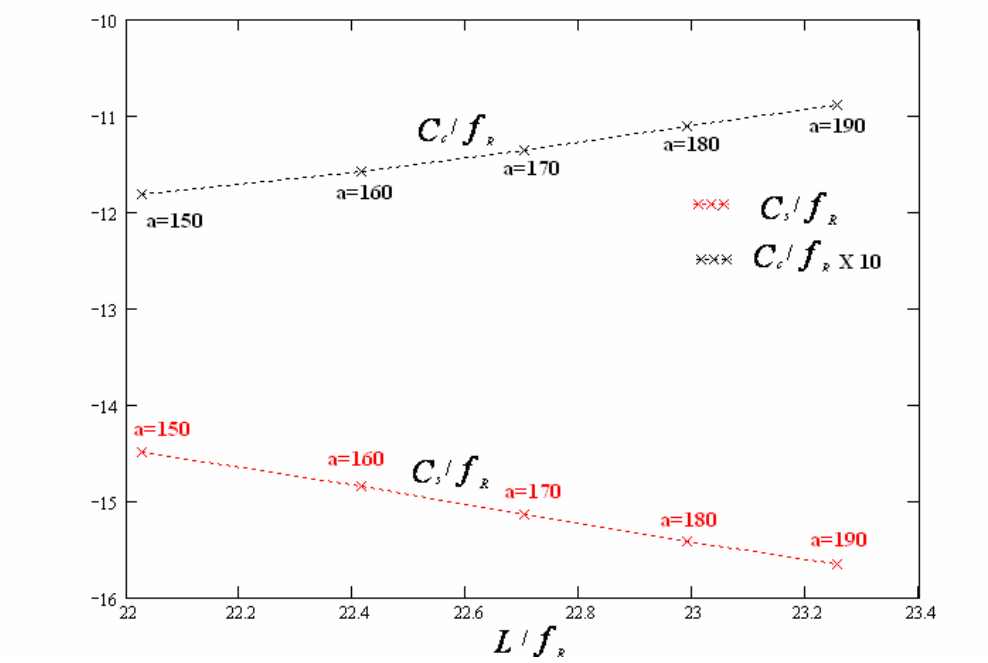

Figure(3.49) show the variation between C_s / f_R ***and*** C_c / f_R ***as a function of relative electrostatic mirror length*** L / f_R ***for different values of a (volt) at b = 15 volt, L = 6 mm, and c = 1.1 mm.***

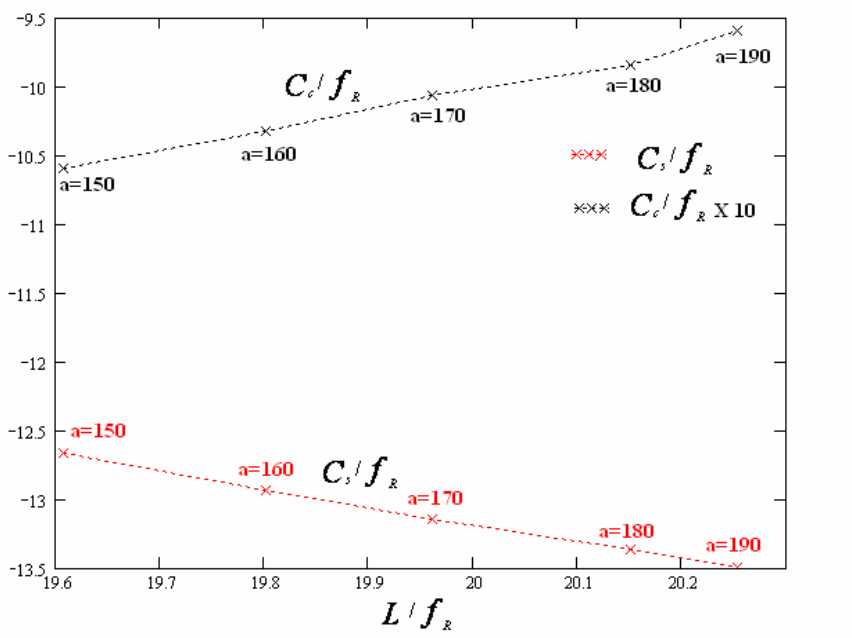

Figure(3.50) show the changeability between C_s / f_R ***and*** C_c / f_R ***as a function of relative electrostatic mirror length*** L / f_R ***for different values of a (volt) at b = 15 volt, L = 8 mm, and c = 1.5 mm.***

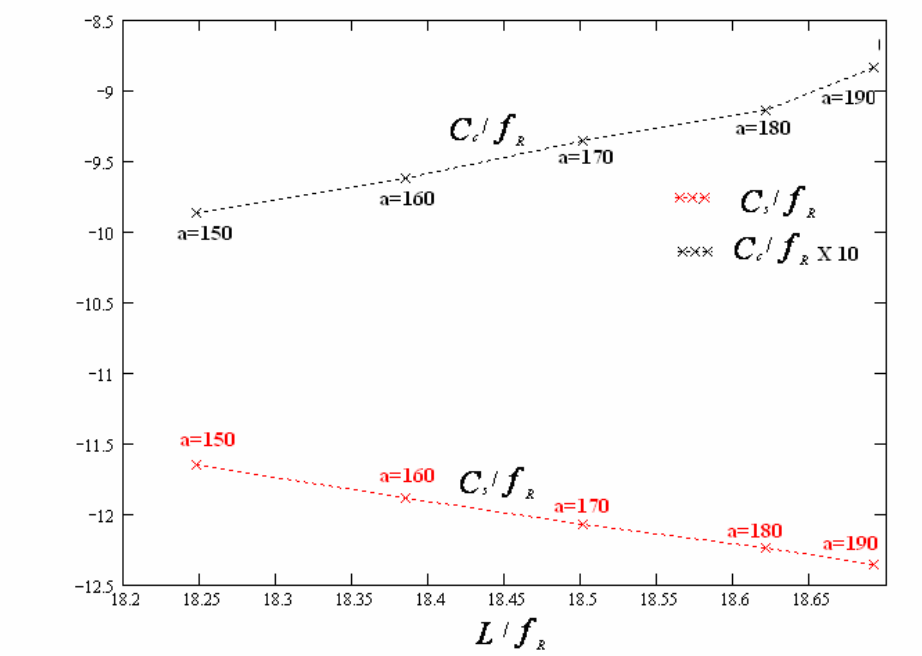

Figure(3.51) show the changeability between C_s / f_R ***and*** C_c / f_R ***as a function of relative electrostatic mirror length*** L / f_R ***for different values of a (volt) at b = 15 volt, L = 10 mm, and c = 1.9 mm.***

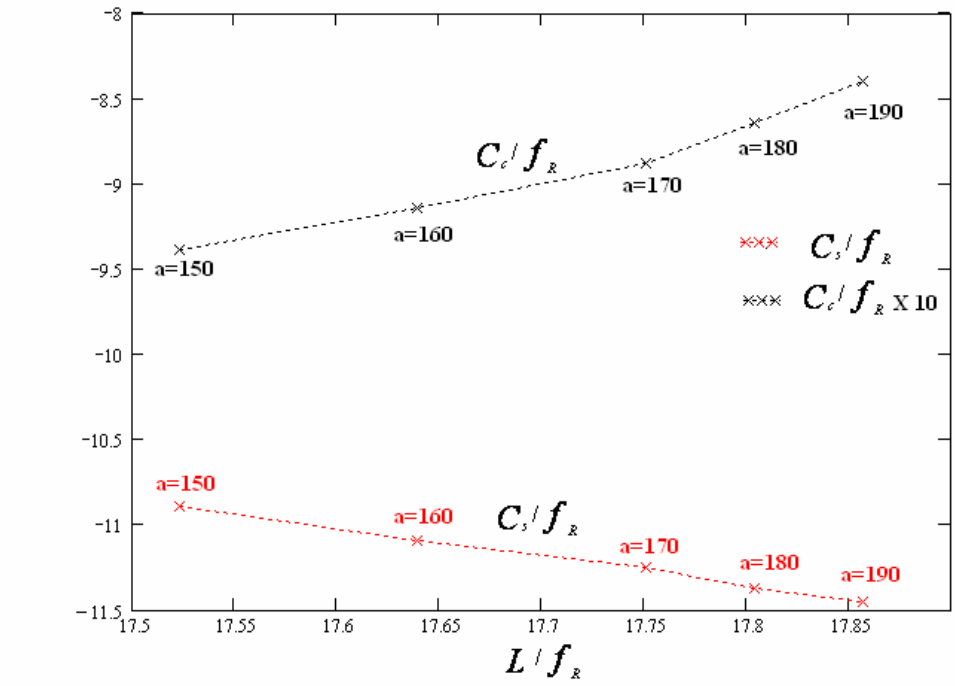

Figure(3.52) show the changeability between C_s / f_R ***and*** C_c / f_R ***as a function of relative electrostatic mirror length*** L / f_R ***for different values of a (volt)at b = 15 volt, L = 12 mm, and c = 2.3 mm.***

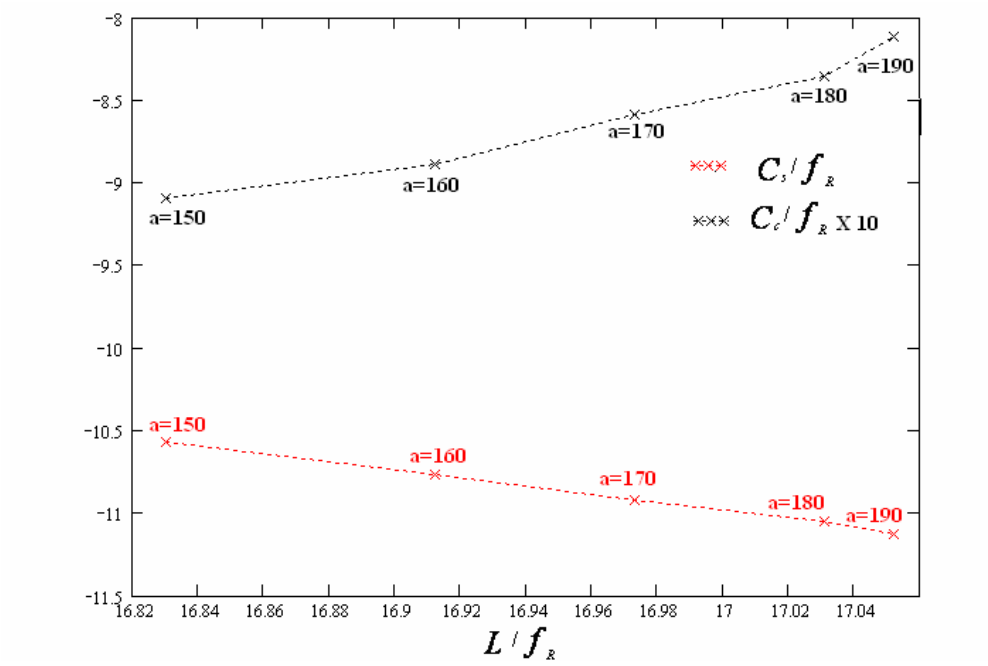

Figure(3.53) show the changeability between C_s / f_R ***and*** C_c / f_R ***as a function of relative electrostatic mirror length*** L / f_R ***for different values of a (volt)at b = 15 volt, L = 14 mm, and c = 2.7 mm.***

For example it is noted from the figure (3.54) that increasing the values of the mirror length **L** and **c** causes to relatively increases in both C_s / f_R, C_c / f_R and decreases value of L / f_R with keeping **a** and **b** constants. Thus under these conditions the most favorable mirror is deduced having the following parameters: **a** = 150, **b** = 15, **L** = 14 mm, **c** = 2.7, C_s = -8.79 mm, C_c = -0.756 mm and f_R = 0.831 mm. the potential distribution of this mirror is shown in figure (3.28) and the trajectory of the beam traversing this field is shown in figure (3.34).

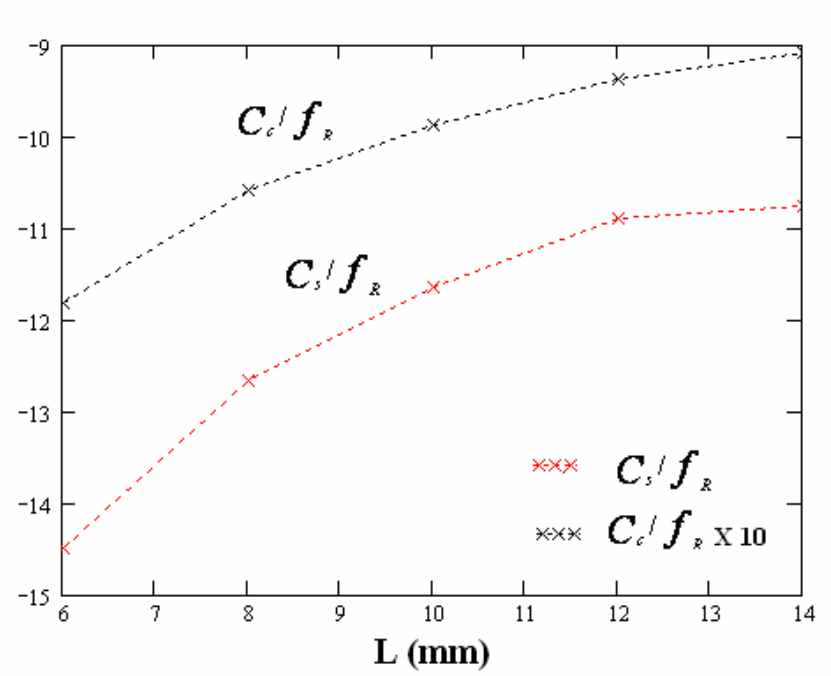

Figure(3.54) show the changeability between C_s / f_R ***and*** C_c / f_R ***as a function of the electrostatic mirror length L (mm) at a = 150 volt, b = 15 volt.***

3.2.4 Mirror electrodes shape

The shape of the electrodes which fulfill the mirror condition for the potential given in equation (3-2) is in general little affected by the various values of the constants. The mirror consists of two electrodes, each with an axial hole to allow passage for the ion beam. Figure (3.55) show the ion mirror electrodes profile using the Bimurzaev technique. This mirror is characterized by low C_c / f_R which is equal to -0.756. This mirror is of the accelerating type, i.e., its mode of operation is subjected to the condition that the voltage applied on the second electrode at the right hand side is usually higher than that on the left hand side electrode.

The electrode at the left hand side has a bore for ion beam entrance of relative radius R/L = 1.785 at z/L = 0.014, a minimum R/L = 0.019 at z/L = 0.307. The electrode at the right hand side have an inner radius of R/L = 0.016 at z/L = 0.329, the outer radius has R/L = 0.381 at z/L = 1.0. The two electrodes are separated by an air gap of relative length z/L = 0.022. Since the favorable value of L for this mirror is found to be 14 mm. The positioning of the specimens it must be located at the adequate vicinity where the deflection of the ion beam occurs. A three-dimensional diagram of the two electrode mirror is shown in figure (3.56).

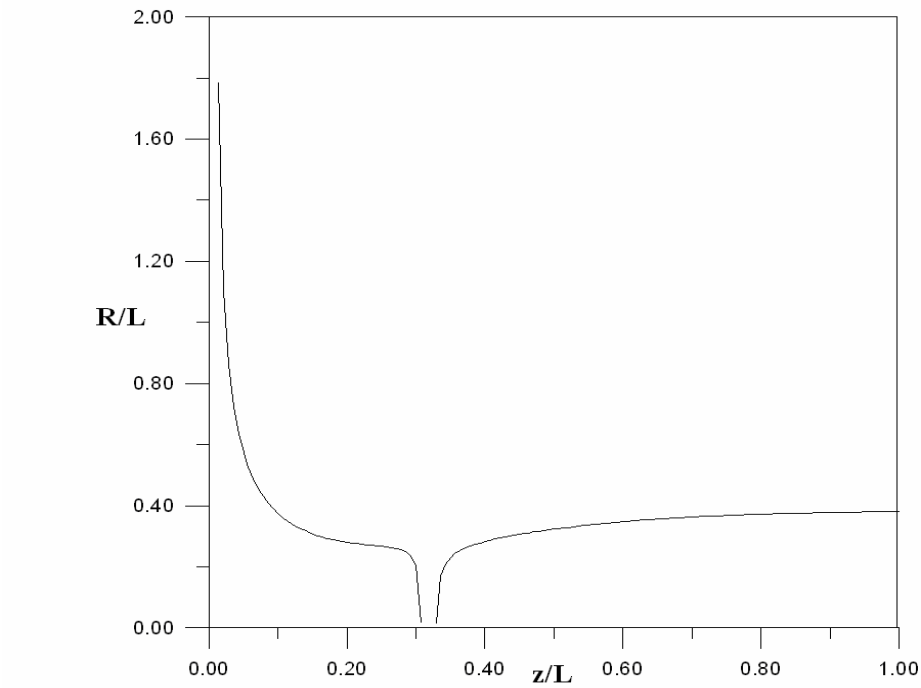

Figure (3.55) the electrodes profile of the two electrodes electrostatic mirror using Bimurzaev technique when the constants a = 150 volt, b = 15 volt, and c = 2.7 mm at the mirror length L = 14 mm.

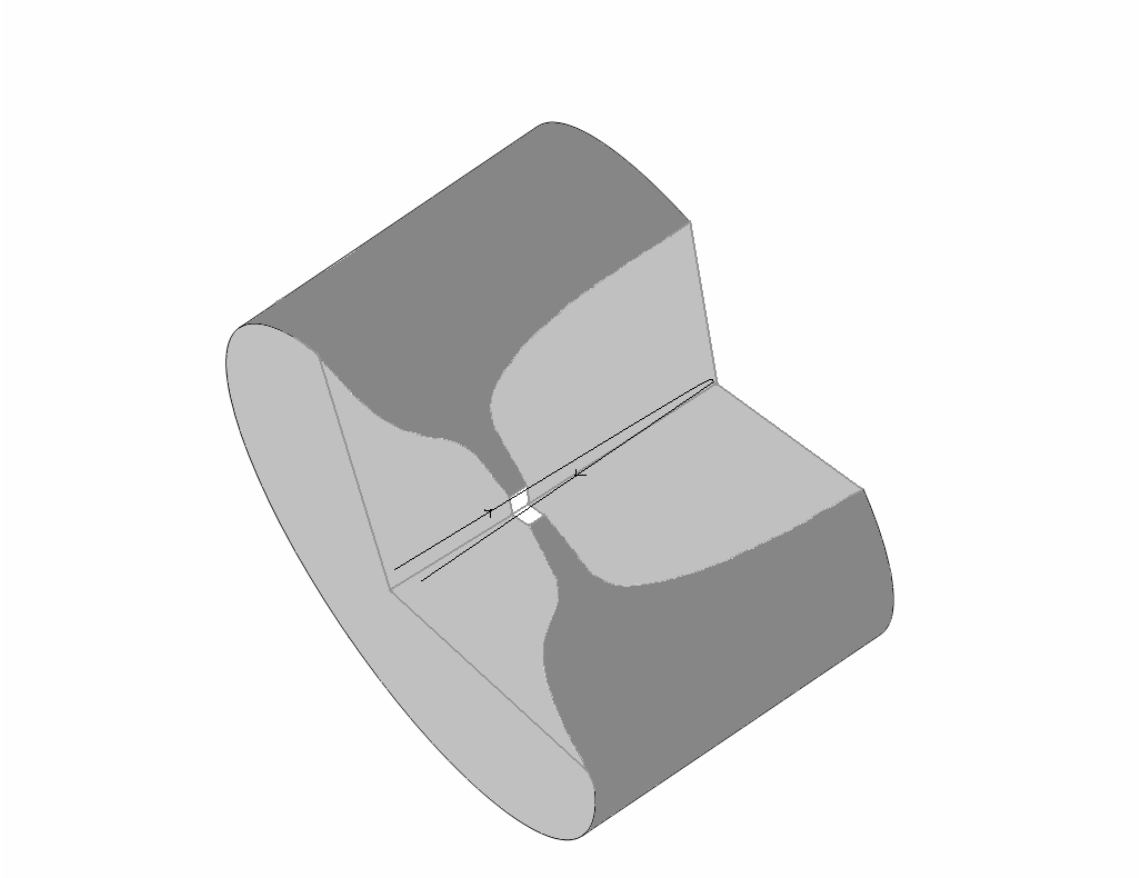

Figure (3.56) A three-dimensional diagram of the two electrodes electrostatic mirror using Bimurzaev technique when the constants a = 150 volt, b = 15 volt, and c = 2.7 mm at the mirror length L = 14 mm.

CHAPTER ONE

INTRODUCTION

CHAPTER TWO

THEORETICAL CONSIDERATION

CHAPTER

THREE

RESULTS AND DISSCUSION

CHAPTER FOUR

CONCLUSIONS AND RECOMMENDATIONS FOR FUTURE WORK

REFERENCES

DEDICATION

TO

MY FAMILY

Synopsis

A computational investigation has been carried out on the design and properties of the electrostatic ion mirrors. The work has been focused on suggesting two mathematical expressions to represent the axial potential of an ion mirror. The functions that have been taken into consideration were those which gave rise to the mirror action. Studying the ion beam path under infinite magnification conditions and study the ion beam path by using the Bimurzaev technique have been investigated as a mirror trajectory with aid of Runge-Kutta method.

The electrodes shapes of each mirror have been determined in two and three dimension. In the present work the profile of the mirror that applied under infinite magnification condition determined from the suggested potential is of the three-electrodes. The profile of the mirror that applied by using Bimurzaev technique determined from the suggested potential is of two-electrodes. Both mirrors have an axial bore to provide a passage for the ion beam undergoing a mirror trajectory.

The spherical and chromatic aberration coefficients of both mirrors have computed and normalized in terms of the focal length. The choice of the mirror depends on the operational requirements, i.e. whether it is intended to operate the mirror in an ion-optical system at low spherical aberration or low chromatic aberration. Computations have shown that the suggested potentials gave rise to mirrors, when the mirror applied under infinite magnification condition the most favorable values of the mirror is deduced

having the following parameters **a** = 500 volt, **b** = 0.01 volt, **c** = 1.05 mm, f_o =-1.618 mm, **L** = 17.8 mm , C_s = 0.42 mm and C_c = 0.42 mm and the most favorable values of the mirror by using Bimurzaev technique is deduced having the following parameters: **a** = 150 volt, **b** = 15 volt, **L** = 14 mm, **c** = 2.7 mm, C_s = -8.79 mm, C_c = -0.756 mm and f_R = 0.831 mm, where the values of the optical properties in the present work have an excellent performance in comparison with those published in the literature.

2. THEORTICAL CONSIDERATION

2.1 The Paraxial-Ray Equation of Charged Particles Moving in an Electric Field

The equations of motion of a charged particle traveling at a non-relativistic velocity in an electric field near the axis of a cylindrically symmetric system can be reduced to the following paraxial ray equation **[Grivet 1972, Paskawski 1968]**,

$$\frac{d^2R}{dz^2} + \frac{U'}{2U}\frac{dR}{dz} + \frac{U''}{4U}R = 0 \qquad \textbf{(2-1)}$$

Where U' and U'' are the first and second derivatives of the axial potential U respectively. R represents the radial displacement of the beam from the optical axis z, and the primes denote a derivative with respect to z. Equation (2-1) is a linear homogeneous second order differential equation. If the potential distribution along the z-axis is known, that is if the function $U(z)$ is known the factors in front of dR/dz and R is also known. It should be noted that three important deductions could be made from equation (2-1) **[El-Kareh and El-Kareh 1972]**:

(a) The quotient of charge to mass (Q/m) does not appear, indicating that the path is the same for any charged particle no matter what may be its Q/m provided it enters the field with the same constant kinetic energy.

(b) The equation is homogeneous in *U(z);* i.e. the trajectory remains unaltered when the voltage is increased proportionally for all the electrodes.

(c) The equation is homogeneous in *R* and which means that n-fold change in the dimensions of the field region and the electrodes produce corresponding change in the dimensions of the trajectory since the equipotentials don't alter the shape of the path. If the electrode is doubled in size, the image will be doubled in size, the ratio between the two remaining constants.

In the second part of the project with the aid its used **Bimurzaev** Technique's and modified on it for solving electrostatic mirror trajectory by using the paraxial ray equation of charge particle moving in an electric field and applied this trajectory equation twice at the first one its applied zero magnification condition when the ray *P(z)* of charge particle is incident (2-2) equation and at the second one its applied the infinite magnification condition when the ray *G(z)* of charge particle is reflected (3-2) equation. By applying this technique we get on complete trajectory of charge particle in electrostatic mirror system.

$P(1)=1 \qquad P'(1)=0$

$$\frac{d^2P}{dz^2}+\frac{U'}{2U}\frac{dP}{dz}+\frac{U''}{4U}P=0 \qquad \textbf{(2-2)}$$

$G(\infty)=0 \qquad G'(\infty)=1$

$$\frac{d^2G}{dz^2}+\frac{U'}{2U}\frac{dG}{dz}+\frac{U''}{4U}G=0 \qquad \textbf{(2-3)}$$

It is often desirable to perform a rapid approximate evaluation of electrostatic mirror properties without actually carrying out a detailed analysis. This can be accomplished with the aid of a new technique by **Bimurzaev** and simple mathematical model for the mirror, i.e. an approximation for the axial potential distribution that is reasonably close to the real one. Thus several expressions have been suggested to represents the axial potential of an electrostatic mirror. The suggested system consists of various types of electrostatic mirrors such as the einzel, immersion mirror where their electrodes configuration and optical properties are determined from suggested mathematical models representing the potential distribution of the different mirrors.

It is important to note that in this project only the axial potential distribution is taken into consideration. Furthermore, because of the complex nature of the present problem under investigation, the following assumptions have been made:

a) The space charge effects are neglected in order to satisfy exactly the following Laplace's equation

$$\nabla^2 U = 0 \qquad \textbf{(2-4)}$$

Where ∇^2 is called the Laplacian operator and U is the electrostatic potential (scalar potential) measured in volts. Equation **(2-4)** determines the function U in charge-free regions.

b) Non-relativistic velocities **v** of the electrons at any point inside the field is determined from the following equation **[Hawkes and Kasper 1989]**:

$$v = \left[\frac{-2e}{m} U \right]^{1/2} \qquad \textbf{(2-5)}$$

Where ***e*** and ***m*** are the charge and mass of the electron.

c) The initial velocity of the electrons i.e. their initial kinetic energy is negligible.

d) Aberrations associated with the source have been neglected.

e) Machining inaccuracies and asymmetries in the mirror are neglected.

A computer program written by **Munro (1975)** and then Modified by **Ahmed (1993)** in Fortran 77 has been used to determine the trajectory of the charged particles using the fourth-order Runge-Kutta method, with initial conditions depending on the magnification of the mirror. Optical properties such as the focal length and aberrations are calculated by integrating the paraxial-ray equation using Simpson's rule. In the second part of the project its used a Mathcad 11 (enterprise edition) program to showed the incident charge particle on the mirror system and the reflected charge particle from the mirror system.

2.2 Types of Electrostatic Lenses

There are various types of electrostatic lenses for different electron and ion optical systems, each with its own optical properties and domain of application. The lenses can be classified from many different points of view, for example, one can talk about (a) strong or weak lenses depending on whether their focal points are situated inside or outside the field, (b) thick or thin lenses, (c) symmetric or asymmetric lenses depending upon whether exists a middle plane perpendicular to the optical axis about which the geometrical arrangement of the lens (and sometime also its field distribution) is symmetric.

Depending on the velocity v_2 of an ion or electron leaving the region of the lens compared to its velocity v_1 when entering this region, the lenses can be classified into the following **[Paszkowski 1968]**:

a) Accelerating when $U_2 > U_1$
b) Decelerating when $U_2 < U_1$
c) Neutral (unipotential) when $U_2 = U_1$

Where U_1 and U_2 are the voltages applied on the first and the last electrode of the electrostatic system respectively. When a charge particle is decelerated and its velocity v_2 becomes zero, and then reverses its direction, one would have in this case an electron mirror.

2.3 Electrostatic Mirror Parameters

With the aid of computer programs, the optical properties (cardinal elements) of an electrostatic mirror are calculated. The coordinates of the two principal points and those of the two focal points, which represent the cardinal elements of the mirror uniquely determine the optical properties of the axially symmetric mirror. The first order optical properties can be determined as follows **[Szilagyi 1988]**:

a) ***focal point***

A beam may enter the mirror parallel to the optical axis and leave it at a certain angle with the optical axis. If the mirror is converging, this straight line will cross the axis at a certain point, which is called the focal point.

b) principal planes

When a straight ray path enters the mirror parallel to the axis it will cross the axis of the mirror at a certain point. The plane through this point normal to the optical axis is called the principal plane.

c) focal length

The focal length represents the distance between the focal point and the corresponding principal plane. It is positive for converging mirror and negative for diverging mirro.

d) magnification

In any optical system the ratio between the transverse dimension of the final image and the corresponding dimension of the original object is called the linear magnification M, i.e.

M=image height/ object height

There are three magnification conditions under which a lens can be operated namely zero, infinite and finite magnification. Figure (2-1) shows a ray diagram for each of the three magnification condition.

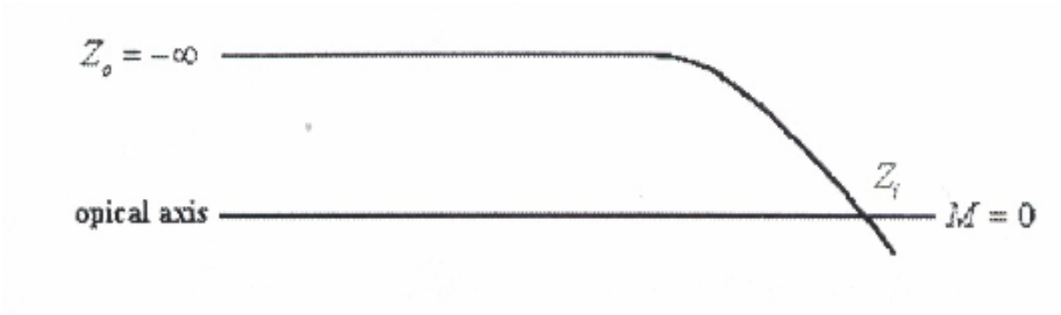

Zero magnification condition

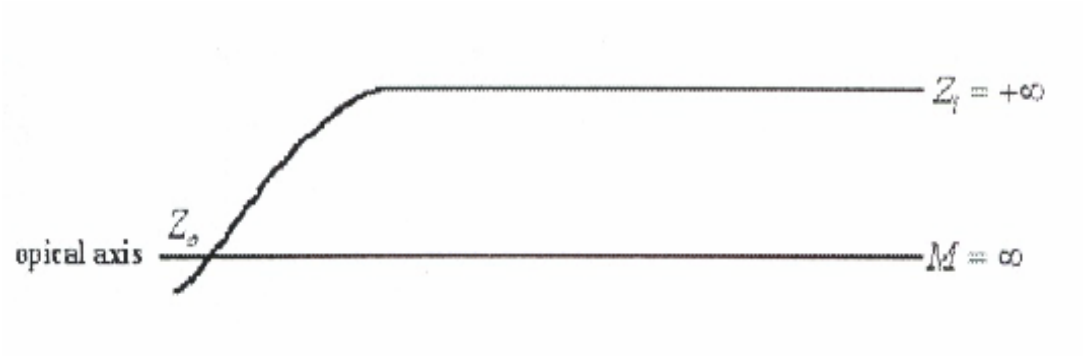

Infinite magnification condition

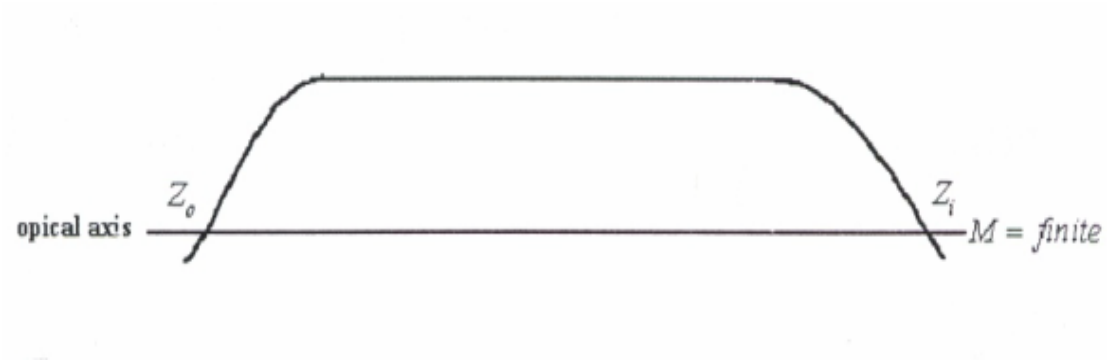

Finite magnification condition

Figure 2.1. Magnification condition **[Szilagyi 1988]**.

2.4 Electrostatic Mirror Aberration

The electron paths, which leave points of the object close to the axis, intersect the image plane in points forming a geometrically similar pattern. This ideal image is known as the ***Gaussian image***, and the plane in which it is formed as the ***Gaussian image plane***. If an electron path leaving an object point a finite distance from the axis with a particular direction and electron velocity intersects the Gaussian image plane at a point displaced from the Gaussian image point, this displacement is defined as the ***aberration***. The quality of any electron optical system depends not only upon the wavelength of the electrons, but also upon the aberrations from which it may suffer [**El-Kareh and El-Kareh 1970]**.

Spherical aberration is one of the most effective geometrical aberrations and can be defined in both light optics and electron optics, as the change in focal properties of a lens with height of the ray. Off-axis electrons spend less time in the field than do paraxial electrons because they do not penetrate as far into the field, and as the result the focal distance is longer for electrons whose trajectories make larger angles with the axis than for paraxial electrons [**Rempfer 1990]**.

Chromatic aberration in light optics refers to the change in focal properties with the wavelength of light. In electron optics it refers to the change in focal properties with kinetic energy of the electrons; lower-energy electrons penetrate less far into the field than do higher-energy electrons, and therefore spend less time in the field and are less strongly converged by the field. Consequently the focal distance is longer for low-energy electrons than for high-energy electrons [**Rempfer 1990]**.

The spherical and chromatic aberration coefficients are denoted by C_S and C_C respectively. In the present investigation the value of C_S and C_C are normalized in terms of the image side focal length, i.e. the relative values of C_S/F_i and C_C/F_i are investigated as figures of merit which are dimensionless. The aberration coefficients of electrostatic mirrors are determined entirely by the geometric arrangement of electrodes and are not adjustable except by changing image and/or object positions **[Shao and Wu 1990]**.

The spherical aberration coefficient C_S and the chromatic aberration coefficient C_C referred to the image side are calculated from the following formula **[Szilagyi and Szép 1987]** :

$$C_S = \frac{U^{-1/2}}{16R'^4}\int_{zo}^{zi}\left(\frac{5}{4}\left(\frac{U''}{U}\right)^2+\frac{5}{24}\left(\frac{U'}{U}\right)^4+\frac{14}{3}\left(\frac{U'}{U}\right)^3\frac{R'}{R}-\frac{3}{2}\left(\frac{U'}{U}\right)^2\frac{R'^2}{R^2}\right)\sqrt{U}R^4dz \qquad \textbf{(2-6)}$$

$$C_C = \frac{U^{1/2}}{R'^2}\int_{zo}^{zi}\left(\frac{U'}{2U}R'R+\frac{U''}{4U}R^2\right)U^{-1/2}dz \qquad \textbf{(2-7)}$$

Where $U=U(z)$ is the axial potential, the primes denote derivative with respect to z, and $U_i=U(z_i)$ is the potential at the image where $z=z_i$. It should be noted that C_S and C_C in the object plane can be expressed in a similar form equations (2-3) and (2-4) where $U^{1/2}$ and R^4 are replaced by $U_o^{1/2}$ and R_o^4 respectively. The integration given in the above equations are executed by means of Simpson's rule.

Two of the various magnification conditions that are well known in electron optics have been taken into account n the present investigation , namely, the infinite and the zero magnification conditions due to their resemblance to the mirror trajectory. With the aid of these two trajectories suggested for the mirror action in this work, new mirror design would be achieved. Such trajectories would be most adequate for a mirror applied for particular specimen investigations rather than for other applications of the mirror.

2.5 How an Electrostatic Mirror Corrects Aberration

The scientific basis for using an electrostatic mirror to correct the spherical and chromatic aberrations of an electrostatic lens is that electrostatic mirrors have aberrations of opposite sign from those of electrostatic lenses. The reason for the signs being opposite can be understood qualitatively by considering the difference in the effects which a focusing field has on a transmitted beam of (electrons or ions) and a reflected beam. The field uses in the example that explain how an electrostatic mirror corrects aberration is called hyperbolic field where figure (2.2) illustrates how spherical arises in electrostatic lenses and mirror. In figure (2.2.A) the field acts as an electrostatic lens transmitting (electrons or ions), and in figure (2.2.B) it acts as a mirror reflecting (electrons or ions). Referring to figure (2.2.A) one can see that the outer (electrons or ions) travel a greater distance through the field, and also encounter a higher part of the potential hill, than do the (electrons or ions) near the axis (paraxial rays). This causes the transit time through the field, and thus the time during which the converging force acts, to be longer for outer (electrons or ions) are more strongly focused and their focal distance is shorter than for paraxial rays. This behavior is known as “undercorrected spherical aberration”. Next consider figure (2.2.B), where the focusing field is show in the mirror field. When the potential of the mirror electrode has been increased so that (electrons or ions) cannot surmount the potential hill, but are turned back at an equipotential surface on the incident slope of the hill. Besides the reversing effect, there are two important ways in which the effect of the field in the mirror mode differs from its effect in the lens mode. First of all, the mirror mode (in contrast to the lens mode) does not require the outer (electrons or ions) to reach a higher level on the potential hill than is

required of the paraxial rays. Thus a major source of undercorrected spherical aberration that is present in the lens mode is not present in the mirror mode. Second, the outer (electrons or ions) travel a shorter distance and spend less time in the focusing field than do the paraxial rays. As a result, the outer (electrons or ions) are less strongly focused and the focal distance is longer than for paraxial rays. This result is opposite to that for the lens mode, and is referred to as “overcorrected spherical aberration”.

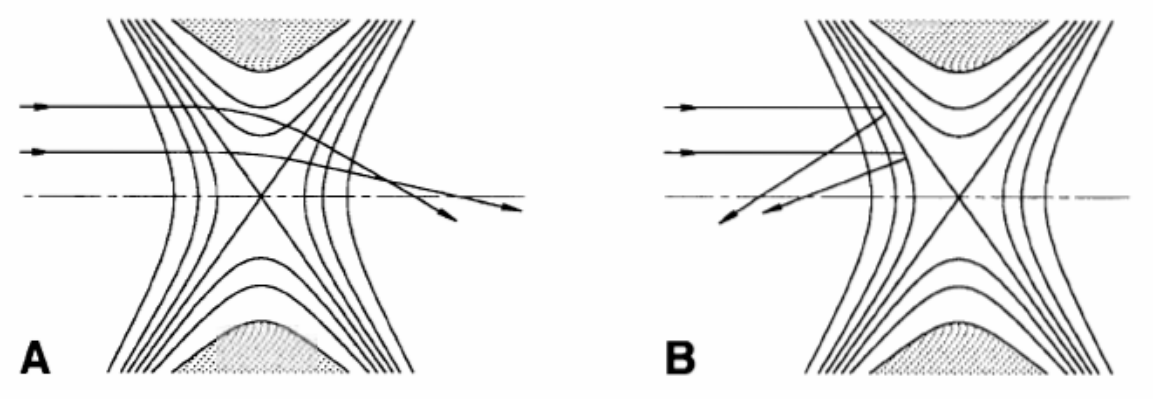

Figure(2.2.) Diagrams illustrating how an electrostatic lens (A) and electrostatic mirror (B) produce spherical aberrations of opposite sign. The contour lines represent equipotential surfaces in the region where the major part of the focusing takes place. The shaded areas are portions of the electrode. Two parallel incident rays are shown, a paraxial ray and another ray farther from the axis.

Chromatic aberration also can be explain qualitatively in terms of the time in the focusing field. For example, if the energy of the incident beam is increased, as illustrate in figure (2.3.A), the transit time through the lens is decreases, so the focusing field becomes less effective and the focal distance increases. This behavior is called “undercorrected chromatic aberration”. In considering chromatic aberration of a mirror, we note that as the energy of an (electrons or ions) is increases, the (electron or ion) penetrates farther into

the mirror field, causing the distance traveled and the time spent in the field to increase figure (2.3.B). The (electrons or ions) is therefore focused more strongly than is a lower energy (electron or ion), and the focal distance is shorter. This decrease in focal distance with increasing energy is opposite to behavior in the lens mode, and is referred to as “overcorrected chromatic aberration” **[Rempfer et al 1997]**.

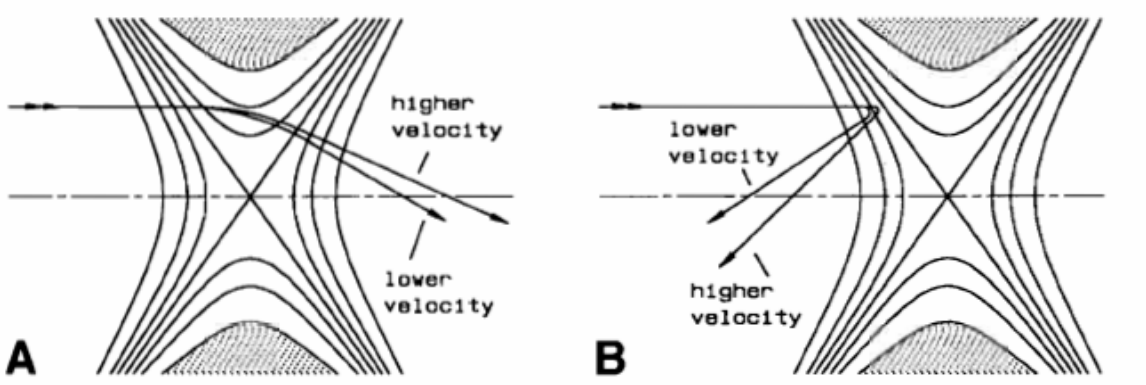

Figure(2.3.) Diagrams illustrating how an electrostatic lens (A) and electrostatic mirror (B) produce chromatic aberrations of opposite sign. The contour lines represent equipotential surfaces in the region where the major part of the focusing takes place. The shaded areas are portions of the electrode. Two parallel incident rays are shown, a paraxial ray and another ray farther from the axis.

2.6 Electrode Shape Program

The shape of the electrodes forming a specific electrostatic lens or mirror has been determined with the aid of a computer program written by **Ahmad (1993)** in Fortran 77 and applied by **Al-Mudarris (2001) and Al-Tabbakh (2000)**. The profile of the electrodes producing a certain electrostatic lens or mirror can be determined by the following equation of an equipotential surface **[Szép and Szilagyi 1987]** :

$$u(r,z) = U(0,z) - r^2 U''(0,z) / 4$$

where $u(r,z)$ is the off-axis potential, $U(0,z)$ is the axial potential function which is first investigated and the number of its inflection points is counted. The radial displacement r approaches infinity at each inflection point since the second derivatives isequal to zero $U''(0,z) = 0$. This equation can be written in the following form :

$$r = 2 ((U(z) - u(r,z)) / U''(z))^{1/2} \qquad \textbf{(2-8)}$$

The number of electrodes is greater than the number of inflection points by one. If the value of the second derivative is negative between two inflection points or between the start/end point and the nearest inflection point, then the electrode potential is chosen slightly higher than the maximum value of the axial potential in this interval is chosen. If the second derivative is positive, the electrode potential must be lower than the minimum value of the axial potential. The finite size of the physical system is a limitation to the accuracy of reconstruction because the electrodes must be cut somewhere at a finite distance from the axis to limit the maximum value of *r* to realistic size, usually half the total length of the focusing element [**Szilagyi 1984, and Szilagyi 1988]**. Figure (2-1)

show a flowchart of the computer program that is based on evaluate the electrodes shape.

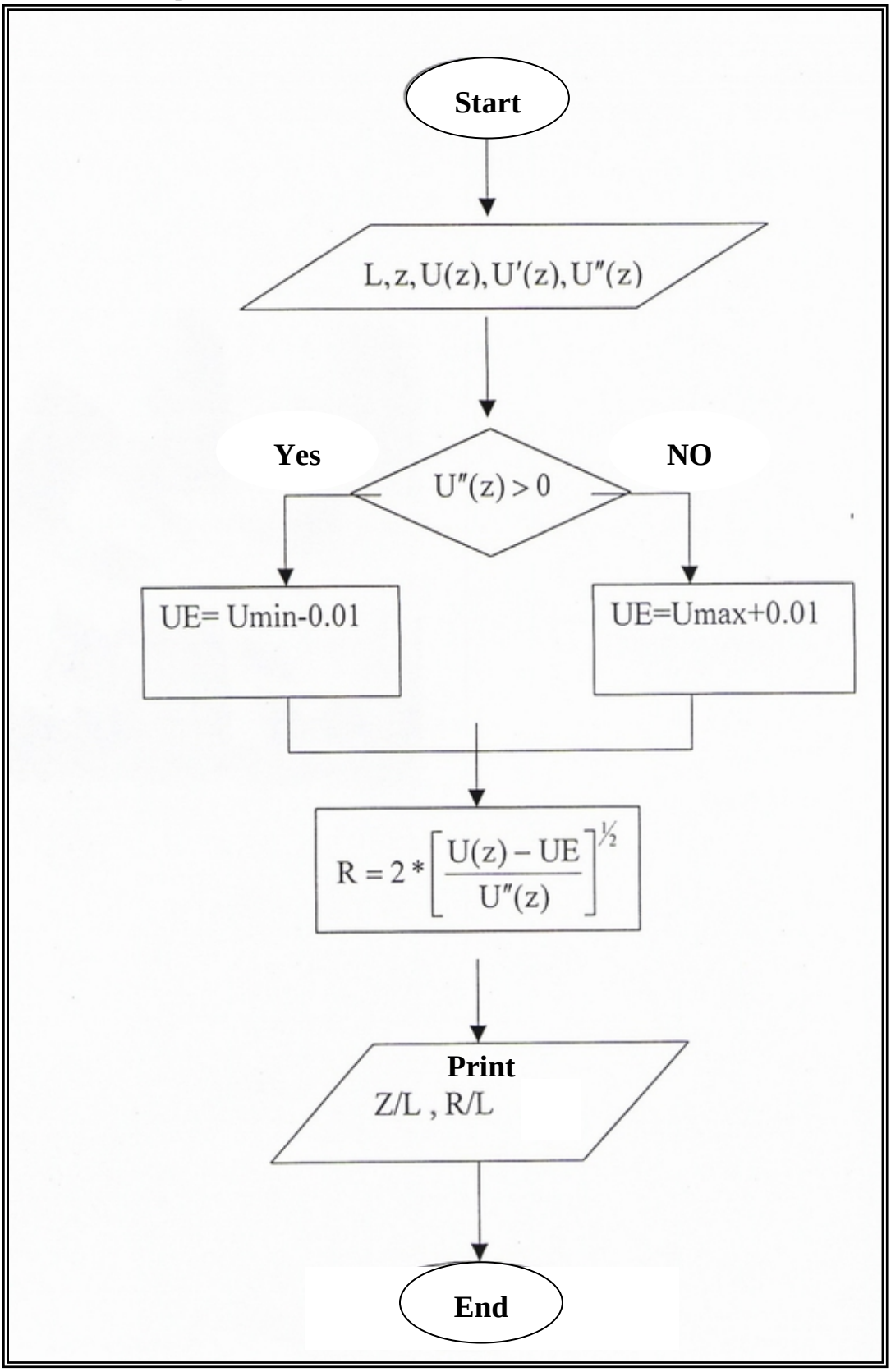

Figure(2-1) Flowchart for the Fortran to evaluate the electrodes shape

Republic of Iraq
Ministry of Higher Education and Scientific Research
AL-Nahrain University
College of Science
Physics Department

DESIGN OF ION MIRROR AS AN ABERRATION CORRECTOR USING BOUNDARY VALUES METHOD

A Thesis

Submitted to the College of Science of Al-Nahrain University in Partial Fulfillment of the Requirements for the Degree of

Master of Science

In

Physics

By

Mohamed Salam Mzahem Al- Obaidy

(B.Sc.2004)

In

Jumadi Al-awal 1428 A. H. **May 2007 A. D.**

بسم الله الرحمن الرحيم

يرفع الله الذين أمنوا منكم والذين أوتوا العلم درجات والله بما تعملون خبير۝ المجادلة ٥٨

صدق الله العظيم

جمهورية العراق
وزارة التعليم العالي و البحث العلمي
جامعة النهرين
كلية العلوم
قسم الفيزياء

تصميم مرآة أيونيه تعمل كمصحح للزيوغ باستخدام طريقه القيم الحدوديه

رسالة

مقدمة إلى كلية العلوم في جامعة النهرين وهي جزء من متطلبات نيل درجة الماجستير في

الفيزياء

من قبل

محمد سلام مزاحم العبيدي
(بكالوريوس ٢٠٠٤)

في

جمادي الأول ١٤٢٨هـ أيار ٢٠٠٧ م

المستخلص

تم إجراء بحث حاسوبي عن تصميم و خواص المرايا ألايونيه الكهروستاتيكية. حيث تم التركيز في البحث على اقتراح عدة صيغ رياضية لتمثيل الجهد المحوري لمرآة أيونية. إن الدوال التي أخذت بنظر الاعتبار كانت تلك التي أعطت عمل المرآة. حيث تم دراسة مسار الحزمة الأيونية تحت ظروف التكبير اللانهائي و دراسة مسار الحزمة الأيونية باستخدام تقنية بمرزايف على إنهما مسار مرآتي بالاستعانة بطريقة رنج-كوتا.

حيث تم إيجاد شكل الأقطاب لكل مرآة ببعدين و بثلاثة أبعاد. إن شكل المرآة التي تعمل تحت ظروف التكبير اللانهائي في هذا البحث و المستحصلة من الجهد المقترح من النوع الثلاثية الأقطاب و إن شكل المرآة التي تعمل بوساطة استخدام تقنية بمرزايف و المستحصلة من الجهد المقترح من النوع الثنائية الأبعاد بفتحه محورية حيث إن كل من المرآتين لهما فتحة محورية لتوفير طريق لحزمة الايونات ذات المسار ألمرآتي.

تم حساب كل من معاملات الزيغ الكروي و اللوني لكل مرآة وتم تعييرها بدلالة البعد البؤري. إن اختيار المرآة يعتمد على مستلزمات التشغيل وذلك فيما إذا كانت الرغبة في تشغيل المرآة في منظومة أيونية بصرية عند زيغ كروي واطئ أو زيغ لوني واطئ. و بينت الحسابات أن الجهود المقترحة قد أعطت عمل المرايا، عندما تعمل المرآة تحت ظرف التكبير اللانهائي فان معظم القيم المفضلة التي استنتجت لها القيم التالية:

a=٥٠٠فولت، b=٠,٠١فولت، c=١,٠٥ملم، f_o =-١,٦١٨ملم، L=١٧,٨ملم، C_s=٠,٤٢ملم، و C_c=٠,٤٢ملم ومعظم القيم المفضلة باستخدام تقنيه بمرزايف التي استنتجت لها القيم التالية:

a=١٥٠٠فولت، b=١٥فولت، L=١٤ ملم، c=٢,٧ملم، C_s=-٨,٧٩ملم، C_c=-٠,٧٥٦ملم و f_R =٠,٨٣١ملم، حيث أن قيم الخواص البصرية في البحث لها أداء ممتاز عند مقارنتها مع تلك المنشورة في الأدبيات.

الى استـــاذنا القديـــر الاستاذ الدكتور

صباح محمود جمعه

رحمه الله

الى من بقي في ثنايا القلب منزله
انـي وان كنت لا القاه.....القـاه

وان نظري لموصول برؤيتـــه
وان تباعد سكناي عن سكنـــاه

ياليته يـعلم انني لست اذكـره
وكيف اذكره اذ لم اكن انســاه